Charles University in Prague, Faculty of Science
Univerzita Karlova v Praze, Přírodovědecká fakulta

Ph.D. study program: Parasitology
Doktorský studijní program: Parazitologie

Mgr. Eva Pyrihová

Characterization of the protein import into *Giardia intestinalis* mitosomes

Charakterizace importu proteinů do mitosomů *Giardia intestinalis*

Ph.D. thesis/Dizertační práce

Supervisor/Školitel: Mgr. Pavel Doležal, Ph.D.
Prague, 2017

Declaration of the author/Prohlášení autorky

I declare that this Ph.D. thesis was written by myself and that all the literary sources were cited properly. Neither this work nor the substantial part of it was used to reach the same or any other academic degree.

Prohlašuji, že jsem předkládanou dizertační práci vypracovala samostatně a že všechny použité literární zdroje jsou řádně uvedeny. Dále prohlašuji, že tato práce ani její podstatná část nebyla předložena k získání stejného či jiného akademického titulu.

Prague/Praha

Mgr. Eva Pyrihová

V Praze, 11.12.2017 _____

Mgr. Eva Pyrihová

Declaration of the supervisor/Prohlášení školitele

I declare that the data presented in this Ph.D. thesis resulted from Eva Pyrihová work and team collaboration in our laboratory. I declare that the involvement of Eva Pyrihová in this work was substantial and that she contributed significantly to obtain the results.

Prohlašuji, že data prezentovaná v předkládané dizertační práci jsou výsledky práce Evy Pyrihové a spolupráce v naší laboratoři. Eva se významně podílela na projektech probíhajících v naší laboratoři i na sepsání uvedených publikací.

V Praze, 11.12.2017 _____

Mgr. Pavel Doležal, Ph.D.

Acknowledgements

Many thanks to my supervisor Pavel Doležal and to all lab members for the support and help during my studies.

TABLE OF CONTENTS

ABSTRACT

Mitochondrial endosymbiosis was a key event in the evolution of eukaryotes. Its proteome evolved into a unique combination of inherited bacterial components as well as novel eukaryotic inventions. Today, mitochondria show a huge variety across eukaryotic species – from aerobic mitochondria with cristae and complex protein apparatus for maintaining its own genome to hydrogen-producing hydrogenosomes and tiny anaerobic mitosomes without their own genome and with only a single metabolic pathway.

Comparing the existing spectra of mitochondria is beneficial for studying their evolution. The only ubiquitous and unifying features are double membrane, ISC pathway for iron-sulfur cluster synthesis and the core of protein import pathway. Therefore, these features could be considered as truly ancestral and essential to mitochondria. Mitosomes of various parasitic protists have evolved independently from complex mitochondria, since they are present in completely unrelated species and yet their evolution led in a surprisingly similar composition of protein import pathway. These retained components are thus believed to be functionally essential and for some reason hard to be replaced by alternate proteins. Mitosomal import pathways were considered very minimalistic for a long time. Nevertheless, the latest research shows, that some of them possess many unique lineage or even species-specific proteins, which likely substitute the loss of canonical components of this pathway.

Mitosomes of *Giardia intestinalis* are one of the most reduced mitochondrial forms discovered so far. However, with the improvement of bioinformatic tools, many distant homologues of proteins involved in protein import pathway such as Tom40, Tim44 and Tim17 were discovered over the last years. Moreover, with the identification of many new *Giardia*-specific proteins, novel unique functions and pathways are likely yet to be discovered.

ABSTRAKT

Pohlcení eubakterie a její přeměna v mitochondrii je klíčovým okamžikem v evoluci eukaryot. Jejich proteom se postupně vyvinul v jedinečnou kombinaci původních bakteriálních komponent s eukaryotickými evolučními novinkami. Dnes můžeme u eukaryot najít obrovskou variabilitu mitochondriálních forem – od klasických mitochondrií s kristy a složitým proteinovým systémem pro údržbu vlastního genomu přes hydrogenosomy se schopností produkovat molekulární vodík a konečně mitosomy, které zcela ztratily jak genom, tak většinu původních mitochondriálních funkcí a proteinů.

Srovnávání různých podob dnešních mitochondrií můžeme použít pro studium jejich evoluce. Jejich jedinými společnými znaky jsou dvojitá membrána, syntéza železo-sirných center pomocí ISC dráhy a centrální komponenty dráhy pro import proteinů. Proto předpokládáme, že právě tyto znaky představují původní a nezbytné vlastnosti mitochondrií. Mitosomy parazitických protist byly objeveny u zcela nepříbuzných druhů, vznikly tedy nezávisle a přesto byly u všech zachovány podobné proteiny mitochondriálního importu. Tyto komponenty jsou proto považovány za esenciální a nenahraditelné. Import proteinů do mitosomů byl dlouhou dobu považován za zcela minimalistický. Nicméně nejnovější studie ukazují, že mitosomální proteomy obsahují druhově-specifické proteiny, které pravděpodobně nahradily stávající komponenty této dráhy.

Mitosomy *Giardia intestinalis* jsou považovány za jedny z nejvíce redukovaných forem mitochondrie vůbec. S neustálým vylepšováním bioinformatických metod však nacházíme další homology proteinů účastnících se importu proteinů, jako Tom40, Tim44 a Tim17. Navíc s identifikací mnoha nových giardiově-specifických proteinů lze očekávat objev nových unikátních funkcí této organely.

1. INTRODUCTION

1.1. Mitochondria acquisition and evolution

Mitochondrion is an organelle of endosymbiotic origin, which originated from the transformation of the endosymbiotic eubacterion in the common eukaryotic ancestor (Gray and Doolittle, 1982). Acquisition of mitochondria was a key event in the early eukaryotic evolution, which enabled the huge expansion of eukaryotes. This endosymbiont of α-proteobacterial origin was gradually transformed to current day mitochondrion by gene loss and gene transfer to host nucleus. It resulted in the creation of genetically dependent organelle integrated into the network of other eukaryotic cellular structures. Key to the transformation was the establishment of an effective system for protein targeting and translocation to the organelle. In canonical mitochondria, the protein import machinery is very complex, comprising more than 35 protein components (Dudek *et al.*, 2013). These components are a combination of bacterial proteins inherited from the bacterial ancestor and novel eukaryotic inventions (Dolezal *et al.*, 2006). Comparative genomics indicate, that the overall design of the protein import machinery is shared among all eukaryotic supergroups and thus was also used by the LECA (last eukaryotic common ancestor) (Fukasawa *et al.*, 2017). However, detailed composition of the mitochondrion of the LECA and its protein import apparatus is difficult to infer from current data.

Our view of the early steps in the mitochondrial evolution is based on the structure of mitochondria of unicellular eukaryotes such as jakobids and malawimonads, which have retained multiple ancestral eubacterial features. Mitochondrial genome of jakobid *Reclinomonas americana* is an exemplary case, since its genome encodes for 97 genes and its proteome contains some proteins which were lost in other eukaryotic lineages (Lang *et al.*, 1997). Recently, many new species with rich mitochondrial genomes were sequenced giving some more insight into mitochondrial genome evolution (Yang *et al.*, 2017).

1.2. Protein import into mitochondria

Most of the studies concerning mitochondrial protein import are focused on mitochondria of *Saccharomyces cerevisiae*. The majority of mitochondrial proteins are translated on cytosolic ribosomes and imported into mitochondria post-translationally. These proteins thus need to carry presequences for proper recognition and translocation. They typically contain N-terminal presequence which is rich in positively charged residues and is able to form amphipatic α-helix (von Heijne, 1986). This presequence is recognized by the outer

mitochondrial membrane (OM) receptors Tom20, Tom22 and Tom70, which also facilitate the translocation itself (Endo and Yamano, 2010). Together with the channel forming protein Tom40 they form the TOM complex (Translocase of the outer membrane) – the main entry gate into mitochondria (Baker *et al.*, 1990).

Proteins of the OM classified as signal-anchored (anchored in the membrane by their N-terminus, the C-terminus facing cytosol) are imported by MIM (mitochondrial import machinery) complex (Bohnert *et al.*, 2015). This complex comprises proteins Mim1 and Mim2 and the transport does not require Tom40 (Becker *et al.*, 2008; Dimmer *et al.*, 2012). Proteins of the OM called tail-anchored (anchored in the membrane by their C-terminus, the N-terminus facing cytosol) are imported by yet-unknown mechanism, which also does not require TOM machinery. However, the lipid composition of the OM seems to be crucial for efficient import (Lee *et al.*, 2014).

Other proteins are transported through the TOM complex to the subcompartments of mitochondria according to their additional signal sequences: to the intermembrane space (IMS) via MIA pathway (Mitochondrial Intermembrane space Assembly), to the OM via SAM complex (Sorting and Assembly Machinery), to the inner membrane (IM) via TIM22 (Translocase of the Inner Membrane) or TIM23 complexes, which also translocates proteins into mitochondrial matrix (reviewed in Chacinska *et al.*, 2009).

Precursors of β-barrel proteins (such as Tom40) are transported through TOM complex to the IMS. There, the precursor is bound to small Tim proteins and guided to SAM complex, with the core formed of Sam50 channel (Endo and Yamano, 2010; Kozjak *et al.*, 2003).

Proteins of the IMS are recognized by MIA machinery, which comprises two components: Mia40 and Erv1 (Chacinska *et al.*, 2004). In the IMS, there are typically small soluble proteins (such as small Tims), which contain conserved cysteine residues. The precursors are transported through TOM complex to the IMS, where they bind Mia40, which cooperates with sulfhydryl oxidase Erv1 in a disulfide relay. A disulfide bond generated by Erv1 is transferred via Mia40 to the substrate proteins. It results in the intramolecular disulfide bridge formation and therefore protein folding, which prevents reverse movement of the proteins from the IMS (Muller *et al.*, 2008). Cysteine residues of Mia40 are reoxidized by Erv1 and the electrons are transported through cytochrome c to the proteins of the respiratory chain (Bihlmaier *et al.*, 2007).

Proteins of mitochondrial matrix and some IM proteins are imported via TIM23 complex, which is connected with the TOM complex by protein Tim50 (Mokranjac *et al.*, 2003). The transport channel of TIM23 is formed by two paralogues of Tim17 protein family, Tim23 and Tim17 (Emtage and Jensen, 1993). The C-terminal part of Tim23 is anchored in the IM and interacts with Tim17 forming the core of the TIM23 complex (Ryan *et al.*, 1998). The exact role of Tim17 in the complex is still unknown, but it interacts with Tim23 via its transmembrane domains (Demishtein-Zohary *et al.*, 2017). Interestingly, part of Tim23 is exposed to the IMS and interacts with Tim50 and is also involved in the membrane potential-dependent dimerization of Tim23 (Bauer *et al.*, 1996).

The transport through the TIM23 channel is propelled by two sources of energy, ATP hydrolysis mediated by PAM complex (Presequence translocase Associated Motor) and the membrane potential generated by the respiratory chain. The membrane potential helps to electrophoretically transport the positively charged residues in the presequence through the channel. Moreover it also directly activates the Tim23 channel (Wiedemann and Pfanner, 2017).

Transport of soluble matrix proteins with the N-terminal presequences requires the interaction of TIM23 with PAM complex with the key component chaperone Hsp70. Upon ATP hydrolysis Hsp70 pulls the substrate proteins into the matrix via entropic pulling mechanism (De Los and Goloubinoff, 2016). PAM complex is associated with TIM23 via protein Tim44, which tethers the two complexes together (Rassow *et al.*, 1994). In mitochondrial matrix, the N-terminal presequences are cut off by MPP (mitochondrial processing peptidase) (Hawlitschek *et al.*, 1988) and folded by Cpn60 and Cpn10 (Martin, 1997). The other group of substrate proteins contains so-called stop-transfer sequence, which is a hydrophobic transmembrane domain, which triggers lateral transfer from TIM23 into the IM. This transport requires the presence of proteins Tim21 and Mgr2, but energy from PAM complex is not needed (Mokranjac and Neupert, 2010). Some of these proteins later undergo cleavage of the stop-transfer sequence by IMP (Inner Membrane Peptidase) and are released into IMS (Gasser *et al.*, 1982).

The core protein of TIM22 complex – Tim22 is also a member of Tim17 family. TIM22 complex imports multi-pass transmembrane proteins, typically metabolite carriers, such as ADP/ATP transporter (Sirrenberg *et al.*, 1996). The precursors of Tim23 and Tim17 proteins are imported via TIM22 as well (Kaldi *et al.*, 1998). The proteins are delivered to the TIM22

complex from TOM complex via IMS, where they bind small Tims, which prevent their aggregation. From the IMS, the proteins go to TIM22 and then they are laterally released into the IM, which requires membrane potential, but no energy from ATP (Endres *et al.*, 1999).

1.3. Mitochondria-related organelles in anaerobic protists

Parasitic protists often contain highly reduced mitochondria, so called mitochondria-related organelles (MROs). MROs as well as mitochondria are derived from the single endosymbiotic organelle that gave rise to LECA (Last eukaryotic common ancestor) and then they underwent reductive evolution independently in different eukaryotic lineages (Leger *et al.*, 2017; van der Giezen and Tovar, 2005). All MROs share some common features with mitochondria, such as double membrane and some components of the protein import pathway (Embley and Martin, 2006). The driving force for the reductive mitochondrial evolution has predominantly been the anaerobic environment, in some cases accompanied by the parasitic lifestyle (Hjort *et al.*, 2010). The comparative analysis of different mitochondrial forms enable us to distinguish the minimal essential set of components of mitochondrial import from the dispensable set of peripheral subunits. Furthermore, studying these simplified pathways may help us to understand the principles of the first functional import pathway in protomitochondria, before all the additional receptors and enhancers were established. Nevertheless, studying these organisms comprises many complications. Mainly the presence of highly divergent gene sequences cause, that the homologues of particular proteins are difficult to be identified.

Hydrogenosomes represent one type of MROs. They are able to produce ATP by substrate level phosphorylation while the molecular hydrogen is produced (Lindmark and Muller, 1973). In most cases, they lost their genome and play role in Fe-S cluster biosynthesis. Hydrogenosomes were firstly discovered in trichomonads (Lindmark and Muller, 1973). Later, they were also found in several groups of ciliates (Embley *et al.*, 1995; Yarlett *et al.*, 1981), chytrid fungi (Yarlett *et al.*, 1986) or diplomonad *Spironucleus salmonicida* (Jerlstrom-Hultqvist *et al.*, 2013). Recently, the reductive evolution was described inside the group Metamonada. For example, the intermediate MRO between hydrogenosome and mitosome was identified in *Dysnectes.* It is an organelle, which is able to produce hydrogen, but the ATP production was lost (Leger *et al.*, 2017). Moreover, the transition organelle between mitochondria and hydrogenosome was recently found in Rhizarian *Brevimastigomonas motovehiculus* (Gawryluk *et al.*, 2016).

The most reduced forms of MROs are recognized as mitosomes. These organelles escaped the attention for a long time due to their very small size – less than 0,2 μm (Tovar *et al.*, 2003). All mitosomes lack organellar genome and they do not generate ATP. They were first discovered in amoeba *Entamoeba histolytica* (Tovar *et al.*, 1999) and later were also experimentally identified in various microsporidians (Katinka *et al.*, 2001; Williams *et al.*, 2002), metamonad *Giardia intestinalis* (Tovar *et al.*, 2003) or apicomplexan *Cryptosporidium parvum* (Henriquez *et al.*, 2005). It is very striking, that even though the reduction was independent in these lineages, it resulted into similar outcome in terms of metabolic functions as well as the characteristics of protein import pathway. With the exception of *E. histolytica*, mitosomes are known to participate in just single pathway, Fe-S cluster synthesis via ISC machinery.

Entamoeba histolytica

E. histolytica is a cosmopolitan human intestinal parasite causing amoebiasis. It belongs to Archamoebae (Amoebozoa). Its mitosomes are extremely reduced and lost even the Fe-S cluster biosynthesis pathway via ISC machinery (Ali *et al.*, 2004). Their only known function is the sulfate activation pathway, which provides metabolites required for the parasite encystation (Mi-ichi *et al.*, 2009; Mi-ichi *et al.*, 2015). The genome sequencing project revealed the presence of only three chaperones involved in the protein import – Hsp70, Cpn60 and Cpn10 (Loftus *et al.*, 2005).

Later, Tom40 and Sam50 were discovered in the OM using sensitive Hidden-Markov (HMM) model based searches, which intrinsically carry the information on the protein structure (Dolezal *et al.*, 2010). It was proposed, that *Entamoeba* lost typical OM receptors such as Tom70 or Tom20 due to the loss of presequences and gained the lineage-specific receptor Tom60 instead (Makiuchi *et al.*, 2013). Moreover, over 20 new lineage-specific OM proteins with yet-unknown functions were discovered recently. Some of these may play role in protein import as well (Santos *et al.*, 2016). Nevertheless, no channel in the IM has ever been found, which putatively makes *Entamoeba* one of the last protists with no known Tim17 homologue.

Microsporidia

Microsporidia were long considered as early branching eukaryotes, but later it was shown, that they represent either highly reduced fungi or a sister group to fungi (Hirt *et al.*, 1999). They are intracellular parasites infecting a wide range of animals from insects to humans.

Microsporidia typically contain highly reduced genome in terms of size and gene length (Biderre *et al.*, 1995; Katinka *et al.*, 2001). The presence of mitosomes was already described in many of them (Mikhailov *et al.*, 2017; Vavra *et al.*, 2016; Williams *et al.*, 2002). However, most of the studies focus on rabbit parasite *Encephalitozoon cuniculi*. Interestingly, unlike in other mitosome containing organisms, mitosomal proteins in *Encephalitozoon* often lack the N-terminal presequence, which makes them difficult to identify (Burri *et al.*, 2006). This truncation probably reflects the overall reduction and compaction of the whole genome. This process very likely went in hand with the loss of MPP, which was no longer needed to maturate the proteins in mitosomal matrix. Nevertheless, it is noteworthy, that some of the mitosomal proteins with no recognizable presequence can be efficiently imported into mitochondria when experimentally expressed in yeast (Burri *et al.*, 2006).

Only remnant mitochondrial import system was found in the genome of *Encephalitozoon*. According to the conceptual model of the mitosome structure, the OM accommodates Tom40, truncated receptor protein Tom70 and Sam50 (Burri *et al.*, 2006; Katinka *et al.*, 2001). The putative TIM complex of microsporidial mitosomes contains single Tim17 homologue with the sequence similarity to Tim22 subfamily and homologue of Tim50 (Waller *et al.*, 2009). The PAM complex has retained Pam16 (Waller *et al.*, 2009) and Hsp70 chaperone in the mitosomal matrix (Burri *et al.*, 2006). In the IMS, only Erv1 protein was found (Katinka *et al.*, 2001), while Mia40 is missing. Erv1 is thus probably directly oxidized by O_2 (Allen *et al.*, 2008).

Interestingly, there was a new species of microsporidia discovered recently named *Mitosporidium daphniae*, which is phylogenetically placed at the root of microsporidia. This gut parasite from a crustacean *Daphnia* shares morphological features with microporidia (the infection apparatus), yet it still bares mitochondrial genome as well as ATP production in mitochondria. This unique parasite demonstrates, that the morphological changes enabling the parasitic lifestyle preceded the mitochondrial reduction during the evolution of microsporidia (Haag *et al.*, 2014).

Cryptosporidium parvum

Cryptosporidium is an apicomplexan (SAR) parasite infecting mammalian intestinal tract where it causes cryptosporidiosis. The OM contains both core components, Tom40 and Sam50 (Abrahamsen *et al.*, 2004; Alcock *et al.*, 2012). Strikingly, one small Tim homologue

is present in the IMS, herein suggested to form unique homohexameric complexes (Alcock *et al.*, 2012).

Single Tim17 family protein in the mitosome is probably able to sustain both TIM23 and TIM22 functions (Strong and Nelson, 2000). Additional conserved subunits include Tim50 and Pam18, which together with chaperone Hsp70 propels the import of proteins (Alcock *et al.*, 2012; Slapeta and Keithly, 2004). Protein folding in the mitosomal matrix is then facilitated by Cpn60 (Riordan *et al.*, 2003).

It is noteworthy, that the closely related species – a gastric parasite *C. muris*, contains fully developed mitochondria with all the enzymes of Krebs cycle and complete respiratory chain (Mogi and Kita, 2010). Subsequent survey of *Cryptosporidium* species revealed general trend of mitochondrial reduction in the intestinal species (Liu *et al.*, 2016). Unfortunately, evolution of the protein import pathways was not addressed in this study, but it is to be expected to show a great variability among *Cryptosporidium* species. *Cryptosporidium* may thus represent an excellent example of the mitosomal evolution hand in hand with the overall cell biology.

Giardia intestinalis

Giardia is an unicellular anaerobic parasite causing a disease called giardiasis. Apart from being an important human pathogen, it serves also as a great model to study mitochondrial evolution, since its mitosomes are one of the simplest MROs (Tovar *et al.*, 2003).

Since the discovery of mitosomes, only few components of protein import pathway were described. In the OM, the main channel Tom40 was identified (Dagley *et al.*, 2009). The classification of the protein within the eukaryotic porin superfamily showed, that *Giardia* Tom40 blurs the boundary between Tom40 and VDAC proteins, which otherwise constitute well separated sequence clusters (Dagley *et al.*, 2009). It is thus possible that the protein act as both, the protein and the metabolite carrier across the OM.

Surprisingly, no other component of TOM complex was found. Recently, it was suggested, that the TOM complex components were replaced by *Giardia*-specific proteins (Rout *et al.*, 2016) but functional data on the newly found components are missing. Surprisingly, it appears that *Giardia* together with several related metamonads lost the entire SAM complex (Jedelsky *et al.*, 2011; Leger *et al.*, 2017b) and thus the possible mechanism of Tom40 assembly into the OM is unknown.

In the IM of *Giardia* mitosome, part of PAM complex was identified – Pam16, Pam18 and the chaperone Hsp70 (Dolezal *et al.*, 2005; Jedelsky *et al.*, 2011). Recently, the diverged sequence of Tim44 was also discovered. It contains the C-terminal part but lacks the N-terminal domain responsible for binding Hsp70 as well as Tim23. However, using coprecipitation, it was shown, that Tim44 probably interacts with Hsp70 in *Giardia* mitosomes anyway (Martincova *et al.*, 2015). Moreover, the single Tim17 homologue was recently discovered in *Giardia* as well (manuscript included in the thesis). Although it lacks some conserved features typical for Tim17 proteins, it likely retained four transmembrane domains as well as one conserved arginine residue responsible for Tim44 binding (Demishtein-Zohary *et al.*, 2017). Furthermore, it was suggested, that the protein translocation pore in *Giardia* might be formed of Tim17 dimer, since the protein is able to dimerize (manuscript included in the thesis). Interestingly, the source of ATP required for protein translocation across the TIM complex in *Giardia* is yet unknown. ATP is probably imported from cytosol, although the responsible transporter has not been found so far. The reductive evolution of *Giardia* mitosome is exemplified by the presence of catalytically active single subunit protease β-MPP, which normally functions together with α-MPP (Smid *et al.*, 2008). In mitosomal matrix, two chaperones are responsible for proper protein folding – Cpn60 and Cpn10 (Jedelsky *et al.*, 2011).

Also, the mode of protein targeting was recently tested for mitochondrial proteins in *Giardia* using various constructs with mitochondrial genes fused to DHFR (dihydrofolate reductase) (Martincova *et al.*, 2015). As DHFR can be forcefully folded by addition of metotrexate, its putative import into mitosomes would be interrupted. Indeed, upon the addition of metotrexate, DHFR fused to mitosomal leader peptide accumulates in the cytosol. Therefore, tested mitosomal proteins are likely translated on cytoplasmic ribosomes and later transported into the organelle in unfolded state.

Trypanosoma brucei

Trypanosoma is extensively studied as a causative agent of the African sleeping sickness. The blood stream parasite *Trypanosoma* is transmitted among the mammalian hosts by tse-tse flies. During the life cycle of *Trypanosoma*, its single mitochondrion undergoes dramatic changes in terms of its morphology as well as biochemical capabilities. While in the blood stream of mammals the energy is generated mainly by glycolysis, upon the transmission into the insect vector the mitochondrial respiration is fully activated (Timms *et al.*, 2002). It is

noteworthy, that even though the mitochondrion is aerobic and contains genome, it has undergone dramatic independent evolution likely due to the parasitic lifestyle. Hand in hand with this change, the mitochondrial protein import apparatus was considerably adapted.

Mitochondrial genome is organized into a structure known as kinetoplast, which is physically connected to the flagellar basal body. It is therefore an interesting link between the mitochondrial division and cytokinesis (Chanez *et al.*, 2006). The genome is encoded on so-called maxi-circles and requires posttranscriptional RNA editing by guide RNA molecules encoded on mini-circles (Jensen and Englund, 2012).

In *Trypanosoma*, the translocase in the OM named as ATOM (archaic translocase of OM), comprises seven subunits with the main transport channel ATOM40 (Mani *et al.*, 2015; Pusnik *et al.*, 2011). The archaic nature of ATOM40 was originally explained as the similarity to Omp85 protein from bacteria, which led to the hypothesis that it represents a functional analogue of Tom40 with distinct origin (Pusnik *et al.*, 2011). This would have a major impact on the phylogenetic position of trypanosomes and the evolution of mitochondria in eukaryotes. Nevertheless, it was later shown that ATOM40 is rather a very distant homologue of Tom40 (Zarsky *et al.*, 2012). However, five other ATOM subunits are kinetoplastid-specific and they are functional analogues of TOM components. ATOM46 and ATOM69 function as peripheral import receptors, ATOM11 and ATOM12 regulate the assembly of ATOM40 with the receptors (Mani *et al.*, 2015). Based on the sequence analyses, they are results of a parallel evolution rather than proteins derived from the ancestral import machinery of LECA (Harsman and Schneider, 2017; Mani *et al.*, 2015; Mani *et al.*, 2016).

There is a well conserved Sam50 protein in the OM responsible for the biogenesis of β-barrel proteins (Sharma *et al.*, 2010). No components of MIM complex were identified, however, it seems that analogous function is performed by trypanosome-specific ATOM36, which facilitates the transport of signal-anchored OM proteins (Kaser *et al.*, 2016; Pusnik *et al.*, 2012). In the IMS, no Mia40 was found, although its possible substrates are present. The import pathway is thus dependent on Erv1 only (Allen *et al.*, 2008).

In the IM, only one protein from the Tim17 family was found (Singha *et al.*, 2008). It was shown, that the depletion of Tim17 results in mitochondrial damage (Gentle *et al.*, 2007). However, it is still unclear, whether it functions as Tim17, Tim23 or Tim22. The protein was shown to interact with trypanosome-specific proteins such as TbTim54 and TbTim62, which are essential for the proper function of the complex (Singha *et al.*, 2012). In addition,

functional homologue of Tim50 was shown to participate in the import of proteins into mitochondria (Duncan *et al.*, 2013). Recently, it was shown that the core trypanosomal TIM complex consists of at least 10 proteins (including simplified PAM complex). They participate in the transport of both, the presequence containing proteins as well as membrane proteins carrying the stop-transfer sequences (Harsman *et al.*, 2016).

The wider taxon sampling showed the presence of Tim17, Tim22 and Tim23 proteins in related kinetoplastid species (Zarsky and Dolezal, 2016). The presence of a single Tim17 family protein is thus likely a product of secondary reduction of the import apparatus in trypanosomes. However, the set of IMS chaperones remained complex as both Tim9/Tim10 and Tim8/Tim13 complexes were identified in *T.brucei* (Gentle *et al.*, 2007).

The presence of mitochondrial genome encoding 18 proteins (Feagin, 2000) requires the function of Oxa1 translocase. Trypanosome contains Oxa1, which mediates the insertion of the proteins encoded on the mitoribosomes from matrix to the IM. The membrane protein assembly further involves a homologue of the inner membrane peptidase Imp (Schneider *et al.*, 2008).

2. DISCUSSION

Eukaryotic cell is characterized by its compartmentalization. It contains a set of membraneous organelles like nucleus, endoplasmic reticulum or mitochondria. These various compartments are defined by specific composition of proteins. Majority of eukaryotic proteins are translated on cytosolic ribosomes and thus have to be efficiently translocated into the final organelle. For this, specialized transport machineries have evolved along with the targeting sequences incorporated in the protein sequences.

The mitochondrial protein import machinery is responsible for the import of hundreds of proteins and thus essential for proper mitochondrial function. Therefore, it is not striking that the core components are conserved across eukaryotic species. Given that most of the studies are focusing on aerobic mitochondria of Opisthokonts, a little is known about the specifics of protein import in parasitic protists. Nevertheless, studying the mitochondria across the eukaryotic diversity can teach us a lot about the evolution of mitochondrial import systems and the variety of metabolic pathways occurring within the organelle. For example, the Fe-S cluster biosynthesis is currently considered to be the only essential mitochondrial function in

yeast (Lill and Muhlenhoff, 2006). The necessity of this function is thus reflected by retention of the pathway in mitosomes of distant species (with the sole exception of *E. histolytica*).

In the early days of mitochondrial evolution the host cell had to develop efficient transport system for proteins encoded by genes, which were transferred from the symbiont genome to the host nucleus. We can only speculate about the precise scenario, but we know, that the fundamentals of protein import machinery were established in the last common ancestor to all eukaryotes (Dolezal *et al.*, 2006).

Most likely the host cell used the current bacterial translocases at first. Some of them were later improved for the needs of the host cell and some of them were lost and replaced with new eukaryotic inventions. We know four systems for protein export in gram-negative bacteria, which can be found in current mitochondria. First, the YidC protein responsible for membrane protein insertion (Kuhn *et al.*, 2003). Second, the SecYEG complex with the core komponent SecY is responsible for insertion of inner bacterial membrane proteins as well as protein export (Cheng, 2010). Third, the TAT system, which is able to transport proteins across the membrane in folded state (Palmer *et al.*, 2010). Fourth, the outer membrane BAM complex with the core component Omp85, which inserts β-barrel proteins in the OM (Gentle *et al.*, 2004; Paschen *et al.*, 2003).

Commonly, in bacteria, these translocases function in the outward direction only. The mechanistic details of the mitochondrial orthologues showed that the complexes have the same membrane topology, serving the insertion of proteins from the mitochondrial matrix to or across the IM (Oxa1/YidC, SecY and TAT) or from the IMS to the OM (Omp85/Sam50).

The mitochondrial homologue of YidC, Oxa1, was retained in all eukaryotes carrying mitochondrial genome. It is encoded in the nucleus and upon its import to mitochondria, it serves as the membrane insertase for the IM proteins encoded in mitochondrial genome (Kuhn *et al.*, 2003). SecY homologue was identified in the mitochondrial genome of only several protist species such as *Reclinomonas americana* (Tong *et al.*, 2011) and other related Jakobids (Burger *et al.*, 2013). The actual substrate of the mitochondrial SecY remains unknown but it is likely another mitochondrially encoded protein. Similarly, while TAT translocase is more frequent in mitochondria of various protists than SecY (Lang *et al.*, 1997; Yen *et al.*, 2002), its substrate protein is still unknown. With regard to TAT being a translocase specialized for transporting folded protein cargos, it has been hypothesized that the Fe-S cluster containing Rieske protein might be the putative substrate (Pett and Lavrov, 2013).

Interestingly, SecY-dependent system is also homologous to a Sec61-dependent pathway in the endoplasmic reticulum and homologue of the translocon also functions in chloroplasts (Veenendaal *et al.*, 2004). Moreover, thylakoid membranes also harbour homologue of YidC/Oxa1 as well as functional TAT system (Celedon and Cline, 2013; Hennon *et al.*, 2015). Therefore, it seems that the very same proteins were very efficiently recycled and used in various types of membranes in different organelles.

The mitochondrial homologue of Omp85 - Sam50 can be found in all but few eukaryotes, where it assembles β-barrels into the OM (Kozjak *et al.*, 2003). Hence it seems, that jakobids are the only organisms known so far, which combine all the ancestral bacterial pathways (Oxa, TAT, SEC, BAM) together with derived eukaryotic machineries (TOM, TIM) (Tong *et al.*, 2011).

The crucial step in the evolution of eukaryotic import system was the establishment of the presequences. It was shown, that some of the bacterial proteins already carry the N-terminal sequences, that can be recognized by isolated mitochondria (Lucattini *et al.*, 2004). Hence, it could be a starting point for the initiation of the evolution of mitochondrial import system. Moreover, the presequence-like peptides can be found scattered in bacterial genomes. These fragments were likely used as preadaptations and by DNA rearrangements placed to N-terminal parts of existing genes (Baker and Schatz, 1987). Moreover, these sequences were later reused by their duplication and recombination to other genes (Kadowaki *et al.*, 1996). These N-terminal extensions are also responsible for their recognition by mitochondrial processing peptidase MPP, which is as well of bacterial origin. MPP is formed of two subunits and it has evolved from single subunit peptidases of α-proteobacteria probably by gene duplication (Kitada *et al.*, 2007). Other mitochondrial peptidase – IMP, which cleaves the hydrophobic stop-transfer sequences is also derived from bacteria. IMP consists of Imp1 and Imp2 which are homologous to bacterial leader peptidase. In bacteria, this enzyme is responsible for the presequence cleavage prior to protein folding (Dalbey, 1991).

Simultaneously with the evolution of presequences, it was necessary to establish new eukaryotic system for recognition of these signals. The ancestry of Tom40 is still unresolved. However, it is broadly accepted that it is derived from an eubacterial β-barrel protein of unknown function (Gabriel *et al.*, 2001). Recently, it was shown, that the primitive TOM complex was likely established in LECA consisting at least from Tom40, Tom22 and Tom7 (Fukasawa *et al.*, 2017). This primitive complex was probably able to transport proteins

without additional components. Later, the complex evolved into various forms across eukaryotic lineages.

The energy providing chaperone Hsp70 in mitochondrial matrix is of clear bacterial origin – it is derived from the bacterial chaperone DnaK (Boorstein *et al.*, 1994). Also, matrix chaperones Cpn60 and Cpn10 are derived from the bacterial GroEL and GroES proteins (Martin, 1997). Multiple small Tims in IMS are of eukaryotic origin and are probably result of gene multiplication (Gentle *et al.*, 2007).

Most of the other IM components are likely of eukaryotic origin, however, a few proteins are derived from bacterial inner membrane proteins, such as Tim44 or Pam18 (Clements *et al.*, 2009). The primitive form of TIM23 complex in LECA is thus estimated to comprise: Tim17, Tim23, Tim50, Tim21, Tim44, Mgr2, Pam18 and Pam16 (Fukasawa *et al.*, 2017). Since the channel proteins from TIM22 and TIM23 complexes are homologous, it was proposed, that there was a single Tim protein in LECA serving as a universal translocase for all mitochondrial proteins. This would represent the ancestral form, which later diverged into three distinct proteins functioning as two different import systems (Schneider *et al.*, 2008).This theory was strongly supported by the presence of single Tim17-like protein in euglenozoan *Trypanosoma brucei* (Schneider *et al.*, 2008), apicomplexan *Cryptosporidium parvum* (Strong and Nelson, 2000) or microsporidian *Encephalitozoon cuniculi* (Waller *et al.*, 2009). However, it was recently shown that in case of trypanosomatids the ancestor of all Euglenozoa including *T. brucei* had three distinct proteins. *T. brucei* thus underwent rather secondary simplification of the system (Zarsky and Dolezal, 2016). Therefore, it is probable that other protists with single Tim17 homologue had also undergone independent reduction of the systems.

Originally, it was proposed, that eukaryotic Tim17 family of proteins could possibly evolve from the bacterial amino acid translocase LivH, which later gained the ability to transport longer amino acid chains (Rassow *et al.*, 1999). However, multiple analyses showed that the original identified sequence similarity between Tim17 family proteins and LivH is in fact very low and does not reflect any evolutionary relationship. Hence, the Tim17 family proteins as key constituents of TIM complexes, represent exclusively eukaryotic proteins (Zarsky and Dolezal, 2016).

Evolution of mitochondria has revealed that while some components can be abandoned or replaced in certain species, there are several proteins, which seem to be indispensable for

mitochondrial function in all organisms. Thus, in very distant lineages the evolution resulted in analogous adaptation of the protein import apparatus. Likely, Tom40 is the only OM protein involved in protein import, which was retained in all known mitochondria or MROs. Nonetheless, there has been a recent discussion, whether ATOM40 in trypanosomatids is a product of parallel evolution or rather a distant homologue of canonical Tom40 (Pusnik *et al.*, 2011). According to the HMM-based analyses, the latter seems to be the case, and ATOM40 is just diverged Tom40 (Zarsky *et al.*, 2012).

Sam50 is also a highly conserved ubiquitously present protein with the only exception of *Giardia* and other metamonads. The selection pressure to retain Sam50 is evident, given that Sam50 is necessary for Tom40 assembly. The mechanism of Tom40 assembly in *Giardia* and related organisms is yet to be discovered, but the absence of Sam50 suggests that unique *Giardia*-specific protein has taken over the Sam50 function or *Giardia* Tom40 may actually be able to self-assemble.

Another ubiquitous protein is Hsp70, which was inherited from bacterial ancestor and was retained across all eukaryotic species, where it mediates the actual transport of the substrate polypeptide. Interestingly, the source of ATP for Hsp70 is not clear in some parasitic protists such as in *Giardia*, where no ATP transporter was found. Nevertheless, the ATP transporters were identified in mitosomes of microsporidia (Tsaousis *et al.*, 2008) or *Entamoeba* (Chan *et al.*, 2005). Since the need for ATP is obvious, we can expect that the ATP transporter in *Giardia* and is yet to be discovered.

In the IM, the main channel forming protein from Tim17 family seems to be well conserved. The distant homologue was recently identified even in several metamonads including *Giardia* (manuscript included in the thesis), which was, according to the genome analysis, for a long time considered a Tim17-lacking lineage. However, until now, homologue of Tim17 was found neither in *Spironucleus* nor in *Entamoeba*.

Surprisingly, the same scenario of mitochondrial adaptation leading to the reduction of three Tim17 members (Tim17/Tim22/Tim23) to just single protein can be observed in multiple parasites (such as *Giardia, Trypanosoma, Cryptosporidium* and micropsoridia). It is striking, that even in *Trypanosoma*, with fully developed aerobic mitochondria with hundreds of mitochondrial proteins, only single-component channel can mediate the import of all IM and matrix proteins. In general, the single Tim17 homologues are often too divergent to be clearly classified as one of the Tim17, Tim22 or Tm23. Nevertheless, it has been suggested, that they

might belong either to Tim17 or Tim22 subfamily (manuscript included in the thesis). In yeast, it was shown, that Tim17 alone is not able to form a functional pore. In trypanosomes, it was proposed, that in order to form pore, Tim17 is associated with rhomboid-like proteins, which are known to form pores in the ERAD (ER-associated protein degradation) system (Harsman *et al.*, 2016; Harsman and Schneider, 2017). In *Giardia*, Tim17 might form a pore by dimerization or oligomerization. It was shown, that in-vivo, GiTim17 is part of a protein complex bound by disulfide bond and of approximately doubled size of single GiTim17. Moreover, upon in-vitro translation it forms a complex of doubled size in experimental membrane and it also specifically interacts with itself in yeast two-hybrid assay (manuscript included in the thesis).

Together with the single homologue of Tim17, part of PAM complex is usually retained in various MROs. Interestingly, no component of PAM complex was found in *Entamoeba*, which might reflect the putative loss of Tim17. It is thus possible, that *Entamoeba* established a new lineage-specific transport system in the IM. Another well-conserved IM protein is Tim44. Only recently the homolog of Tim44 was found by coprecipitation approach in *G. intestinalis*. Although the sequence of GiTim44 is highly derived and N-terminally truncated, the protein likely functions together with Hsp70 as in other organisms (Martincova *et al.*, 2015). The C-terminal part of Tim44, which is responsible for Tim17 binding (Banerjee *et al.*, 2015) is conserved though. Moreover, these two proteins were coprecipitated together and hence it was suggested, that they interact with each other in *Giardia* (manuscript included in the thesis).

What seems to be typical to all mitosomes is the loss of membrane potential, which in canonical mitochondria contributes to efficient mitochondrial transport. It is noteworthy, that a small set of IM proteins can be efficiently transported via TIM23 in a membrane potential independent manner (Turakhiya *et al.*, 2016). These proteins are characterized by the lack of positively charged residues on their N-terminus. Thus the loss of these residues in some mitosomal proteins might correspond to the loss of membrane potential. It is possible, that the N-terminal truncation of many mitosomal proteins without canonical presequence is due to this very adaptation (Garg and Gould, 2016).

Mitochondrial protein import pathway is one of the unifying and determining features of mitochondria across all eukaryotic supergroups. As mitochondrial acquisition enabled the huge expansion of eukaryotic species, studying its evolution is a subject of interest for many

years. The discovery of highly reduced mitochondria-related organelles has provided us great models for studying simplified mitochondria. Recent publications showing that mitosomes in fact contain many unique proteins suggested, that they might be far more complex than previously thought. Analogously, while it might seem that only core protein apparatus was conserved in mitosomes, the recent studies show, that mitosomes of anaerobes or mitochondria of trypanosomes combine the „classical“ components with their specific proteins to establish a functional import pathway.

3. AIMS OF THE STUDY

- To characterize mitosomal proteome in *Giardia*
- To test the mode of mitosomal protein targeting in *Giardia*
- To identify new mitosomal proteins and pathways associated with mitosomes in *Giardia*
- To find the putative mitosomal inner membrane translocase in *Giardia*

4. LIST OF PUBLICATION AND AUTHOR CONTRIBUTION

- Pyrih, J., Harant, K., Martincová, E., Šuťák, R., Lesuisse, E., Hrdý, I., Tachezy, J. (2014) ***Giardia intestinalis*** **incorporates heme into cytosolic cytochrome b(5).** *Eukaryotic Cell* **13:** 231-239.
    - Cloning, preparation and production of recombinant cytochrom b5 proteins in *E. coli*, preparation of mutated gCYTb5-4 recombinant protein

- Martincová E., Voleman L., Pyrih J., Žárský V., Vondráčková P., Kolísko M., Tachezy J., Doležal, P. (2015) **Probing the biology of *Giardia intestinalis* mitosomes using in vivo enzymatic tagging.** Molecular and Cellular Biology. 2015 Jun;35(16):2864- 74.
    - Cloning, Coprecipitation protocol development, protein isolation (Pam18, Tim44, Hsp70, Tom40), analysis of proteomic data, experiments with DHFR, immunofluorescence

- Pyrih, J., Pyrihová, E., Kolísko, M., Stojanovová, D., Basu, S., Harant, K., Haindrich, A. C., Doležal, P., Lukeš, J., Roger, A., Tachezy, J. (2016) **Minimal cytosolic iron-sulfur cluster assembly machinery of *Giardia intestinalis* is partially associated with mitosomes.** *Mol Microbiol* **102:** 701-714.
    - Together with Jan Pyrih: coprecipitation of GiOR-1 interacting proteins, analysis of proteomic data.

- Pyrihová, E., Krupičková, A., Voleman L., Wandyszewska, N., Roger, A., Kolísko, M., Doležal, P. **Single Tim translocase in the mitosomes of *Giardia intestinalis* illustrates the convergence of the protein import machines in anaerobic eukaryotes.** Manuscript in preparation
    - Cloning, protein localization, Co-precipitation of Tim17, analysis of proteomic data, construction of vectors for Yeast two hybrid, membrane solubility tests, manuscript preparation

REFERENCES

Abrahamsen, M. S., Templeton, T. J., Enomoto, S., Abrahante, J. E., Zhu, G., Lancto, C. A. *et al.* (2004) Complete genome sequence of the apicomplexan, *Cryptosporidium parvum*. *Science* **304:** 441-445.

Alcock, F., Webb, C. T., Dolezal, P., Hewitt, V., Shingu-Vasquez, M., Likic, V. A. *et al.* (2012) A small Tim homohexamer in the relict mitochondrion of *Cryptosporidium*. *Mol Biol Evol* **29:** 113-122.

Ali, V., Shigeta, Y., Tokumoto, U., Takahashi, Y., and Nozaki, T. (2004) An intestinal parasitic protist, *Entamoeba histolytica*, possesses a non-redundant nitrogen fixation-like system for iron-sulfur cluster assembly under anaerobic conditions. *J Biol Chem* **279:** 16863-16874.

Allen, J. W., Ferguson, S. J., and Ginger, M. L. (2008) Distinctive biochemistry in the trypanosome mitochondrial intermembrane space suggests a model for stepwise evolution of the MIA pathway for import of cysteine-rich proteins. *FEBS Lett* **582:** 2817-2825.

Banerjee, R., Gladkova, C., Mapa, K., Witte, G., and Mokranjac, D. (2015) Protein translocation channel of mitochondrial inner membrane and matrix-exposed import motor communicate via two-domain coupling protein. *Elife* **4:** e11897.

Baker, A. and Schatz, G. (1987) Sequences from a prokaryotic genome or the mouse dihydrofolate reductase gene can restore the import of a truncated precursor protein into yeast mitochondria. *Proc Natl Acad Sci U S A* **84:** 3117-3121.

Baker, K. P., Schaniel, A., Vestweber, D., and Schatz, G. (1990) A yeast mitochondrial outer membrane protein essential for protein import and cell viability. *Nature* **348:** 605-609.

Bauer, M. F., Sirrenberg, C., Neupert, W., and Brunner, M. (1996) Role of Tim23 as voltage sensor and presequence receptor in protein import into mitochondria. *Cell* **87:** 33-41.

Becker, T., Pfannschmidt, S., Guiard, B., Stojanovski, D., Milenkovic, D., Kutik, S. *et al.* (2008) Biogenesis of the mitochondrial TOM complex: Mim1 promotes insertion and assembly of signal-anchored receptors. *J Biol Chem* **283:** 120-127.

Biderre, C., Pages, M., Metenier, G., Canning, E. U., and Vivares, C. P. (1995) Evidence for the smallest nuclear genome (2.9 Mb) in the microsporidium *Encephalitozoon cuniculi*. *Mol Biochem Parasitol* **74:** 229-231.

Bihlmaier, K., Mesecke, N., Terziyska, N., Bien, M., Hell, K., and Herrmann, J. M. (2007) The disulfide relay system of mitochondria is connected to the respiratory chain. *J Cell Biol* **179:** 389-395.

Bohnert, M., Pfanner, N., and van der Laan, M. (2015) Mitochondrial machineries for insertion of membrane proteins. *Curr Opin Struct Biol* **33:** 92-102.

Boorstein, W. R., Ziegelhoffer, T., and Craig, E. A. (1994) Molecular evolution of the HSP70 multigene family. *J Mol Evol* **38:** 1-17.

Burger, G., Gray, M. W., Forget, L., and Lang, B. F. (2013) Strikingly bacteria-like and gene-rich mitochondrial genomes throughout jakobid protists. *Genome Biol Evol* **5:** 418-438.

Burri, L., Williams, B. A., Bursac, D., Lithgow, T., and Keeling, P. J. (2006) Microsporidian mitosomes retain elements of the general mitochondrial targeting system. *Proc Natl Acad Sci U S A* **103:** 15916-15920.

Celedon, J. M. and Cline, K. (2013) Intra-plastid protein trafficking: how plant cells adapted prokaryotic mechanisms to the eukaryotic condition. *Biochim Biophys Acta* **1833:** 341-351.

Chacinska, A., Koehler, C. M., Milenkovic, D., Lithgow, T., and Pfanner, N. (2009) Importing mitochondrial proteins: machineries and mechanisms. *Cell* **138:** 628-644.

Chacinska, A., Pfannschmidt, S., Wiedemann, N., Kozjak, V., Sanjuan Szklarz, L. K., Schulze-Specking, A. *et al.* (2004) Essential role of Mia40 in import and assembly of mitochondrial intermembrane space proteins. *EMBO J* **23:** 3735-3746.

Chan, K. W., Slotboom, D. J., Cox, S., Embley, T. M., Fabre, O., van der Giezen, M. *et al.* (2005) A novel ADP/ATP transporter in the mitosome of the microaerophilic human parasite *Entamoeba histolytica*. *Curr Biol* **15:** 737-742.

Chanez, A. L., Hehl, A. B., Engstler, M., and Schneider, A. (2006) Ablation of the single dynamin of *T. brucei* blocks mitochondrial fission and endocytosis and leads to a precise cytokinesis arrest. *J Cell Sci* **119:** 2968-2974.

Cheng, Z. (2010) Protein translocation through the Sec61/SecY channel. *Biosci Rep* **30:** 201-207.

Clements, A., Bursac, D., Gatsos, X., Perry, A. J., Civciristov, S., Celik, N. *et al.* (2009) The reducible complexity of a mitochondrial molecular machine. *Proc Natl Acad Sci U S A* **106:** 15791-15795.

Dagley, M. J., Dolezal, P., Likic, V. A., Smid, O., Purcell, A. W., Buchanan, S. K. *et al.* (2009) The protein import channel in the outer mitosomal membrane of *Giardia intestinalis*. *Molecular Biology and Evolution* **26:** 1941-1947.

Dalbey, R. E. (1991) Leader peptidase. *Mol Microbiol* **5:** 2855-2860.

De Los, R. P. and Goloubinoff, P. (2016) Hsp70 chaperones use ATP to remodel native protein oligomers and stable aggregates by entropic pulling. *Nat Struct Mol Biol* **23:** 766-769.

Demishtein-Zohary, K., Gunsel, U., Marom, M., Banerjee, R., Neupert, W., Azem, A. *et al.* (2017) Role of Tim17 in coupling the import motor to the translocation channel of the mitochondrial presequence translocase. *Elife* **6**.

Dimmer, K. S., Papic, D., Schumann, B., Sperl, D., Krumpe, K., Walther, D. M. *et al.* (2012) A crucial role for Mim2 in the biogenesis of mitochondrial outer membrane proteins. *J Cell Sci* **125:** 3464-3473.

Dolezal, P., Dagley, M. J., Kono, M., Wolynec, P., Likic, V. A., Foo, J. H. *et al.* (2010) The essentials of protein import in the degenerate mitochondrion of *Entamoeba histolytica*. *Plos Pathogens* **6**.

Dolezal, P., Likic, V., Tachezy, J., and Lithgow, T. (2006) Evolution of the molecular machines for protein import into mitochondria. *Science* **313:** 314-318.

Dolezal, P., Smid, O., Rada, P., Zubacova, Z., Bursac, D., Sutak, R. *et al.* (2005) Giardia mitosomes and trichomonad hydrogenosomes share a common mode of protein targeting. *Proceedings of the National Academy of Sciences of the United States of America* **102:** 10924-10929.

Dudek, J., Rehling, P., and van der Laan, M. (2013) Mitochondrial protein import: common principles and physiological networks. *Biochim Biophys Acta* **1833:** 274-285.

Duncan, M. R., Fullerton, M., and Chaudhuri, M. (2013) Tim50 in *Trypanosoma brucei* possesses a dual specificity phosphatase activity and is critical for mitochondrial protein import. *J Biol Chem* **288:** 3184-3197.

Embley, T. M., Finlay, B. J., Dyal, P. L., Hirt, R. P., Wilkinson, M., and Williams, A. G. (1995) Multiple origins of anaerobic ciliates with hydrogenosomes within the radiation of aerobic ciliates. *Proc Biol Sci* **262:** 87-93.

Embley, T. M. and Martin, W. (2006) Eukaryotic evolution, changes and challenges. *Nature* **440:** 623-630.

Emtage, J. L. and Jensen, R. E. (1993) MAS6 encodes an essential inner membrane component of the yeast mitochondrial protein import pathway. *J Cell Biol* **122:** 1003-1012.

Endo, T. and Yamano, K. (2010) Transport of proteins across or into the mitochondrial outer membrane. *Biochim Biophys Acta* **1803:** 706-714.

Endres, M., Neupert, W., and Brunner, M. (1999) Transport of the ADP/ATP carrier of mitochondria from the TOM complex to the TIM22.54 complex. *EMBO J* **18:** 3214-3221.

Feagin, J. E. (2000) Mitochondrial genome diversity in parasites. *Int J Parasitol* **30:** 371-390.

Fukasawa, Y., Oda, T., Tomii, K., and Imai, K. (2017) Origin and Evolutionary Alteration of the Mitochondrial Import System in Eukaryotic Lineages. *Mol Biol Evol*.

Gabriel, K., Buchanan, S. K., and Lithgow, T. (2001) The alpha and the beta: protein translocation across mitochondrial and plastid outer membranes. *Trends Biochem Sci* **26:** 36-40.

Garg, S. G. and Gould, S. B. (2016) The Role of Charge in Protein Targeting Evolution. *Trends Cell Biol* **26:** 894-905.

Gasser, S. M., Ohashi, A., Daum, G., Bohni, P. C., Gibson, J., Reid, G. A. *et al.* (1982) Imported mitochondrial proteins cytochrome b2 and cytochrome c1 are processed in two steps. *Proc Natl Acad Sci U S A* **79:** 267-271.

Gawryluk, R. M. R., Kamikawa, R., Stairs, C. W., Silberman, J. D., Brown, M. W., and Roger, A. J. (2016) The Earliest Stages of Mitochondrial Adaptation to Low Oxygen Revealed in a Novel Rhizarian. *Curr Biol* **26:** 2729-2738.

Gentle, I., Gabriel, K., Beech, P., Waller, R., and Lithgow, T. (2004) The Omp85 family of proteins is essential for outer membrane biogenesis in mitochondria and bacteria. *J Cell Biol* **164:** 19-24.

Gentle, I. E., Perry, A. J., Alcock, F. H., Likic, V. A., Dolezal, P., Ng, E. T. *et al.* (2007) Conserved motifs reveal details of ancestry and structure in the small TIM chaperones of the mitochondrial intermembrane space. *Mol Biol Evol* **24:** 1149-1160.

Gray, M. W. and Doolittle, W. F. (1982) Has the endosymbiont hypothesis been proven? *Microbiol Rev* **46:** 1-42.

Haag, K. L., James, T. Y., Pombert, J. F., Larsson, R., Schaer, T. M., Refardt, D. *et al.* (2014) Evolution of a morphological novelty occurred before genome compaction in a lineage of extreme parasites. *Proc Natl Acad Sci U S A* **111:** 15480-15485.

Harsman, A., Oeljeklaus, S., Wenger, C., Huot, J. L., Warscheid, B., and Schneider, A. (2016) The non-canonical mitochondrial inner membrane presequence translocase of trypanosomatids contains two essential rhomboid-like proteins. *Nat Commun* **7:** 13707.

Harsman, A. and Schneider, A. (2017) Mitochondrial protein import in trypanosomes: Expect the unexpected. *Traffic* **18:** 96-109.

Hawlitschek, G., Schneider, H., Schmidt, B., Tropschug, M., Hartl, F. U., and Neupert, W. (1988) Mitochondrial protein import: identification of processing peptidase and of PEP, a processing enhancing protein. *Cell* **53:** 795-806.

Hennon, S. W., Soman, R., Zhu, L., and Dalbey, R. E. (2015) YidC/Alb3/Oxa1 Family of Insertases. *J Biol Chem* **290:** 14866-14874.

Henriquez, F. L., Richards, T. A., Roberts, F., McLeod, R., and Roberts, C. W. (2005) The unusual mitochondrial compartment of Cryptosporidium parvum. *Trends Parasitol* **21:** 68-74.

Hirt, R. P., Logsdon, J. M., Jr., Healy, B., Dorey, M. W., Doolittle, W. F., and Embley, T. M. (1999) Microsporidia are related to Fungi: evidence from the largest subunit of RNA polymerase II and other proteins. *Proc Natl Acad Sci U S A* **96:** 580-585.

Hjort, K., Goldberg, A. V., Tsaousis, A. D., Hirt, R. P., and Embley, T. M. (2010) Diversity and reductive evolution of mitochondria among microbial eukaryotes. *Philos Trans R Soc Lond B Biol Sci* **365:** 713-727.

Jedelsky, P. L., Dolezal, P., Rada, P., Pyrih, J., Smid, O., Hrdy, I. *et al.* (2011) The minimal proteome in the reduced mitochondrion of the parasitic protist *Giardia intestinalis*. *PLoS One* **6:** e17285.

Jensen, R. E. and Englund, P. T. (2012) Network news: the replication of kinetoplast DNA. *Annu Rev Microbiol* **66:** 473-491.

Jerlstrom-Hultqvist, J., Einarsson, E., Xu, F., Hjort, K., Ek, B., Steinhauf, D. *et al.* (2013) Hydrogenosomes in the diplomonad *Spironucleus salmonicida*. *Nat Commun* **4:** 2493.

Kadowaki, K., Kubo, N., Ozawa, K., and Hirai, A. (1996) Targeting presequence acquisition after mitochondrial gene transfer to the nucleus occurs by duplication of existing targeting signals. *EMBO J* **15:** 6652-6661.

Kaldi, K., Bauer, M. F., Sirrenberg, C., Neupert, W., and Brunner, M. (1998) Biogenesis of Tim23 and Tim17, integral components of the TIM machinery for matrix-targeted preproteins. *EMBO J* **17:** 1569-1576.

Kaser, S., Oeljeklaus, S., Tyc, J., Vaughan, S., Warscheid, B., and Schneider, A. (2016) Outer membrane protein functions as integrator of protein import and DNA inheritance in mitochondria. *Proc Natl Acad Sci U S A* **113:** E4467-E4475.

Katinka, M. D., Duprat, S., Cornillot, E., Metenier, G., Thomarat, F., Prensier, G. *et al.* (2001) Genome sequence and gene compaction of the eukaryote parasite *Encephalitozoon cuniculi*. *Nature* **414:** 450-453.

Kitada, S., Uchiyama, T., Funatsu, T., Kitada, Y., Ogishima, T., and Ito, A. (2007) A protein from a parasitic microorganism, *Rickettsia prowazekii*, can cleave the signal sequences of proteins targeting mitochondria. *J Bacteriol* **189:** 844-850.

Kozjak, V., Wiedemann, N., Milenkovic, D., Lohaus, C., Meyer, H. E., Guiard, B. *et al.* (2003) An essential role of Sam50 in the protein sorting and assembly machinery of the mitochondrial outer membrane. *J Biol Chem* **278:** 48520-48523.

Kuhn, A., Stuart, R., Henry, R., and Dalbey, R. E. (2003) The Alb3/Oxa1/YidC protein family: membrane-localized chaperones facilitating membrane protein insertion? *Trends Cell Biol* **13:** 510-516.

Lang, B. F., Burger, G., O'Kelly, C. J., Cedergren, R., Golding, G. B., Lemieux, C. *et al.* (1997) An ancestral mitochondrial DNA resembling a eubacterial genome in miniature. *Nature* **387:** 493-497.

Lee, J., Kim, D. H., and Hwang, I. (2014) Specific targeting of proteins to outer envelope membranes of endosymbiotic organelles, chloroplasts, and mitochondria. *Front Plant Sci* **5:** 173.

Leger, M. M., Kolisko, M., Kamikawa, R., Stairs, C. W., Kume, K., Cepicka, I. *et al.* (2017) Organelles that illuminate the origins of *Trichomonas* hydrogenosomes and *Giardia* mitosomes. *Nat Ecol Evol* **1:** 0092.

Lill, R. and Muhlenhoff, U. (2006) Iron-sulfur protein biogenesis in eukaryotes: components and mechanisms. *Annu Rev Cell Dev Biol* **22:** 457-486.

Lindmark, D. G. and Muller, M. (1973) Hydrogenosome, a cytoplasmic organelle of the anaerobic flagellate *Tritrichomonas foetus*, and its role in pyruvate metabolism. *J Biol Chem* **248:** 7724-7728.

Liu, S., Roellig, D. M., Guo, Y., Li, N., Frace, M. A., Tang, K. *et al.* (2016) Evolution of mitosome metabolism and invasion-related proteins in *Cryptosporidium*. *BMC Genomics* **17:** 1006.

Loftus, B., Anderson, I., Davies, R., Alsmark, U. C., Samuelson, J., Amedeo, P. *et al.* (2005) The genome of the protist parasite *Entamoeba histolytica*. *Nature* **433:** 865-868.

Lucattini, R., Likic, V. A., and Lithgow, T. (2004) Bacterial proteins predisposed for targeting to mitochondria. *Mol Biol Evol* **21:** 652-658.

Makiuchi, T., Mi-ichi, F., Nakada-Tsukui, K., and Nozaki, T. (2013) Novel TPR-containing subunit of TOM complex functions as cytosolic receptor for *Entamoeba* mitosomal transport. *Sci Rep* **3:** 1129.

Mani, J., Desy, S., Niemann, M., Chanfon, A., Oeljeklaus, S., Pusnik, M. *et al.* (2015) Mitochondrial protein import receptors in Kinetoplastids reveal convergent evolution over large phylogenetic distances. *Nat Commun* **6:** 6646.

Mani, J., Meisinger, C., and Schneider, A. (2016) Peeping at TOMs-Diverse Entry Gates to Mitochondria Provide Insights into the Evolution of Eukaryotes. *Mol Biol Evol* **33:** 337-351.

Martin, J. (1997) Molecular chaperones and mitochondrial protein folding. *J Bioenerg Biomembr* **29:** 35-43.

Martincova, E., Voleman, L., Pyrih, J., Zarsky, V., Vondrackova, P., Kolisko, M. *et al.* (2015) Probing the biology of *Giardia intestinalis* mitosomes using in vivo enzymatic tagging. *Molecular and Cellular Biology* **35:** 2864-2874.

Mi-ichi, F., Abu Yousuf, M., Nakada-Tsukui, K., and Nozaki, T. (2009) Mitosomes in *Entamoeba histolytica* contain a sulfate activation pathway. *Proceedings of the National Academy of Sciences of the United States of America* **106:** 21731-21736.

Mi-ichi, F., Miyamoto, T., Takao, S., Jeelani, G., Hashimoto, T., Hara, H. *et al.* (2015) *Entamoeba* mitosomes play an important role in encystation by association with cholesteryl sulfate synthesis. *Proc Natl Acad Sci U S A* **112:** E2884-E2890.

Mikhailov, K. V., Simdyanov, T. G., and Aleoshin, V. V. (2017) Genomic Survey of a Hyperparasitic Microsporidian *Amphiamblys sp*. (Metchnikovellidae). *Genome Biol Evol* **9:** 454-467.

Mogi, T. and Kita, K. (2010) Diversity in mitochondrial metabolic pathways in parasitic protists *Plasmodium* and *Cryptosporidium*. *Parasitol Int* **59:** 305-312.

Mokranjac, D. and Neupert, W. (2010) The many faces of the mitochondrial TIM23 complex. *Biochim Biophys Acta* **1797:** 1045-1054.

Mokranjac, D., Paschen, S. A., Kozany, C., Prokisch, H., Hoppins, S. C., Nargang, F. E. *et al.* (2003) Tim50, a novel component of the TIM23 preprotein translocase of mitochondria. *EMBO J* **22:** 816-825.

Muller, J. M., Milenkovic, D., Guiard, B., Pfanner, N., and Chacinska, A. (2008) Precursor oxidation by Mia40 and Erv1 promotes vectorial transport of proteins into the mitochondrial intermembrane space. *Mol Biol Cell* **19:** 226-236.

Palmer, T., Sargent, F., and Berks, B. C. (2010) The Tat Protein Export Pathway. *EcoSal Plus* **4**.

Paschen, S. A., Waizenegger, T., Stan, T., Preuss, M., Cyrklaff, M., Hell, K. *et al.* (2003) Evolutionary conservation of biogenesis of beta-barrel membrane proteins. *Nature* **426:** 862-866.

Pett, W. and Lavrov, D. V. (2013) The twin-arginine subunit C in Oscarella: origin, evolution, and potential functional significance. *Integr Comp Biol* **53:** 495-502.

Pusnik, M., Mani, J., Schmidt, O., Niemann, M., Oeljeklaus, S., Schnarwiler, F. *et al.* (2012) An essential novel component of the noncanonical mitochondrial outer membrane protein import system of trypanosomatids. *Mol Biol Cell* **23:** 3420-3428.

Pusnik, M., Schmidt, O., Perry, A. J., Oeljeklaus, S., Niemann, M., Warscheid, B. *et al.* (2011) Mitochondrial preprotein translocase of trypanosomatids has a bacterial origin. *Curr Biol* **21:** 1738-1743.

Rassow, J., Dekker, P. J., van, W. S., Meijer, M., and Soll, J. (1999) The preprotein translocase of the mitochondrial inner membrane: function and evolution. *J Mol Biol* **286:** 105-120.

Rassow, J., Maarse, A. C., Krainer, E., Kubrich, M., Muller, H., Meijer, M. *et al.* (1994) Mitochondrial protein import: biochemical and genetic evidence for interaction of matrix hsp70 and the inner membrane protein MIM44. *J Cell Biol* **127:** 1547-1556.

Riordan, C. E., Ault, J. G., Langreth, S. G., and Keithly, J. S. (2003) *Cryptosporidium parvum* Cpn60 targets a relict organelle. *Curr Genet* **44:** 138-147.

Rout, S., Zumthor, J. P., Schraner, E. M., Faso, C., and Hehl, A. B. (2016) An Interactome-Centered Protein Discovery Approach Reveals Novel Components Involved in Mitosome Function and Homeostasis in *Giardia lamblia*. *PLoS Pathog* **12:** e1006036.

Ryan, K. R., Leung, R. S., and Jensen, R. E. (1998) Characterization of the mitochondrial inner membrane translocase complex: the Tim23p hydrophobic domain interacts with Tim17p but not with other Tim23p molecules. *Mol Cell Biol* **18:** 178-187.

Santos, H. J., Imai, K., Hanadate, Y., Fukasawa, Y., Oda, T., Mi-ichi, F. *et al.* (2016) Screening and discovery of lineage-specific mitosomal membrane proteins in *Entamoeba histolytica*. *Mol Biochem Parasitol* **209:** 10-17.

Schneider, A., Bursac, D., and Lithgow, T. (2008) The direct route: a simplified pathway for protein import into the mitochondrion of trypanosomes. *Trends Cell Biol* **18:** 12-18.

Sharma, S., Singha, U. K., and Chaudhuri, M. (2010) Role of Tob55 on mitochondrial protein biogenesis in *Trypanosoma brucei*. *Mol Biochem Parasitol* **174:** 89-100.

Singha, U. K., Hamilton, V., Duncan, M. R., Weems, E., Tripathi, M. K., and Chaudhuri, M. (2012) Protein translocase of mitochondrial inner membrane in *Trypanosoma brucei*. *J Biol Chem* **287:** 14480-14493.

Singha, U. K., Peprah, E., Williams, S., Walker, R., Saha, L., and Chaudhuri, M. (2008) Characterization of the mitochondrial inner membrane protein translocator Tim17 from *Trypanosoma brucei*. *Mol Biochem Parasitol* **159:** 30-43.

Sirrenberg, C., Bauer, M. F., Guiard, B., Neupert, W., and Brunner, M. (1996) Import of carrier proteins into the mitochondrial inner membrane mediated by Tim22. *Nature* **384:** 582-585.

Slapeta, J. and Keithly, J. S. (2004) Cryptosporidium parvum mitochondrial-type HSP70 targets homologous and heterologous mitochondria. *Eukaryot Cell* **3:** 483-494.

Smid, O., Matuskova, A., Harris, S. R., Kucera, T., Novotny, M., Horvathova, L. *et al.* (2008) Reductive evolution of the Mitochondrial Processing Peptidases of the unicellular parasites *Trichomonas vaginalis* and *Giardia intestinalis*. *Plos Pathogens* **4**.

Strong, W. B. and Nelson, R. G. (2000) Preliminary profile of the *Cryptosporidium parvum* genome: an expressed sequence tag and genome survey sequence analysis. *Mol Biochem Parasitol* **107:** 1-32.

Timms, M. W., van Deursen, F. J., Hendriks, E. F., and Matthews, K. R. (2002) Mitochondrial development during life cycle differentiation of African trypanosomes: evidence for a kinetoplast-dependent differentiation control point. *Mol Biol Cell* **13:** 3747-3759.

Tong, J., Dolezal, P., Selkrig, J., Crawford, S., Simpson, A. G., Noinaj, N. *et al.* (2011) Ancestral and derived protein import pathways in the mitochondrion of *Reclinomonas americana*. *Mol Biol Evol* **28:** 1581-1591.

Tovar, J., Fischer, A., and Clark, C. G. (1999) The mitosome, a novel organelle related to mitochondria in the amitochondrial parasite *Entamoeba histolytica*. *Mol Microbiol* **32:** 1013-1021.

Tovar, J., Leon-Avila, G., Sanchez, L. B., Sutak, R., Tachezy, J., van der Giezen, M. *et al.* (2003) Mitochondrial remnant organelles of *Giardia* function in iron-sulphur protein maturation. *Nature* **426:** 172-176.

Tsaousis, A. D., Kunji, E. R., Goldberg, A. V., Lucocq, J. M., Hirt, R. P., and Embley, T. M. (2008) A novel route for ATP acquisition by the remnant mitochondria of *Encephalitozoon cuniculi*. *Nature* **453:** 553-556.

Turakhiya, U., von der, M. K., Gold, V. A., Guiard, B., Chacinska, A., van der Laan, M. *et al.* (2016) Protein Import by the Mitochondrial Presequence Translocase in the Absence of a Membrane Potential. *J Mol Biol* **428:** 1041-1052.

van der Giezen, M. and Tovar, J. (2005) Degenerate mitochondria. *EMBO Rep* **6:** 525-530.

Vavra, J., Hylis, M., Fiala, I., and Nebesarova, J. (2016) *Globulispora mitoportans* n. g., n. sp., (Opisthosporidia: Microsporidia) a microsporidian parasite of daphnids with unusual spore organization and prominent mitosome-like vesicles. *J Invertebr Pathol* **135:** 43-52.

Veenendaal, A. K., van der Does, C., and Driessen, A. J. (2004) The protein-conducting channel SecYEG. *Biochim Biophys Acta* **1694:** 81-95.

von Heijne, H. G. (1986) Mitochondrial targeting sequences may form amphiphilic helices. *EMBO J* **5:** 1335-1342.

Waller, R. F., Jabbour, C., Chan, N. C., Celik, N., Likic, V. A., Mulhern, T. D. *et al.* (2009) Evidence of a reduced and modified mitochondrial protein import apparatus in microsporidian mitosomes. *Eukaryot Cell* **8:** 19-26.

Wiedemann, N. and Pfanner, N. (2017) Mitochondrial Machineries for Protein Import and Assembly. *Annu Rev Biochem* **86:** 685-714.

Williams, B. A., Hirt, R. P., Lucocq, J. M., and Embley, T. M. (2002) A mitochondrial remnant in the microsporidian *Trachipleistophora hominis*. *Nature* **418:** 865-869.

Yang, J., Harding, T., Kamikawa, R., Simpson, A. G. B., and Roger, A. J. (2017) Mitochondrial Genome Evolution and a Novel RNA Editing System in Deep-Branching Heteroloboseids. *Genome Biol Evol* **9:** 1161-1174.

Yarlett, N., Hann, A. C., Lloyd, D., and Williams, A. (1981) Hydrogenosomes in the rumen protozoon *Dasytricha ruminantium* Schuberg. *Biochem J* **200:** 365-372.

Yarlett, N., Orpin, C. G., Munn, E. A., Yarlett, N. C., and Greenwood, C. A. (1986) Hydrogenosomes in the rumen fungus *Neocallimastix patriciarum*. *Biochem J* **236:** 729-739.

Yen, M. R., Tseng, Y. H., Nguyen, E. H., Wu, L. F., and Saier, M. H., Jr. (2002) Sequence and phylogenetic analyses of the twin-arginine targeting (Tat) protein export system. *Arch Microbiol* **177:** 441-450.

Zarsky, V. and Dolezal, P. (2016) Evolution of the Tim17 protein family. *Biol Direct* **11:** 54.

Zarsky, V., Tachezy, J., and Dolezal, P. (2012) Tom40 is likely common to all mitochondria. *Current Biology* **22:** R479-R481.

EC
Journals.ASM.org

Giardia intestinalis Incorporates Heme into Cytosolic Cytochrome b_5

Jan Pyrih,[a] Karel Harant,[b] Eva Martincová,[a] Robert Sutak,[a] Emmanuel Lesuisse,[c] Ivan Hrdý,[a] Jan Tachezy[a]

Department of Parasitology, Faculty of Science, Charles University in Prague, Prague, Czech Republic[a]; Department of Genetics and Microbiology, Faculty of Science, Charles University in Prague, Prague, Czech Republic[b]; Laboratoire Mitochondries, Métaux et Stress Oxydant, Institut Jacques Monod, UMR 7592 CNRS-Université Paris-Diderot, Paris, France[c]

The anaerobic intestinal pathogen *Giardia intestinalis* does not possess enzymes for heme synthesis, and it also lacks the typical set of hemoproteins that are involved in mitochondrial respiration and cellular oxygen stress management. Nevertheless, *G. intestinalis* may require heme for the function of particular hemoproteins, such as cytochrome b_5 (cytb_5). We have analyzed the sequences of eukaryotic cytb_5 proteins and identified three distinct cytb_5 groups: group I, which consists of C-tail membrane-anchored cytb_5 proteins; group II, which includes soluble cytb_5 proteins; and group III, which comprises the fungal cytb_5 proteins. The majority of eukaryotes possess both group I and II cytb_5 proteins, whereas three *Giardia* paralogs belong to group II. We have identified a fourth *Giardia* cytb_5 paralog (gCYTb5-IV) that is rather divergent and possesses an unusual 134-residue N-terminal extension. Recombinant *Giardia* cytb_5 proteins, including gCYTb5-IV, were expressed in *Escherichia coli* and exhibited characteristic UV-visible spectra that corresponded to heme-loaded cytb_5 proteins. The expression of the recombinant gCYTb5-IV in *G. intestinalis* resulted in the increased import of extracellular heme and its incorporation into the protein, whereas this effect was not observed when gCYTb5-IV containing a mutated heme-binding site was expressed. The electrons for *Giardia* cytb_5 proteins may be provided by the NADPH-dependent Tah18-like oxidoreductase GiOR-1. Therefore, GiOR-1 and cytb_5 may constitute a novel redox system in *G. intestinalis*. To our knowledge, *G. intestinalis* is the first anaerobic eukaryote in which the presence of heme has been directly demonstrated.

Heme, an iron-coordinating porphyrin, serves as a prosthetic group for hemoproteins that are involved in a number of vital functions, such as carrying diatomic gases, participating in electron transport in the mitochondrial respiratory chain, and providing defense against oxidative and nitrosative stress (1, 2). To fulfill their heme requirements, a vast majority of organisms possess a heme biosynthetic pathway that converts δ-aminolevulinic acid to heme in seven consecutive steps, which are conserved in all domains of life. Eukaryotes partially inherited this pathway from the bacterial predecessor of mitochondria and partially retained the original preeukaryotic system (3). The loss of the pathway in some organisms is typically associated with the evolution of a mechanism to acquire heme from exogenous sources, such as feeding on bacteria by *Caenorhabditis elegans* or free-living bodonids (4, 5) or parasitic lifestyles for blood-sucking ticks and trypanosomes (4, 6). An additional group of organisms devoid of heme synthesis is parasitic protists that are adapted for life in anaerobic or oxygen-poor environments. These organisms include intestinal parasites, such as *Giardia*, *Entamoeba*, *Cryptosporidium*, and *Blastocystis*, and urogenital tract parasites, such as *Trichomonas*. They all possess highly reduced forms of mitochondria, such as mitosomes or hydrogenosomes, that have lost the majority of their mitochondrial functions, including heme-dependent respiratory complexes (7, 8). In addition, common hemoproteins (oxidases, catalases, and hydrolases) that are involved in oxidative-stress management in aerobes are replaced by different protective enzymes that were likely acquired by the anaerobic protists through lateral gene transfer from anaerobic bacteria. These enzymes include flavodiiron protein, hydroperoxide reductase, rubrerythrin, and NADH oxidase (9–11). The anaerobic protists were previously hypothesized to live entirely without heme (12), which may be true for *Entamoeba histolytica*, because no gene encoding any hemoprotein has been identified in the *Entamoeba* genome. However, genome analyses of all other anaerobic parasites have revealed that they retain several genes encoding hemoproteins, which are most frequently members of the cytochrome b_5 (cytb_5) family (13).

The archetypal cytb_5 is a small acidic membrane protein consisting of two domains, an amino-terminal hydrophilic heme-binding domain and a carboxy-terminal domain consisting of hydrophobic residues (transmembrane segment) that is followed by positively charged residues at the carboxy terminus. The carboxy-terminal domain, which is a C-tail anchor, facilitates post-translational targeting and integration of cytb_5 into the membranes of various organelles, such as the endoplasmic reticulum and the outer membrane of mitochondria. The charged C terminus is typically present in the organellar matrix or intermembrane space of mitochondria, whereas the heme-binding domain faces the cytosol. The heme is inserted into the hydrophobic pocket of the N-terminal cytb_5 domain, which contains two invariable histidines, H44 and H68 (numbered according to the human cytb_5 [accession number P00167]), that coordinate the heme iron (14). H44 lies within the highly conserved HPGG motif, which is surrounded by several acidic residues. These residues have been implicated in the redox potential of cytb_5 (15). cytb_5 is a multifunctional protein that acts as an electron carrier in several oxidative reactions between reductases, such as NADH-cytochrome b_5 reductase and NADPH-cytochrome P450 reductase, and various

Received 29 August 2013 **Accepted** 22 November 2013
Published ahead of print 2 December 2013
Address correspondence to Jan Tachezy, tachezy@natur.cuni.cz.
Supplemental material for this article may be found at http://dx.doi.org/10.1128/EC.00200-13.

doi:10.1128/EC.00200-13

oxidases and fatty acid desaturases that are involved in lipid and cholesterol biosynthesis (16, 17). Additionally, cytb_5 is a component of various fusion enzymes (18, 19). However, the function of cytb_5 in anaerobic protists and its possible partners for electron transfer are unknown.

Giardia intestinalis, one of the most important intestinal pathogens, possesses two types of heme-binding proteins, a flavohemoglobin (gFLHb) (20) and cytb_5 (15). Recombinant gFLHb binds heme and flavin and exhibits NADH and NADPH oxidase activity. This activity is stimulated *in vitro* by the addition of the nitric oxide donor diethylammonium (Z)-1-(*N*,*N*-diethylamino) diazen-1-ium-1,2-diolate (diethylamine NONOate), which suggests that gFLHb may play a role in protecting *Giardia* against oxygen and nitric oxide (20). cytb_5 is encoded in *Giardia* by three paralogous genes, *gCYTb5-I*, *gCYTb5-II*, and *gCYTb5-III*. Recombinant gCYTb5-I that was expressed in *Escherichia coli* exhibited spectroscopic and electrochemical properties of heme-loaded cytb_5. Interestingly, the conserved heme-binding domains of all three gCYTb5 proteins are flanked by unconventional, highly charged N- and C-terminal sequences. Although these sequences are decisive for protein targeting to subcellular compartments, the localization of gCYTb5 in *Giardia* remains unclear. The ability of recombinant gCYTb5-I and gFLHb to bind heme in *E. coli* strongly suggests that functional heme-binding proteins may also exist in *Giardia*. However, direct evidence for the incorporation of heme into target proteins in an anaerobic protist has not yet been demonstrated.

Here, we investigated the cytb_5 proteins in *G. intestinalis* to determine (i) whether the unusual structure of gCYTb5 proteins is unique to *Giardia* or whether these proteins represent a distinct branch of the cytb_5 family of proteins, (ii) the cellular localization of these cytb_5 proteins, (iii) whether the parasite can incorporate exogenous heme into hemoproteins *in situ*, and (iv) whether *Giardia* possesses suitable redox partners that can reduce the cytb_5 proteins. We found that, in addition to the known gCYTb5 proteins, *Giardia* possesses an additional cytb_5-like protein that contains a long C-terminal extension (gCYTb5-IV) and a heme-binding domain. We demonstrate that this protein efficiently binds heme when *Giardia* cells are cultured in the presence of hemin and that functional gCYTb5-IV can be reduced by electrons that are provided by the recently identified diflavin oxidoreductase GiOR-1 (7). All *Giardia* cytb_5 paralogs appear to belong to a novel group of soluble cytosolic cytb_5 proteins that are ubiquitous in eukaryotes.

MATERIALS AND METHODS

Cell cultivation:. *G. intestinalis* cells (strain WB; ATCC 30975) were grown in TYI-S-33 medium supplemented with 10% heat-inactivated bovine serum (PAA Laboratories GmbH, Austria) and 0.1% bovine bile (Sigma) (21). For the determination of the heme content of *G. intestinalis*, the cells were cultured in TYI-S-33 medium supplemented with 4 μM hemin (Fluka).

Selectable transformation of *G. intestinalis*. The genes encoding the *Giardia* cytb_5 proteins (GiardiaDB accession numbers GL50803_9089, GL50803_27747, GL50803_33870, and GL50803_2972) were amplified using PCR and inserted into the plasmid pTG3039 (a kind gift from Frances D. Gillin, San Diego, CA) (22), which was modified for the expression of proteins that contain N-terminal hemagglutinin (HA) tags. The cells were transformed and selected as previously described (23).

Immunofluorescence microscopy. *G. intestinalis* cells were fixed with 1% formaldehyde as previously described (24) and stained for immunofluorescence microscopy using a rat monoclonal anti-HA antibody (Roche), a rabbit polyclonal TOM40 antibody (25), and an anti-PDI-2 (protein disulfide isomerase 2) antibody (a kind gift from Adrian B. Hehl) (26). Alexa Fluor 488 (green) donkey anti-mouse and anti-rabbit antibodies and Alexa Fluor 594 (red) donkey anti-rat antibody (all from Invitrogen) were used as the secondary antibodies. The slides were examined using an Olympus IX81 microscope equipped with an MT20 illumination system. The images were processed using ImageJ 1.41e software (NIH).

Preparation of subcellular fractions and immunoblot analysis. *Giardia* trophozoites were harvested, washed twice in phosphate-buffered saline (PBS), pH 7.4, and resuspended in SM buffer (250 mM sucrose and 20 mM MOPS [morpholinepropanesulfonic acid], pH 7.2) containing protease inhibitors (Complete EDTA-free Protease Inhibitor Cocktail; Roche). The cells were disrupted by sonication using approximately 15 1-s pulses at an amplitude of 40 (Bioblock Scientific Vibra-Cell 72405) and centrifuged twice at 1,000 × *g* for 10 min each time to remove any undisrupted cells. The supernatant was centrifuged at 50,000 × *g* for 30 min to obtain the organellar fraction (sediment). The high-speed supernatant that was obtained after an additional centrifugation at 200,000 × *g* for 30 min was used as the cytosolic fraction.

The cell fractionation samples were separated by SDS-13.5% PAGE and transferred to a nitrocellulose membrane. The HA-tagged proteins were detected using a rat monoclonal anti-HA antibody (Roche). Enolase, which is a cytosolic marker protein, was detected using a rabbit polyclonal antibody against *Trypanosoma brucei* enolase (a kind gift from Julius Lukes, Ceske Budejovice, Czech Republic) (27).

Protein expression and purification. The genes encoding gCYTb5-I to -IV and the mutant gCYTb5-IVH_{178}L, in which histidine 178 was replaced with leucine, were inserted into the pET42b (Qiagen) vector for the expression of the recombinant proteins containing a C-terminal hexahistidine tag in *E. coli*. Protein purification was performed under native conditions using Ni-nitrilotriacetic acid affinity chromatography according to the manufacturer's instructions (Qiagen GmbH, Hilden, Germany). The PCR fragment corresponding to gCYTb5-IVH_{178}L was amplified using two-step PCR and primers described in Table S1 in the supplemental material.

Determination of the heme content of *G. intestinalis*. The heme content of *G. intestinalis* was determined in wild-type (wt) cells and cells expressing gCYTb5-IV and gCYTb5-IVH_{178}L. The cells were cultured for 72 h in medium in the presence or absence of 4 μM hemin. Subsequently, approximately 4 × 10^8 cells were harvested and washed twice with sterile cold PBS. The high-speed cellular fraction (cytosol) was obtained as previously described and concentrated using Amicon Ultra Centrifugal Filters with Ultracel 30-kDa membrane filters (Millipore) to a final protein concentration of approximately 25 μg/μl. Heme extraction was performed as described previously (28). Briefly, 200 μl of 1% HCl in acetone was added to 50 μl of each sample, rigorously mixed, and centrifuged at 4,000 × *g* for 10 min at room temperature. The supernatant was collected, and the sediment was reextracted in 30 μl of HCl-acetone. The concentrations of heme were immediately determined by high-performance liquid chromatography (HPLC) (UltiMate 3000 RSLC; Dionex; DAD diode array detector) using a C_{18} (Acclaim 120 C_{18}; 3 μm; 120 Å; 4.6 by 150 mm; Dionex) reverse-phase column and absorbance detection at 400 nm, as previously described (28, 29). The linear gradient from 60% to 40% (vol/vol) solvent A-solvent B to 100% solvent B was run for 11 min using solvents A (56 mM ammonium phosphate in 40% methanol) and B (methanol) at a flow rate of 1.2 ml/min. Then, 100% solvent B was maintained for another 6.5 min. The column was restored to the original conditions over 2 min and maintained under these conditions for another 6 min.

UV-visible spectroscopy. The UV-visible spectra of the freshly purified gCYTb5 proteins in 50 mM NaH_2PO_4 and 300 mM NaCl, pH 8.0, were recorded at room temperature between 260 and 700 nm using a Shimadzu UV-1601 spectrophotometer. The low-temperature visible

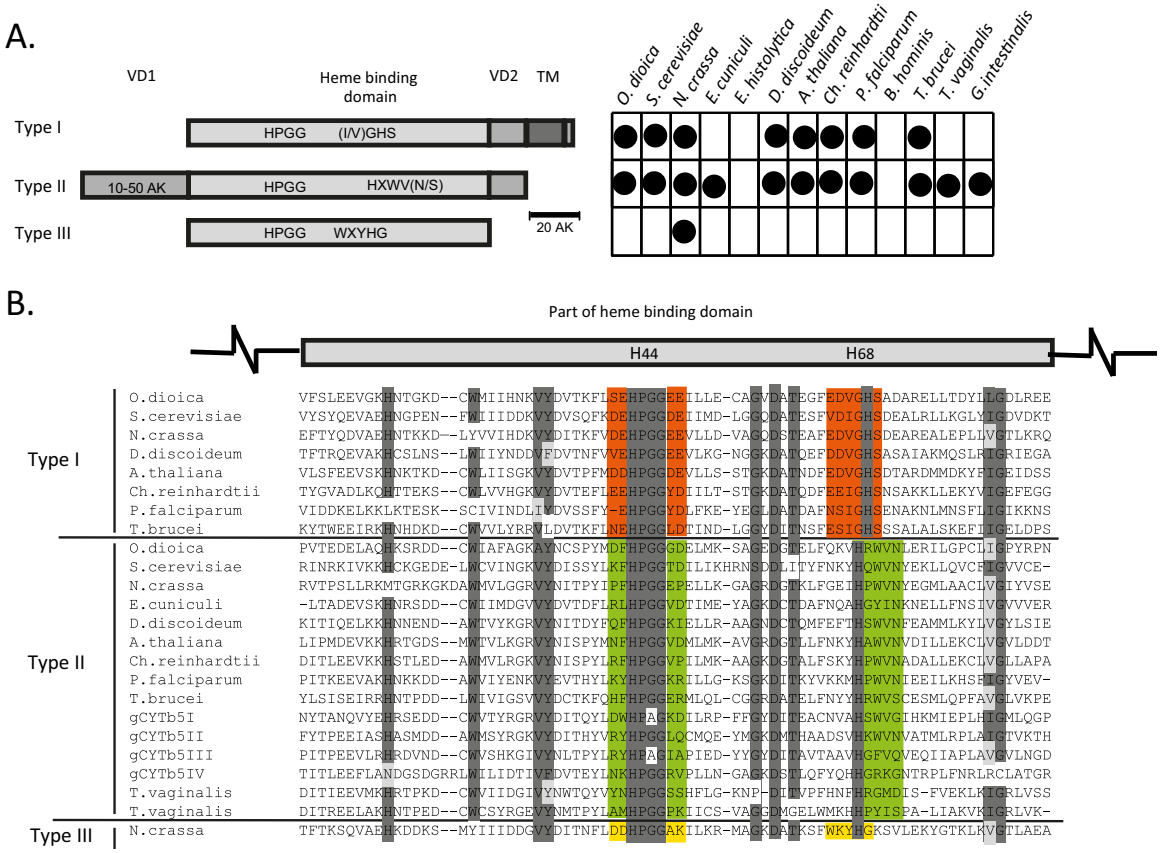

FIG 1 The three groups of cytb_5 proteins. (A) Schematic representation of the structural differences between the canonical group I cytb_5, group II soluble cytb_5, and fungal group III cytb_5 proteins. The chart indicates the distribution of cytochromes in representative eukaryotes. VD, variable domain; TM, transmembrane domain. *O. dioica*, *Oikopleura dioica*; *S. cerevisiae*, *Saccharomyces cerevisiae*; *N. crassa*, *Neurospora crassa*; *E. cuniculi*, *Encephalitozoon cuniculi*; *D. discoideum*, *Dictyostelium discoideum*; *A. thaliana*, *Arabidopsis thaliana*; *Ch. reinhardtii*, *Chlamydomonas reinhardtii*; *P. falciparum*, *Plasmodium falciparum*. (B) Alignment of partial heme-binding domains. The two histidine residues that are critical for heme iron coordination are highlighted in the schematic above the alignment. Highly conserved regions are shaded in dark gray, and similar amino acids in conserved regions are shaded in light gray. Red, green, and yellow highlight typical motifs for each type of cytb_5.

spectrum of whole cells was measured as previously described (30) using a Varian Cary 4000 spectrophotometer.

GiOR-1-dependent reduction of the gCYTb5 proteins. Recombinant GiOR-1 was prepared as previously described (7). The cytochrome reductase activity of GiOR-1 was spectrophotometrically assayed at 550 nm. The reaction mixture consisted of the gCYTb5 protein, GiOR-1, and NADPH (0.25 mM) in phosphate buffer (100 mM KH_2PO_4-KOH and 150 mM NaCl, pH 7.4). The reaction proceeded in anaerobic cuvettes under a nitrogen atmosphere at 25°C. The spectra were recorded using a Shimadzu UV-1601 spectrophotometer. The protein concentration was determined according to the Bradford method.

Bioinformatics analysis. The cytb_5 protein sequences were retrieved using protein BLAST searches (31) against a nonredundant GenBank protein database. The sequences were aligned using the ClustalX program (32). Columns with more than 25% gaps were stripped out. The final alignment retained 102 taxa and 68 sites. Phylogenetic analysis was performed using the WAG model with PhyML 3.0 (33). Support values are shown next to the branches as the maximum-likelihood bootstrap support (WAG model; PhyML).

RESULTS

Cytochrome b_5-like proteins in *Giardia*. *Giardia* cytb_5 gCYTb5-I (GL50803_9089) was used for BLAST searches in the GiardiaDB database to identify paralogous genes. The searches identified two other cytb_5-encoding genes that were previously reported as gCYTb5-II (GL50803_27747) and gCYTb5-III (GL50803_33870). In addition, we identified two cytb_5-like proteins named gCYTb5-IV (GL50803_2972) and GiTax (GL50803_17116).

An alignment of the *Giardia* proteins with eukaryotic orthologs revealed that cytb_5 forms three groups based on the primary structure of the heme-binding domain (Fig. 1; see Fig. S1 in the supplemental material). This domain includes the N-terminal (H44) and C-terminal (H68) histidines, which are two heme iron ligands. In all of the cytb_5 proteins, H44 is highly conserved within the HPGG motif. Group I represents canonical cytb_5 proteins that possess a HPGG motif that is surrounded by acidic residues (E and D), and H68 is flanked by the small amino acids glycine and serine (GHS). The group I cytb_5 proteins typically contain a C-terminal hydrophobic tail sequence (30 to 40 residues) that allows cytb_5 to attach to the cytosolic face of the endoplasmic reticulum or mitochondria (34). The C-tail anchor is connected to the heme-binding domain by a short variable domain of approximately 15 to 20 residues. In the group II cytb_5 proteins, the HPGG motif is not surrounded by acidic residues, and H68 lies within the distinct HXWV(N/S) motif. These proteins lack a C-tail anchor; however, they possess an N-terminal variable extension of approximately 10

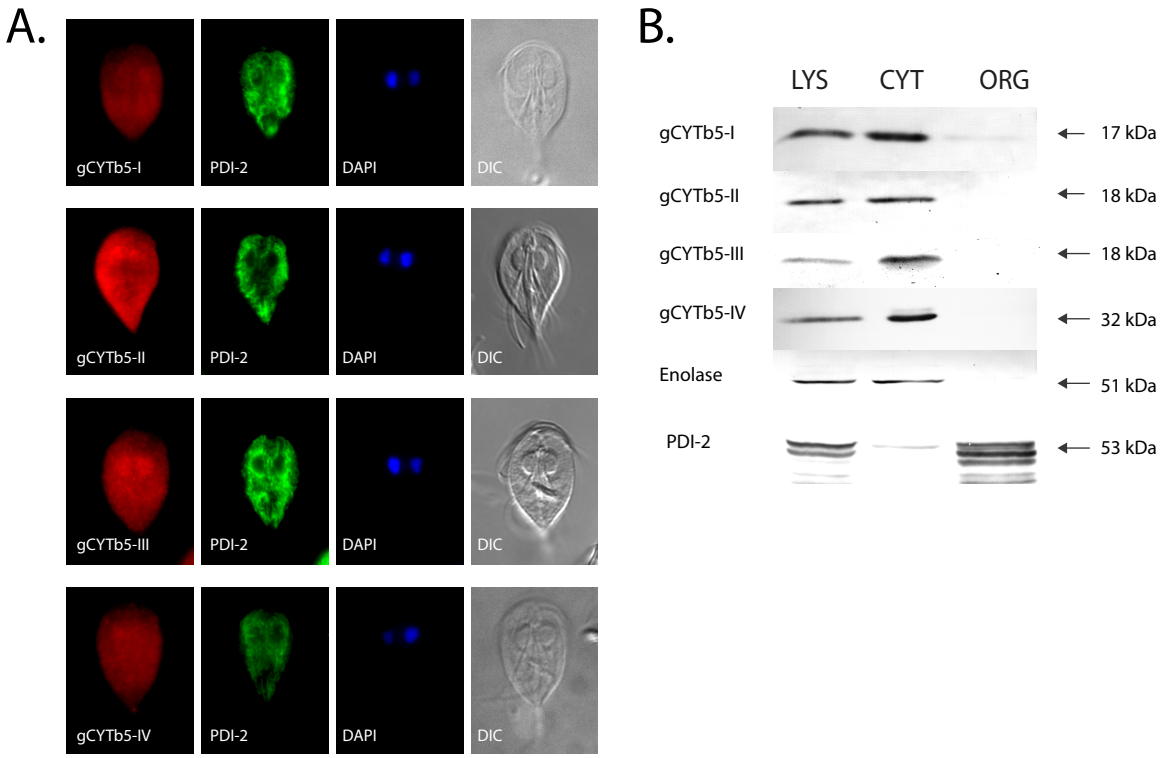

FIG 2 Localization of gCYTb5 proteins in *Giardia*. (A) The cytosolic localization of gCYTb5-I to -IV visualized using immunofluorescence microscopy. The gCYTb5 proteins were visualized using rat anti-HA tag and anti-rat Alexa Fluor 594 (red) antibodies. PDI-2 was detected using mouse anti-PDI-2 and anti-mouse Alexa Fluor 488 (green) antibodies. The nuclei were stained with DAPI (4′,6-diamidino-2-phenylindole) (blue). DIC, differential interference contrast. (B) Localization of gCYTb5 in subcellular fractions of *Giardia* using immunoblot analysis. LYS, cell lysate; CYT, cytoplasm; ORG, organellar fraction; Enolase, a cytosolic marker protein; PDI-2, an endoplasmic reticulum marker protein.

to 50 residues (Fig. 1). The group III cytb_5 proteins are short and lack both C- and N-terminal extensions. These proteins possess a unique conserved motif flanking H68 (WXYHG), and the HPGG motif is surrounded by acidic and basic residues at the N- and C-terminal sites, respectively (Fig. 1). The vast majority of eukaryotes appear to possess members of both group I and group II cytb_5 proteins, whereas group III cytb_5 proteins are present only in certain fungi (Fig. 1). Interestingly, *G. intestinalis* and *Trichomonas vaginalis* lack the canonical C-tail-anchored cytb_5, and cytb_5 proteins were not found in the parasitic protists *E. histolytica* and *Blastocystis hominis*.

The three *Giardia* cytochromes gCYTb5-I, -II, and -III exhibit characteristics of group II cytb_5 proteins, although gCYTb5-I and -III contain an alanine instead of a glycine at position 67. However, gCYTb5-IV appears to differ from the other *Giardia* cytb_5 proteins in several respects. Although gCYTb5-IV lacks acidic residues surrounding the HPGG motif, which is characteristic of group II cytb_5 proteins, two histidines are present at positions 67 and 68, and the protein lacks the conserved WV(N/S) residues. This double-histidine motif has been observed only in the cytb_5 of *T. vaginalis*. Additionally, gCYTb5-IV possesses a long N-terminal extension of 134 residues. However, an analysis of this extension using motif/domain search tools in the Pfam 27.0 and PROSITE 20.91 databases did not identify any known structure. Based on a phylogenetic reconstruction and according to the similarity of the key residues in proximity to both histidine binding motifs, gCYTb5-IV may represent a highly divergent member of group II cytb_5 proteins (Fig. 1; see Fig. S1 in the supplemental material). The cytb_5-like protein GiTax appears to be an ortholog of the *T. brucei* axonemal protein TAX-2, which is important for flagellar function (35). This protein represents a highly divergent cytb_5 protein that has lost both its conserved heme iron-coordinating histidine ligands. Therefore, we excluded the protein from further analysis.

Giardia gCYTb5 proteins are soluble cytosolic proteins. To determine the cellular localization of the *Giardia* cytb_5 proteins, all of the gCYTb5 genes were subcloned into expression vectors that were used for *G. intestinalis* transformation. To avoid any possible interference from the membrane-targeting signal that is located in the C-terminal portion of the membrane-associated cytb_5 (35, 36), we overexpressed these proteins in *Giardia* using a hemagglutinin tag located at the N terminus. Immunofluorescence microscopy of the HA-tagged gCYTb5-I to -IV revealed that all of the proteins are present in the cytosol, in addition to minor localization in the nuclei (Fig. 2A). All of the cells were additionally stained with the anti-PDI-2 antibody to confirm that the fluorescence of cytb_5 is distinct from that of the endoplasmic reticulum. The cytosolic localization of gCYTb5-I to -IV was confirmed by immunoblot analysis of the subcellular fractions (Fig. 2B) using enolase as a cytosolic marker protein. Because the PSORT II program (http://psort.hgc.jp/form2.html) identified a putative N-terminal cleavable mitochondrial targeting sequence in the gCYTb5-II and -III proteins, we additionally expressed these proteins with a C-terminal hemagglutinin tag in *G. intestinalis*. However, the two C-terminally tagged proteins demonstrated cytosolic

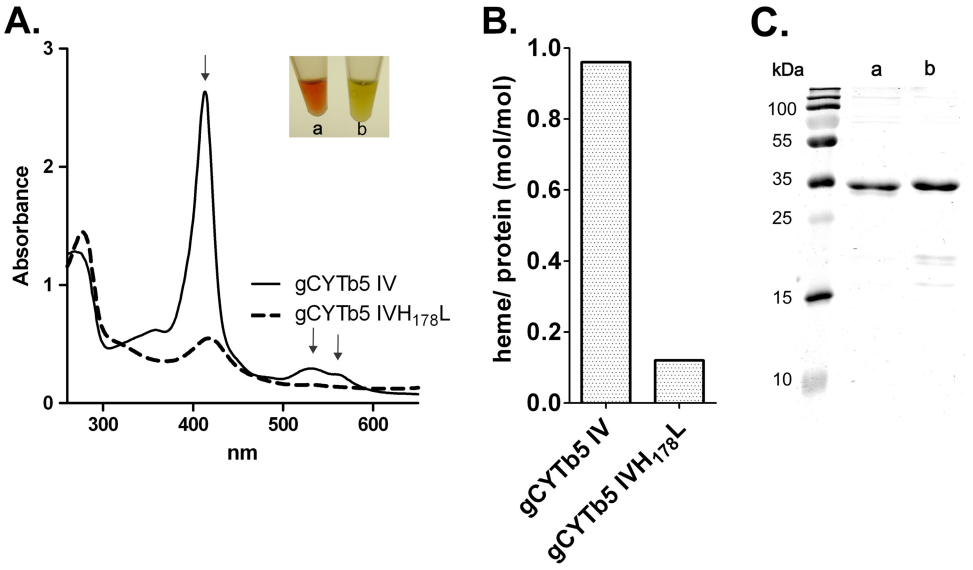

FIG 3 gCYTb5-IV coordinates heme. (A) UV-visible spectrum of recombinant gCYTb5-IV compared with that of the gCYTb5-IVH$_{178}$L mutant. The arrows indicate characteristic absorption maxima of oxidized gCYTb5-IV. The inset shows the colors of the purified proteins gCYTb5-IV (a) and gCYTb5-IVH$_{178}$L (b). The 280-nm peaks show that comparable amounts of proteins were used. (B) Determination of the heme contents in gCYTb5-IV and gCYTb5-IVH$_{178}$L using HPLC. (C) Purity of recombinant gCYTb5-IV (a) and gCYTb5-IVH$_{178}$L (b) tested by SDS-PAGE analysis using 13.5% gel. The proteins were stained with Coomassie brilliant blue.

localizations identical to those of the N-terminally tagged proteins (see Fig. S2 in the supplemental material). The cytosolic localization of the group II gCYTb5-I to -IV proteins is consistent with the absence of a C-tail hydrophobic anchor in these proteins.

Recombinant gCYTb5 proteins bind heme. The unorthodox structure of gCYTb5-IV, including the unusual motif surrounding H68, prompted us to determine whether gCYTb5-IV coordinates heme. As a positive control, we included gCYTb5-I, which was previously shown to bind heme, and we additionally characterized the paralogs gCYTb5-II and gCYTb5-III. All of the proteins were expressed with a C-terminal polyhistidine tag in *E. coli*, using the pET42b vector, and were isolated under native conditions. The presence of a heme cofactor was determined using UV-visible spectroscopy and HPLC analysis. All of the isolated proteins displayed the characteristic strong absorption at 413 nm and two absorption peaks at 529 and 563 nm. A typical spectrum for gCYTb5-IV is shown in Fig. 3A. Additionally, we expressed a mutant of gCYTb5-IV in which the histidine residue in the HPGG motif was replaced by leucine (gCYTb5-IVH$_{178}$L) (Fig. 3A). As expected, we observed a dramatic decrease (8-fold) in the heme-binding ability of the mutant (Fig. 3B; see Fig. S3 in the supplemental material).

gCYTb5 is reduced by the NADPH-dependent oxidoreductase GiOR-1. *G. intestinalis* does not contain genes encoding the typical cytb_5 partners, such as cytb_5 reductase or cytochrome P450 reductase, which deliver electrons for cytb_5 reduction (13). However, *G. intestinalis* does possess the oxidoreductase GiOR-1, which contains a flavodoxin-like flavin mononucleotide (FMN)-binding domain that is connected to a cytochrome P450 reductase-like domain, including a flavin adenine dinucleotide (FAD)-binding pocket and an NADP(H)-binding site (7). Therefore, we determined whether GiOR-1 is able to reduce the gCYTb5 proteins. Indeed, GiOR-1 reduced the *Giardia* cytochrome b_5 I, III, and IV proteins (gCYTb5-II was not evaluated) in the presence of NADPH, which was observed as a shift of the electronic absorption band from 413 to 426 nm and the appearance of sharp α and β bands at 559 and 529 nm. A representative spectrum of GiOR-1 reduction of gCYTb5 is shown for gCYTb5-IV in Fig. 4.

Heme is present in *G. intestinalis*. To provide direct evidence that *G. intestinalis* contains the heme cofactor, we initially attempted to detect the presence of heme in the cytosolic fraction that was isolated from wild-type cells grown in standard culture

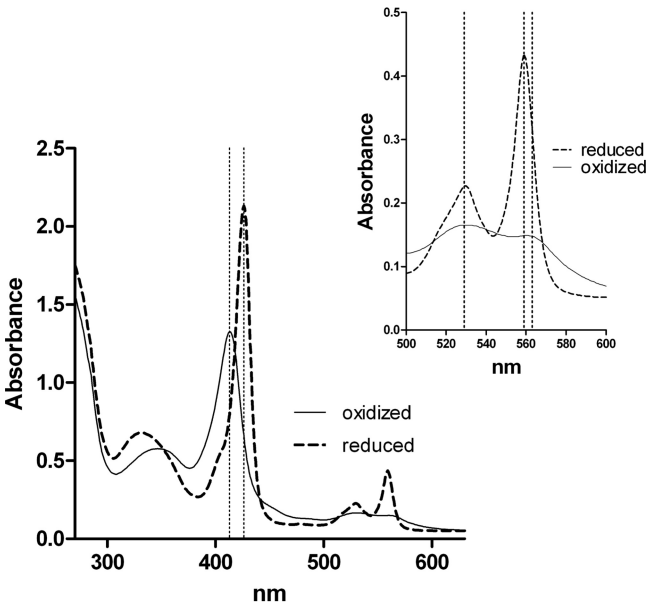

FIG 4 Reduction of gCYTb5-IV by GiOR-1. UV-visible spectra of reduced gCYTb5-IV (dashed lines) were recorded after incubation of oxidized gCYTb5-IV (solid lines) in the presence of NADPH and GiOR-1 for 10 min at 25°C in an anaerobic cuvette. The region between 500 and 600 nm is enlarged in the inset. The wavelengths 413, 426, 529, 559, and 563 nm are indicated by dotted lines.

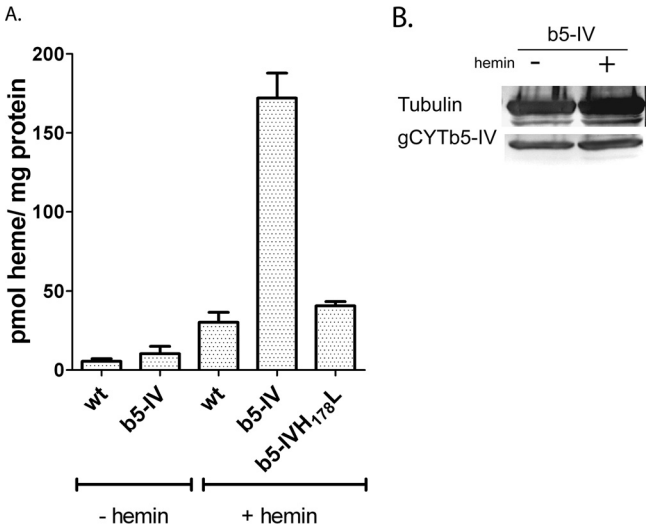

FIG 5 Detection of heme in *G. intestinalis*. (A) The concentration of heme was determined in *Giardia* cytosol using HPLC. The highest heme concentration was found in cells that expressed recombinant gCYTb5-IV (b5-IV) when the cells were cultured in TYI-S-33 medium supplemented with 4 μM hemin (+ hemin). The heme content was significantly lower in the strain harboring the gCYTb5-IVH_{178}L mutant. (B) Western blot analysis indicated comparable levels of recombinant gCYTb5-IV in the lysates of cells cultured in the presence and absence of hemin. An anti-tubulin antibody (TAT-1; Sigma-Aldrich) was used as a loading control. The error bars indicate standard deviations.

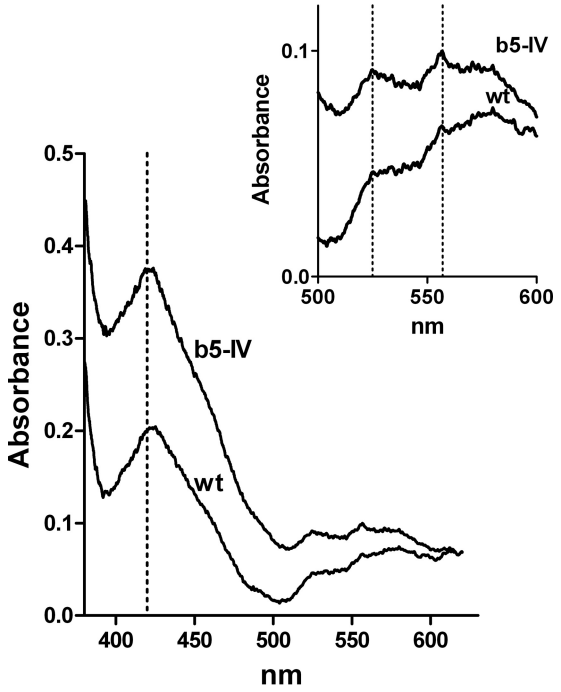

FIG 6 Detection of heme in *G. intestinalis*. A low-temperature visible spectrum of whole-cell lysates was obtained for wild-type cells (wt) and cells expressing the recombinant gCYTb5-IV (b5-IV). The region containing the characteristic absorption maxima for heme-loaded cytb_5 (420, 525, and 557 nm) is enlarged in the inset.

medium. Under these conditions, the amount of detected heme was at the detection limit of our HPLC system (approximately 1 pmol of heme per mg of protein), and we were unable to determine whether the low heme signal was intrinsic to the *Giardia* cells or was due to contamination from the complex culture medium, in which we detected heme at a concentration of 8 nM. Therefore, we compared the amount of endogenous heme in wild-type cells to that found in cells expressing recombinant gCYTb5-IV. The results indicated that the cells expressing gCYTb5-IV contained an approximately 2-fold-larger amount of heme than wild-type cells (Fig. 5A; see Fig. S4 in the supplemental material). Subsequently, we cultured *Giardia* in a medium that was supplemented with 4 μM hemin to increase the availability of heme in the cellular environment. The addition of hemin had no effect on cell growth (see Fig. S6 in the supplemental material), but the amount of heme in the wild-type cells increased to 32 pmol heme/mg protein, and a 6-fold-larger amount of heme was observed in the gCYTb5-IV-expressing cells. To determine whether the observed increase was specifically associated with heme incorporation into gCYTb5-IV, we also prepared a cell line that expressed a gCYTb5-IVH_{178}L mutant. As the expression of a gene with a negative mutation may be deleterious, we compared the growth of the wild-type strain and the strains expressing gCYTb5-IV and its mutated version. Only a subtle decrease in cell growth was observed in the gCYTb5-IVH_{178}L mutant (see Fig. S7 in the supplemental material). The amount of heme in this cell line was only slightly greater than that of the wild-type cells. We also determined whether the addition of exogenous heme affected the expression of recombinant gCYTb5-IV (Fig. 5B). Immunoblot analysis revealed comparable levels of gCYTb5-IV in the cytosol of cells that were grown in standard medium and in that of cells grown in medium containing hemin. Therefore, the observed changes in heme content within *Giardia* cells are related to the levels of heme incorporated into gCYTb5-IV, while the expression of the protein remained unaffected.

We further analyzed the presence of heme in *Giardia* cells using low-temperature spectroscopy. This complementary approach allows us to determine whether heme is incorporated by specific ligands. The analysis of homogenates of wild-type cells and gCYTb5-IV transformants that were cultured for 72 h in medium that contained hemin revealed a significantly higher Soret band at 420 nm in the transformed cells (Fig. 6). To determine whether the heme was bound to cytb_5, we determined the visible spectrum in the region between 500 and 600 nm, which is characteristic of distinct types of cytochromes (37, 38). The observed spectrum displayed maxima at 525 and 557 nm, which are typical for cytb_5 (Fig. 6) (39, 40). As a control, we determined the visible spectrum of *E. coli* cells expressing gCYTb5-IV, which exhibited characteristic absorption maxima identical to those observed for the *Giardia* cells (see Fig. S5 in the supplemental material). Altogether, these results demonstrate that *Giardia* cells are able to utilize an exogenous heme source and can incorporate heme into cytochrome b_5 proteins.

DISCUSSION

In this study, we demonstrated that the anaerobic protist *G. intestinalis*, despite lacking a heme synthesis pathway and the typical set of hemoproteins, is able to utilize extracellular heme and incorporate it into cytosolic group II cytb_5 proteins. To our knowledge, this is the first report that provides direct evidence for the presence of heme in an anaerobic eukaryote.

cytb_5 proteins form a large protein family with many biological

roles that appeared very early in evolution (16). They are known as typical C-tail-anchored proteins and are incorporated into organellar membranes. However, our analysis of *Giardia* CYTb5-I to -IV revealed the absence of the C-terminal transmembrane domain in these proteins. Surprisingly, searches for orthologs of *Giardia* cytb_5 proteins revealed that the vast majority of eukaryotes possess a soluble cytb_5 that does not contain the C-tail anchor (group II), in addition to the archetypal membrane-bound cytb_5 (group I). Moreover, fungi have evolved another cytb_5, which is most likely a soluble group III cytb_5. These three cytb_5 groups can be distinguished based on the characteristic vicinity of the highly conserved iron-coordinating histidines of the heme-binding pocket, and members of the groups form distinct branches in phylogenetic reconstructions. Interestingly, anaerobic protists, including *G. intestinalis*, exclusively possess members of the group II cytb_5 proteins. The lack of group I cytb_5 proteins in *Giardia* and other anaerobes suggests that these proteins preferentially provide electrons to oxygen-dependent acceptors, such as monooxygenases, that are not present in anaerobes. Importantly, the group II cytb_5 proteins are distinct from the well-known soluble cytb_5 proteins in erythrocytes that function in the reduction of methemoglobin (41). The erythrocyte cytb_5, which lacks a C-tail anchor, is a splice variant of a gene that additionally encodes a group I cytb_5 that is anchored in the membrane of the endoplasmic reticulum (42). An identical type of soluble cytb_5 is also involved in the activation of mammalian methionine synthase (43). However, despite the ubiquitous distribution of the group II cytb_5 proteins, the pathway in which these soluble cytb_5 proteins serve as electron transport proteins remains unknown.

In *G. intestinalis* and other anaerobic protists, electron transport is primarily dependent on ferredoxins that mediate single electron transfers. These FeS proteins are involved in energy metabolism that occurs in the *Giardia* cytosol and in the formation of FeS clusters in mitosomes. Recently, a novel *Giardia* oxidoreductase, GiOR-1, has been described (7). This enzyme efficiently transfers electrons from NADPH to artificial electron acceptors, such as dichlorophenolindophenol. However, it is unable to reduce [2Fe-2S] ferredoxin (7). The architecture of GiOR-1 corresponds to that of the multifunctional protein Tah18. Tah18 has been shown to form a complex with the FeS protein Dre2 and participates in the cytosolic assembly of FeS clusters (44). Under oxidative stress, Tah18 translocates to the mitochondria, where it interacts with cytochrome *c* and acts as a proapoptotic protein (45). In addition, yeast Tah18 is involved in NO synthesis (46). Human Tah18 (NR1) has been shown to act as a methionine synthase reductase that uses cytb_5 as a proximal electron donor for methionine synthase (43). Therefore, we determined whether GiOR-1 is able to reduce *Giardia* CYTb5 proteins. We found that CYTb5-I, -III, and -IV are efficiently reduced by GiOR-1 in the presence of NADPH as a source of reducing equivalents. However, the proximal partner of reduced CYTb5 remains unknown. Genes encoding Dre2 or methionine synthase have not been identified in the *G. intestinalis* genome thus far (47). Moreover, differences in the *Giardia* CYTb5 paralogs, particularly the presence of the unusual N-terminal extension of CYTb5-IV, suggest that they likely interact with different proximal partners. We further hypothesize that the function of the CYTb5 proteins may be related to the function of mitosomes, because GiOR-1 has been shown to be associated with these organelles (7). Moreover, *G. intestinalis* contains a paralogous gene encoding GiOR-2 that is associated with distinct vesicles, the characteristics of which remain to be clarified (7). Altogether, our results indicate that, in addition to ferredoxin-dependent electron transport, *G. intestinalis* contains a functional redox system that consists of an NADPH-dependent Tah18-like oxidoreductase and soluble group II CYTb5 proteins.

In anaerobic protists, there are several reasons for the absence of the heme synthesis pathway, which was likely lost during ancestral adaptations to anaerobic niches: (i) the organisms lost mitochondrial heme-dependent respiration and its high demand for heme, which was replaced by FeS protein-dependent energy metabolism; (ii) they replaced common hemoproteins that are involved in the defense against oxidative stress with heme-independent bacterial protective enzymes (9, 10); and (iii) two steps of the heme synthetic pathway that are catalyzed by the mitochondrial enzymes coproporphyrinogen III oxidase and protoporphyrinogen IX oxidase depend on molecular oxygen, which is not available in anaerobic niches (48, 49). Consequently, anaerobic protists retained a very limited set of hemoproteins, such as *G. intestinalis* cytb_5 and flavohemoglobin (15, 20). Not surprisingly, our results indicated a rather low level of heme in the cytosol of *G. intestinalis* when the parasite was grown in standard culture medium ($<$2.5 pmol per mg of protein) compared with 25 pmol heme/mg protein in macrophages (50). However, the amount of cytosolic heme increased upon the addition of hemin to the medium as an exogenous heme source. In particular, an increased level of heme was found in the strain expressing recombinant CYTb5-IV. This effect primarily reflects the incorporation of acquired heme into CYTb5-IV, because such an increase was not observed in the strain that expressed the mutant containing an impaired heme-binding site. The presence of heme-loaded CYTb5-IV in transformed *Giardia* was confirmed using low-temperature visible spectroscopy. These results indicated that *G. intestinalis* is able to compensate for the apparent lack of a heme synthesis pathway by utilizing an exogenous source of heme for its heme requirements. We cannot completely rule out the possibility that *Giardia* synthesizes heme via an undiscovered novel pathway, given that the functions of a large number of genes in the *Giardia* genome are unknown (46). Nevertheless, the heme-synthetic pathway is highly conserved in eukaryotes (13), and no alternative mechanisms for heme synthesis have been found in any organisms.

It is noteworthy that overexpression of CYTb5-IV caused the increase in cellular heme content. This observation suggests that import of heme in *Giardia* is a regulated process. We can speculate that overexpression of CYTb5-IV results in increased demand for cellular heme, which may provide a signal to increase the import of heme from the environment. Heme regulatory motifs were identified in a transcription factor in yeast (51), δ-aminolevulinate synthase (52), and several other diverse proteins (53). Moreover, iron regulates components of heme import machinery in enterocytes (54). Further studies are required to clarify whether heme transport is indeed a regulated process in *G. intestinalis* and to identify the molecular mechanism.

Parasites that lack genes for heme synthesis pathways but may require exogenous heme sources are not uncommon (13, 55). For example, bloodstream forms of trypanosomes satisfy their heme requirements via the uptake of hemoglobin (56). Intestinal parasites such as *G. intestinalis* may utilize dietary heme that is present in the small intestine (54). It is tempting to speculate that *G. intestinalis* may compete for heme with enterocytes that are able to take up intact

heme as a source of iron (54). However, the utilization of exogenous heme by parasitic protists has been experimentally assessed only in certain trypanosomatids (56–59). Moreover, the mechanisms for heme acquisition and its transport in trypanosomatids are poorly understood and are virtually unknown in other parasitic protists. In *Trypanosoma cruzi*, the uptake of heme analogs was shown to be reduced in the presence of ABC transporter inhibitors, which suggests a role for heme scavenging (57). ABC transporters were also suggested to be involved in the heme scavenging of *Leishmania* (60), a range of bacteria, and mammals (61, 62). More recently, the *Leishmania* heme response 1 (LHR1) protein was proposed to be the major heme importer in the parasite and other kinetoplastids (58). In the *G. intestinalis* genome, we did not find an LHR1 ortholog; however, the genome contains at least 27 ABC domain-containing proteins that are heme transporter candidates, although there is currently no information regarding the functions of these proteins.

It is unknown whether heme is essential for *G. intestinalis*, and the lack of a defined medium for the parasite did not allow us to address this question (13). However, the heme concentration in standard medium is rather low (8 nM), and the addition of 4 μM hemin showed no effect on cell growth. Therefore, either the heme requirements of *Giardia* fall below a concentration of 8 nM or heme may not be essential for parasite growth *in vitro*. Thus far, the kinetoplastid *Phytomonas serpens* is the only eukaryote that has been found to be able to survive entirely without heme (59). Similar to *Giardia* and other anaerobes, *P. serpens* lacks most of the known hemoproteins, although it is a protist with aerobic metabolism. However, *P. serpens* possesses unique metabolic adaptations that allow it to bypass the functions of proteins that are dependent on heme (59). Interestingly, group II cytb_5 appears to be the only heme-binding protein that is encoded in the *P. serpens* genome. This finding, together with the conservation of cytb_5 proteins in the majority of anaerobes, suggests that although cytb_5 proteins are potentially not essential for cell growth *in vitro*, they may play a role important for cells in their native environments.

In conclusion, we defined three groups of cytb_5 proteins in eukaryotes and determined that *G. intestinalis* exclusively possesses group II soluble cytb_5 proteins. We demonstrated that *Giardia* can utilize hemin as an exogenous heme source and incorporates it into the heme-binding site of gCYTb5-IV. The NADPH-dependent oxidoreductase GiOR-1 reduces CYTb5 proteins *in vitro*, which constitutes a novel redox system in *Giardia*. However, there is much to learn about the mechanisms by which *G. intestinalis*, which lacks a heme synthesis pathway, acquires and transports exogenous heme, in addition to the functions of group II cytb_5 proteins in *Giardia* and other eukaryotes.

ACKNOWLEDGMENTS

This work was supported by the Czech Ministry of Education (MSM 0021620858), Charles University in Prague (UNCE 204017 and GAUK 153010), and the project BIOCEV—Biotechnology and Biomedicine Centre of the Academy of Sciences and Charles University (CZ.1.05/1.1.00/02.0109) from the European Regional Development Fund.

REFERENCES

1. **Green J, Crack JC, Thomson AJ, Lebrun NE.** 2009. Bacterial sensors of oxygen. Curr. Opin. Microbiol. **12:**145–151. http://dx.doi.org/10.1016/j.mib.2009.01.008.
2. **Poole RK, Hughes MN.** 2000. New functions for the ancient globin family: bacterial responses to nitric oxide and nitrosative stress. Mol. Microbiol. **36:**775–783. http://dx.doi.org/10.1046/j.1365-2958.2000.01889.x.
3. **Koreny L, Sobotka R, Janouskovec J, Keeling PJ, Obornik M.** 2011. Tetrapyrrole synthesis of photosynthetic chromerids is likely homologous to the unusual pathway of apicomplexan parasites. Plant Cell **23:**3454–3462. http://dx.doi.org/10.1105/tpc.111.089102.
4. **Koreny L, Lukeš J, Obornik M.** 2010. Evolution of the haem synthetic pathway in kinetoplastid flagellates: an essential pathway that is not essential after all? Int. J. Parasitol. **40:**149–156. http://dx.doi.org/10.1016/j.ijpara.2009.11.007.
5. **Rao AU, Carta LK, Lesuisse E, Hamza I.** 2005. Lack of heme synthesis in a free-living eukaryote. Proc. Natl. Acad. Sci. U. S. A. **102:**4270–4275. http://dx.doi.org/10.1073/pnas.0500877102.
6. **Lara FA, Lins U, Bechara GH, Oliveira PL.** 2005. Tracing heme in a living cell: hemoglobin degradation and heme traffic in digest cells of the cattle tick *Boophilus microplus*. J. Exp. Biol. **208:**3093–3101. http://dx.doi.org/10.1242/jeb.01749.
7. **Jedelsky PL, Dolezal P, Rada P, Pyrih J, Smid O, Hrdy I, Sedinova M, Marcincikova M, Voleman L, Perry AJ, Beltran NC, Lithgow T, Tachezy J.** 2011. The minimal proteome in the reduced mitochondrion of the parasitic protist *Giardia intestinalis*. PLoS One **6:**e17285. http://dx.doi.org/10.1371/journal.pone.0017285.
8. **Rada P, Dolezal P, Jedelsky PL, Bursac D, Perry AJ, Sedinova M, Smiskova K, Novotny M, Beltran NC, Hrdy I, Lithgow T, Tachezy J.** 2011. The core components of organelle biogenesis and membrane transport in the hydrogenosomes of *Trichomonas vaginalis*. PLoS One **6:**e24428. http://dx.doi.org/10.1371/journal.pone.0024428.
9. **Coombs GH, Westrop GD, Suchan P, Puzova G, Hirt RP, Embley TM, Mottram JC, Müller S.** 2004. The amitochondriate eukaryote *Trichomonas vaginalis* contains a divergent thioredoxin-linked peroxiredoxin antioxidant system. J. Biol. Chem. **279:**5249–5256. http://dx.doi.org/10.1074/jbc.M304359200.
10. **Nixon JEJ, Wang A, Field J, Morrison HG, McArthur AG, Sogin ML, Loftus BJ, Samuelson J.** 2002. Evidence for lateral transfer of genes encoding ferredoxins, nitroreductases, NADH oxidase, and alcohol dehydrogenase 3 from anaerobic prokaryotes to *Giardia lamblia* and *Entamoeba histolytica*. Eukaryot. Cell **1:**181–190. http://dx.doi.org/10.1128/EC.1.2.181-190.2002.
11. **Smutna T, Goncalves VL, Saraiva LM, Tachezy J, Teixeira M, Hrdy I.** 2009. Flavodiiron protein from *Trichomonas vaginalis* hydrogenosomes: the terminal oxygen reductase. Eukaryot. Cell **8:**47–55. http://dx.doi.org/10.1128/EC.00276-08.
12. **Lindmark DG.** 1980. Energy metabolism of the anaerobic protozoon *Giardia lamblia*. Mol. Biochem. Parasitol. **1:**1–12.
13. **Koreny L, Obornik M, Lukeš J.** 2013. Make it, take it, or leave it: heme metabolism of parasites. PLoS Pathog. **9:**e1003088. http://dx.doi.org/10.1371/journal.ppat.1003088.
14. **Nakanishi N, Takeuchi F, Okamoto H, Tamura A, Hori H, Tsubaki M.** 2006. Characterization of heme-coordinating histidyl residues of cytochrome b5 based on the reactivity with diethylpyrocarbonate: a mechanism for the opening of axial imidazole rings. J. Biochem. **140:**561–571. http://dx.doi.org/10.1093/jb/mvj189.
15. **Alam S, Yee J, Couture M, Takayama SJ, Tseng WH, Mauk AG, Rafferty S.** 2012. Cytochrome b(5) from *Giardia lamblia*. Metallomics **4:**1255–1261. http://dx.doi.org/10.1039/c2mt20152f.
16. **Schenkman JB, Jansson I.** 2003. The many roles of cytochrome b(5). Pharmacol. Ther. **97:**139–152. http://dx.doi.org/10.1016/S0163-7258(02)00327-3.
17. **Vergeres G, Waskell L.** 1995. Cytochrome B(5), its functions, structure and membrane topology. Biochimie **77:**604–620.
18. **Guiard B, Lederer F.** 1977. The "b5-like" domain from chicken-liver sulfite oxidase: a new case of common ancestral origin with liver cytochrome b5 and bakers' yeast cytochrome b2 core. Eur. J. Biochem. **74:**181–190.
19. **Napier JA, Sayanova O, Stobart AK, Shewry PR.** 1997. A new class of cytochrome b5 fusion proteins. Biochem. J. **328:**717–718.
20. **Rafferty S, Luu B, March RE, Yee J.** 2010. *Giardia lamblia* encodes a functional flavohemoglobin. Biochem. Biophys. Res. Commun. **399:**347–351. http://dx.doi.org/10.1016/j.bbrc.2010.07.073.
21. **Keister DB.** 1983. Axenic culture of *Giardia lamblia* in Tyi-S-33 medium supplemented with bile. Trans. R. Soc. Trop. Med. Hyg. **77:**487–488.
22. **Lauwaet T, Davids BJ, Torres-Escobar A, Birkeland SR, Cipriano MJ, Preheim SP, Palm D, Svard SG, McArthur AG, Gillin FD.** 2007. Protein phosphatase 2A plays a crucial role in *Giardia lamblia* differentiation. Mol. Biochem. Parasitol. **152:**80–89. http://dx.doi.org/10.1016/j.molbiopara.2006.12.001.
23. **Sun CH, Chou CF, Tai JH.** 1998. Stable DNA transfection of the primitive

protozoan pathogen *Giardia lamblia*. Mol. Biochem. Parasitol. **92:**123–132.
24. **Dawson SC, Sagolla MS, Mancuso JJ, Woessner DJ, House SA, Fritz-Laylin L, Cande WZ.** 2007. Kinesin-13 regulates flagellar, interphase, and mitotic microtubule dynamics in *Giardia intestinalis*. Eukaryot. Cell **6:**2354–2364. http://dx.doi.org/10.1128/EC.00128-07.
25. **Dagley MJ, Dolezal P, Likic VA, Smid O, Purcell AW, Buchanan SK, Tachezy J, Lithgow T.** 2009. The protein import channel in the outer mitosomal membrane of *Giardia intestinalis*. Mol. Biol. Evol. **26:**1941–1947. http://dx.doi.org/10.1093/molbev/msp117.
26. **Sonda S, Stefanic S, Hehl AB.** 2008. A sphingolipid inhibitor induces a cytokinesis arrest and blocks stage differentiation in *Giardia lamblia*. Antimicrob. Agents Chemother. **52:**563–569. http://dx.doi.org/10.1128/AAC.01105-07.
27. **Long SJ, Changmai P, Tsaousis AD, Skalicky T, Verner Z, Wen YZ, Roger AJ, Lukeš J.** 2011. Stage-specific requirement for Isa1 and Isa2 proteins in the mitochondrion of *Trypanosoma brucei* and heterologous rescue by human and Blastocystis orthologues. Mol. Microbiol. **81:**1403–1418. http://dx.doi.org/10.1111/j.1365-2958.2011.07769.x.
28. **Sinclair PR, Gorman N, Jacobs JM.** 2001. Measurement of heme concentration. Curr. Protoc. Toxicol. Chapter 8: Unit 8.3. http://dx.doi.org/10.1002/0471140856.tx0803s00.
29. **Tzagoloff A, Nobrega M, Gorman N, Sinclair P.** 1993. On the functions of the yeast COX10 and COX11 gene products. Biochem. Mol. Biol. Int. **31:**593–598.
30. **Labbe P, Chaix P.** 1971. Inexpensive device for recording difference absorption spectra at low temperature (-196 degrees). Anal. Biochem. **39:**322.
31. **Altschul SF, Madden TL, Schaffer AA, Zhang JH, Zhang Z, Miller W, Lipman DJ.** 1997. Gapped BLAST and PSI-BLAST: a new generation of protein database search programs. Nucleic Acids Res. **25:**3389–3402.
32. **Jeanmougin F, Thompson JD, Gouy M, Higgins DG, Gibson TJ.** 1998. Multiple sequence alignment with Clustal X. Trends Biochem. Sci. **23:**403–405.
33. **Guindon S, Dufayard JF, Lefort V, Anisimova M, Hordijk W, Gascuel O.** 2010. New algorithms and methods to estimate maximum-likelihood phylogenies: assessing the performance of PhyML 3.0. Syst. Biol. **59:**307–321. http://dx.doi.org/10.1093/sysbio/syq010.
34. **Hwang YT, Pelitire SM, Henderson MP, Andrews DW, Dyer JM, Mullen RT.** 2004. Novel targeting signals mediate the sorting of different isoforms of the tail-anchored membrane protein cytochrome b5 to either endoplasmic reticulum or mitochondria. Plant Cell **16:**3002–3019. http://dx.doi.org/10.1105/tpc.104.026039.
35. **Farr H, Gull K.** 2009. Functional studies of an evolutionarily conserved, cytochrome b5 domain protein reveal a specific role in axonemal organisation and the general phenomenon of post-division axonemal growth in Trypanosomes. Cell Motil. Cytoskeleton **66:**24–35. http://dx.doi.org/10.1002/cm.20322.
36. **D'Arrigo A, Manera E, Longhi R, Borgese N.** 1993. The specific subcellular-localization of 2 isoforms of cytochrome-B5 suggests novel targeting pathways. J. Biol. Chem. **268:**2802–2808.
37. **Seguin A, Sutak R, Bulteau AL, Garcia-Serres R, Oddou JL, Lefevre S, Santos R, Dancis A, Camadro JM, Latour JM, Lesuisse E.** 2010. Evidence that yeast frataxin is not an iron storage protein in vivo. Biochim. Biophys. Acta **1802:**531–538. http://dx.doi.org/10.1016/j.bbadis.2010.03.008.
38. **Falk JE.** 1964. Porphyrins and metalloporphyrins. Elsevier Publishing Co. New York, NY.
39. **Bonnerot C, Galle AM, Jolliot A, Kader JC.** 1985. Purification and properties of plant cytochrome-B5. Biochem. J. **226:**331–334.
40. **Smith MA, Napier JA, Stymne S, Tatham AS, Shewry PR, Stobart AK.** 1994. Expression of a biologically-active plant cytochrome b(5) in *Escherichia coli*. Biochem. J. **303:**73–79.
41. **Hultquist DE, Passon PG.** 1971. Catalysis of methaemoglobin reduction by erythrocyte cytochrome B5 and cytochrome B5 reductase. Nat. New Biol. **229:**252–254.
42. **Giordano SJ, Steggles AW.** 1991. The human liver and reticulocyte cytochrome b5 mRNAs are products from a single gene. Biochem. Biophys. Res. Commun. **178:**38–44.
43. **Olteanu H, Banerjee R.** 2003. Redundancy in the pathway for redox regulation of mammalian methionine synthase: reductive activation by the dual flavoprotein, novel reductase 1. J. Biol. Chem. **278:**38310–38314. http://dx.doi.org/10.1074/jbc.M306282200.
44. **Netz DJ, Stumpfig M, Dore C, Muhlenhoff U, Pierik AJ, Lill R.** 2010. Tah18 transfers electrons to Dre2 in cytosolic iron-sulfur protein biogenesis. Nat. Chem. Biol. **6:**758–765. http://dx.doi.org/10.1038/nchembio.432.
45. **Vernis L, Facca C, Delagoutte E, Soler N, Chanet R, Guiard B, Faye G, Baldacci G.** 2009. A newly identified essential complex, Dre2-Tah18, controls mitochondria integrity and cell death after oxidative stress in yeast. PLoS One **4:**e4376. http://dx.doi.org/10.1371/journal.pone.0004376.
46. **Nishimura A, Kawahara N, Takagi H.** 2013. The flavoprotein Tah18-dependent NO synthesis confers high-temperature stress tolerance on yeast cells. Biochem. Biophys. Res. Commun. **430:**137–143. http://dx.doi.org/10.1016/j.bbrc.2012.11.023.
47. **Morrison HG, McArthur AG, Gillin FD, Aley SB, Adam RD, Olsen GJ, Best AA, Cande WZ, Chen F, Cipriano MJ, Davids BJ, Dawson SC, Elmendorf HG, Hehl AB, Holder ME, Huse SM, Kim UU, Lasek-Nesselquist E, Manning G, Nigam A, Nixon JE, Palm D, Passamaneck NE, Prabhu A, Reich CI, Reiner DS, Samuelson J, Svard SG, Sogin ML.** 2007. Genomic minimalism in the early diverging intestinal parasite *Giardia lamblia*. Science **317:**1921–1926. http://dx.doi.org/10.1126/science.1143837.
48. **Xu K, Elliott T.** 1993. An oxygen-dependent coproporphyrinogen oxidase encoded by the hemF gene of *Salmonella typhimurium*. J. Bacteriol. **175:**4990–4999.
49. **Dailey TA, Dailey HA.** 1996. Human protoporphyrinogen oxidase: expression, purification, and characterization of the cloned enzyme. Protein Sci. **5:**98–105.
50. **Chang CS, Chang KP.** 1985. Heme requirement and acquisition by extracellular and intracellular stages of *Leishmania mexicana amazonensis*. Mol. Biochem. Parasitol. **16:**267–276.
51. **Pfeifer K, Kim KS, Kogan S, Guarente L.** 1989. Functional dissection and sequence of yeast HapI activator. Cell **56:**291–301.
52. **Munakata H, Sun JY, Yoshida K, Nakatani T, Honda E, Hayakawa S, Furuyama K, Hayashi N.** 2004. Role of the heme regulatory motif in the heme-mediated inhibition of mitochondrial import of 5-aminolevulinate synthase. J. Biochem. **136:**233–238. http://dx.doi.org/10.1093/jb/mvh112.
53. **Zhang L, Guarente L.** 1995. Heme binds to a short sequence that serves a regulatory function in diverse proteins. EMBO J. **14:**313–320.
54. **West AR, Thomas C, Sadlier J, Oates PS.** 2006. Haemochromatosis protein is expressed on the terminal web of enterocytes in proximal small intestine of the rat. Histochem. Cell Biol. **125:**283–292. http://dx.doi.org/10.1007/s00418-005-0060-6.
55. **van Dooren GG, Kennedy AT, McFadden GI.** 2012. The use and abuse of heme in apicomplexan parasites. Antioxid. Redox Signal. **17:**634–656. http://dx.doi.org/10.1089/ars.2012.4539.
56. **Vanhollebeke B, De Muylder G, Nielsen MJ, Pays A, Tebabi P, Dieu M, Raes M, Moestrup SK, Pays E.** 2008. A haptoglobin-hemoglobin receptor conveys innate immunity to *Trypanosoma brucei* in humans. Science **320:**677–681. http://dx.doi.org/10.1126/science.1156296.
57. **Lara FA, Sant'anna C, Lemos D, Laranja GA, Coelho MG, Reis S, Michel IA, Oliveira PL, Cunha-E-Silva Salmon D, Paes MC.** 2007. Heme requirement and intracellular trafficking in *Trypanosoma cruzi* epimastigotes. Biochem. Biophys. Res. Commun. **355:**16–22. http://dx.doi.org/10.1016/j.bbrc.2006.12.238.
58. **Huynh C, Yuan X, Miguel DC, Renberg RL, Protchenko O, Philpott CC, Hamza I, Andrews NW.** 2012. Heme uptake by *Leishmania amazonensis* is mediated by the transmembrane protein LHR1. PLoS Pathog. **8:**e1002795. http://dx.doi.org/10.1371/journal.ppat.1002795.
59. **Koreny L, Sobotka R, Kovarova J, Gnipova A, Flegontov P, Horvath A, Obornik M, Ayala FJ, Lukes J.** 2012. Aerobic kinetoplastid flagellate Phytomonas does not require heme for viability. Proc. Natl. Acad. Sci. U. S. A. **109:**3808–3813. http://dx.doi.org/10.1073/pnas.1201089109.
60. **Campos-Salinas J, Cabello-Donayre M, Garcia-Hernandez R, Perez-Victoria I, Castanys S, Gamarro F, Perez-Victoria JM.** 2011. A new ATP-binding cassette protein is involved in intracellular haem trafficking in Leishmania. Mol. Microbiol. **79:**1430–1444. http://dx.doi.org/10.1111/j.1365-2958.2010.07531.x.
61. **Koster W.** 2001. ABC transporter-mediated uptake of iron, siderophores, heme and vitamin B12. Res. Microbiol. **152:**291–301. http://dx.doi.org/10.1016/S0923-2508(01)01200-1.
62. **Krishnamurthy PC, Du G, Fukuda Y, Sun D, Sampath J, Mercer KE, Wang J, Sosa-Pineda B, Murti KG, Schuetz JD.** 2006. Identification of a mammalian mitochondrial porphyrin transporter. Nature **443:**586–589. http://dx.doi.org/10.1038/nature05125.

MCB
Journals.ASM.org

Probing the Biology of *Giardia intestinalis* Mitosomes Using *In Vivo* Enzymatic Tagging

Eva Martincová,[a] Luboš Voleman,[a] Jan Pyrih,[a] Vojtěch Žárský,[a] Pavlína Vondráčková,[a] Martin Kolísko,[b] Jan Tachezy,[a] Pavel Doležal[a]

Department of Parasitology, Faculty of Science, Charles University in Prague, Prague, Czech Republic[a]; Centre for Microbial Diversity and Evolution, Department of Botany, University of British Columbia, Vancouver, BC, Canada[b]

Giardia intestinalis **parasites contain mitosomes, one of the simplest mitochondrion-related organelles. Strategies to identify the functions of mitosomes have been limited mainly to homology detection, which is not suitable for identifying species-specific proteins and their functions. An *in vivo* enzymatic tagging technique based on the *Escherichia coli* biotin ligase (BirA) has been introduced to *G. intestinalis*; this method allows for the compartment-specific biotinylation of a protein of interest. Known proteins involved in the mitosomal protein import were *in vivo* tagged, cross-linked, and used to copurify complexes from the outer and inner mitosomal membranes in a single step. New proteins were then identified by mass spectrometry. This approach enabled the identification of highly diverged mitosomal Tim44 (*Gi*Tim44), the first known component of the mitosomal inner membrane translocase (TIM). In addition, our subsequent bioinformatics searches returned novel diverged Tim44 paralogs, which mediate the translation and mitosomal insertion of mitochondrially encoded proteins in other eukaryotes. However, most of the identified proteins are specific to *G. intestinalis* and even absent from the related diplomonad parasite *Spironucleus salmonicida*, thus reflecting the unique character of the mitosomal metabolism. The *in vivo* enzymatic tagging also showed that proteins enter the mitosome posttranslationally in an unfolded state and without vesicular transport.**

Giardia intestinalis causes intestinal infection in diverse vertebrate species, including humans, where it causes the disease giardiasis (1). In addition to its medical and veterinary importance, *Giardia* is an interesting unicellular eukaryote (protist) from cell biology and evolutionary perspectives (2).

The binucleated *Giardia* trophozoite is equipped with eight flagella and an adhesive disc, which mediates attachment to its host's intestine. The interior of the cell is dominated by an endoplasmic reticulum (ER) network (3) and lysosome-like peripheral vacuoles that mediate the uptake and digestion of nutrients (4). There are also Golgi body-like encystation vesicles that distribute the cyst wall material to the cell surface during encystation of the parasite (5).

The mitosomes of *Giardia* are highly adapted forms of mitochondria and are approximately 100 nm in size. These organelles are surrounded by two membranes, but unlike mitochondria, they do not contain DNA. The mitosomal proteome is currently limited to 21 proteins, which primarily participate in iron-sulfur cluster biosynthesis and protein import and folding (6–8). The identification of mitosomal proteins has been accomplished mostly using bioinformatics techniques, such as phylogenetics (9, 10) and hidden Markov model (HMM)-based searches (6, 11), that detect homologous proteins. Thus, in contrast to hydrogenosomes and mitochondria, in which 20 to 50% of proteins have no assigned function (12–14), the vast majority of mitosomal proteins have known functions and orthologs in the mitochondria of other eukaryotes. Attempts to identify the mitosomal proteome using cell fractionation techniques have been largely stymied by the abundance of the ER and cytoskeletal structures in the cell (7). Analogous studies of the proteomes of encystation vesicles and peripheral vacuoles of *Giardia* using sophisticated organelle purification procedures have demonstrated the limits of direct organelle isolation approaches (15). As a result, several essential aspects of the mitosome, such as the nature of the translocase of the inner membrane (TIM) complex or the protein composition of the outer mitosomal membrane, remain unknown.

Here, we addressed the difficulty of the biochemical characterization of giardial mitosomes by employing an *in vivo* enzymatic tagging approach. The highly specific purification of biotinylated mitosomal proteins led to the identification of divergent *Gi*Tim44, the first component of the mitosomal TIM complex. In addition, over 10 novel mitosomal proteins from the mitosomal matrix and the outer mitosomal membrane were also identified, increasing the known mitosomal proteome by one-half. Most of these proteins reflect the unique and unpredictable character of giardial mitosome biology. Moreover, the compartment-specific protein tagging allowed us to identify the mode of mitosomal protein transport.

MATERIALS AND METHODS

Cell culture and fractionation. Trophozoites of *G. intestinalis* strain WB (ATCC 30957) were grown in TY-S-33 medium (16) supplemented with 10% heat-inactivated bovine serum (PAA Laboratories), 0.1% bovine bile, and antibiotics. Cells expressing the dihydrofolate reductase (DHFR)

Received 8 May 2015 **Returned for modification** 18 May 2015
Accepted 3 June 2015
Accepted manuscript posted online 8 June 2015
Citation Martincová E, Voleman L, Pyrih J, Žárský V, Vondráčková P, Kolísko M, Tachezy J, Doležal P. 2015. Probing the biology of *Giardia intestinalis* mitosomes using *in vivo* enzymatic tagging. Mol Cell Biol 35:2864–2874. doi:10.1128/MCB.00448-15.
Address correspondence to Pavel Doležal, pavel.dolezal@natur.cuni.cz.
Supplemental material for this article may be found at http://dx.doi.org/10.1128/MCB.00448-15.

doi:10.1128/MCB.00448-15

fusion protein were grown in medium supplemented with 100 μM pyrimethamine (PM).

Preparation of cell fractions. The cells were harvested by centrifugation at 1,000 × *g* at 4°C for 10 min in ice-cold phosphate-buffered saline (PBS), washed once in SM buffer (250 mM sucrose, 20 mM MOPS [morpholinepropanesulfonic acid], pH 7.4), and resuspended in SM buffer with protease inhibitors (cOmplete, EDTA-free; Roche). Cells were disrupted on ice by sonication with 1-s pulses and an amplitude of 40 for 1 min (Bioblock Scientific Vibra-Cell 72405). The lysate was then centrifuged at 2,750 × *g* for 10 min. The centrifugation step was repeated until the pellet containing unbroken cells, nuclei, and the cytoskeleton was no longer visible. The clear supernatant was centrifuged at 180,000 × *g* at 4°C for 30 min. The resulting high-speed supernatant represented the cytosolic fraction; the high-speed pellet (HSP) containing the mitosomes was resuspended in SM buffer containing protease inhibitors.

Fluorescence microscopy. *G. intestinalis* trophozoites were fixed and immunolabeled as previously described (17). Mitosomal *Gi*Tom40 was detected with a specific polyclonal antibody raised in rabbits (18), and the hemagglutinin epitope (HA tag) was recognized by a rat monoclonal antibody (Roche). The primary antibodies were detected by a donkey Alexa Fluor 594 (red)-conjugated anti-rabbit antibody and Alexa Fluor 594 (red)- or Alexa Fluor 488 (green)-conjugated anti-rat antibodies (Life Technologies), respectively. Alexa Fluor 488 (green)-conjugated streptavidin (Life Technologies) was used to detect biotinylation. Slides were mounted with Vectashield containing DAPI (4′,6-diamidino-2-phenylindole; Vector Laboratories). The slides were imaged with an Olympus Cell-R, IX81 microscope system, and the images were processed using ImageJ 1.41e software (NIH).

Cloning and transfection. The pTG vector was used for *Escherichia coli* biotin ligase (BirA) cloning and protein expression (17). The gene encoding BirA (WP_023308552) was amplified from pET21a-BirA (19). Table S1 in the supplemental material lists all the primers used in this study. To coexpress proteins with BirA, biotin acceptor peptide (BAP) was introduced into the pONDRA vector (6) using a reverse primer for *Gi*Pam18-BAP. This vector carrying the C-terminal BAP was used for the subsequent cloning of the other genes. All *Giardia* genes were amplified from genomic DNA. Mouse DHFR was amplified from pARL2-GDG (20) (kindly provided by Jude Przyborski, Philipps University Marburg). *G. intestinalis* transfection was performed as previously described (6). Briefly, 300 μl of *G. intestinalis* trophozoites (3.3×10^7 cells/ml) was electroporated with a Bio-Rad Gene Pulser using an exponential protocol (U = 350 V; C = 1,000 μF; R = 750 Ω). The transfected cells were grown in medium supplemented with antibiotics (57 μg/ml puromycin and 600 μg/ml G418).

Cross-linking, protein isolation, and mass spectrometry (MS). *G. intestinalis* cells were grown in standard medium supplemented with 50 μM biotin for 24 h prior to harvesting. The cells were harvested and fractionated as described above. The HSP (40 mg) was used for the cross-linking and protein isolation. The pellet was resuspended in PBS (pH 7.4) supplemented with protease inhibitors (Roche) at a final protein concentration of 1.5 mg/ml. Then, a 25 μM concentration of the cross-linker DSP (dithiobis [succinimidyl propionate]; Thermo Scientific) was added, followed by 1 h of incubation on ice. After the incubation, Tris (pH 8) was added at a final concentration of 50 mM, and the sample was incubated at room temperature for 15 min. The sample was centrifuged at 30,000 × *g* for 10 min at 4°C, and the resulting pellet was resuspended in boiling buffer (50 mM Tris, 1 mM EDTA, 1% SDS, pH 7.4) supplemented with protease inhibitors at a final protein concentration of 1.5 mg/ml. The sample was incubated at 80°C for 10 min and was centrifuged at 30,000 × *g* for 10 min at room temperature. The resulting supernatant was diluted 1:10 in incubation buffer (50 mM Tris, 150 mM NaCl, 5 mM EDTA, 1% Triton X-100, pH 7.4) supplemented with protease inhibitors. Then, 200 μl of streptavidin-coupled magnetic beads (Dynabeads MyOne Streptavidin C1; Invitrogen) was washed 3 times with incubation buffer, mixed with the sample, and incubated overnight at 4°C with gentle rotation. The beads were then subjected to the following washes: 3 times for 5 min each in incubation buffer supplemented with 0.1% SDS, once for 5 min in boiling buffer, once for 5 min in washing buffer (60 mM Tris, 2% SDS, 10% glycerol), and twice for 5 min each in incubation buffer supplemented with 0.1% SDS. Finally, proteins were eluted from the beads in SDS-PAGE sample buffer supplemented with 20 mM biotin for 5 min at 95°C.

The samples were analyzed by Western blotting using streptavidin-conjugated Alexa Fluor 488 and were visualized using a Molecular Imager FX imager (Bio-Rad). The eluate was resolved by SDS-PAGE and stained with Coomassie brilliant blue. The gel was cut, destained, trypsin digested, and analyzed on a mass spectrometer.

Mass spectrometry and MS/MS analyses. Spectra were acquired using a (4800 Plus MALDI-TOF/TOF) analyzer (Applied Biosystems/MDS Sciex) equipped with an Nd:YAG laser (355 nm) with a firing rate of 200 Hz. The tandem mass spectrometry (MS/MS) analyses were performed as previously described (21).

Protease protection assay. To determine whether proteins were embedded in the outer mitosomal membrane, 150 μg of the HSP fraction in SM buffer supplemented with protease inhibitors was incubated with 200 μg/ml trypsin for 10 min at 37°C. The control sample also contained 0.1% Triton X-100 to completely digest the proteins of the solubilized organelles. The samples were separated by SDS-PAGE and blotted onto a nitrocellulose membrane, and proteins were detected with antibodies.

To determine whether proteins were in the mitosomal matrix, 1 mg of the HSP fraction was resuspended in 400 μl of either hypotonic buffer (1 mM EDTA, 10 mM MOPS, pH 7.2), isotonic buffer (hypotonic buffer supplemented with 250 mM sucrose), or NaCl buffer (500 mM NaCl, 10 mM Tris, pH 7.4). Pellets were resuspended by gentle pipetting or by sonication with 1-s pulses and amplitude of 60 for 2 times 1 min (Bioblock Scientific Vibra Cell 72405). Subsequently, 100 μl of each sample was treated with a different concentration of proteinase K (PK) and incubated on ice for 20 min. The reaction was stopped by the addition of 2 μl of 1 mM phenylmethanesulfonyl fluoride (PMSF), and the mixture was incubated on ice for 10 min. For the protein precipitation, 20 μl of 100% trichloroacetic acid (TCA) was added, and the samples were incubated on ice for 30 min. The samples were then centrifuged at 30,000 × *g* at 4°C for 30 min. The resulting pellets were washed in acetone and centrifuged at 30,000 × *g* at 4°C for 30 min, air dried, and resuspended in SDS-PAGE sample buffer.

Electron microscopy. For transmission electron microscopy (TEM) studies, *G. intestinalis* cell pellets were fixed for 24 h in 2.5% glutaraldehyde in 0.1 M cacodylate buffer (pH 7.2) and were postfixed in 2% OsO_4 in the same buffer. The fixed samples were dehydrated by passage through an ascending ethanol and acetone series and were embedded in an Araldite-Poly/Bed 812 mixture. Thin sections were cut on a Reichert-Jung Ultracut E ultramicrotome and were stained using uranyl acetate and lead citrate. The sections were examined and photographed with a JEOL JEM-1011 electron microscope. Fine-structure measurements were performed with a Veleta camera and iTEM 5.1 software (Olympus Soft Imaging Solution GmbH).

Bioinformatic analyses. To identify the copurified proteins, their amino acid sequences were analyzed by BLASTP against the NCBI nr database using the following algorithms: HHpred at http://toolkit.tuebingen.mpg.de/hhpred# (22); HMMER3 at http://hmmer.janelia.org/ (23); and I-TASSER at http://zhanglab.ccmb.med.umich.edu/I-TASSER/ (24). The subcellular localization and topology of the proteins were predicted using TargetP at http://www.cbs.dtu.dk/services/ (25) and Phobius at http://phobius.sbc.su.se (26), respectively.

RESULTS

***In vivo* enzymatic tagging in *Giardia intestinalis*.** To gain insights into the composition of protein import pathways and other processes in giardial mitosomes, we took a direct biochemical ap-

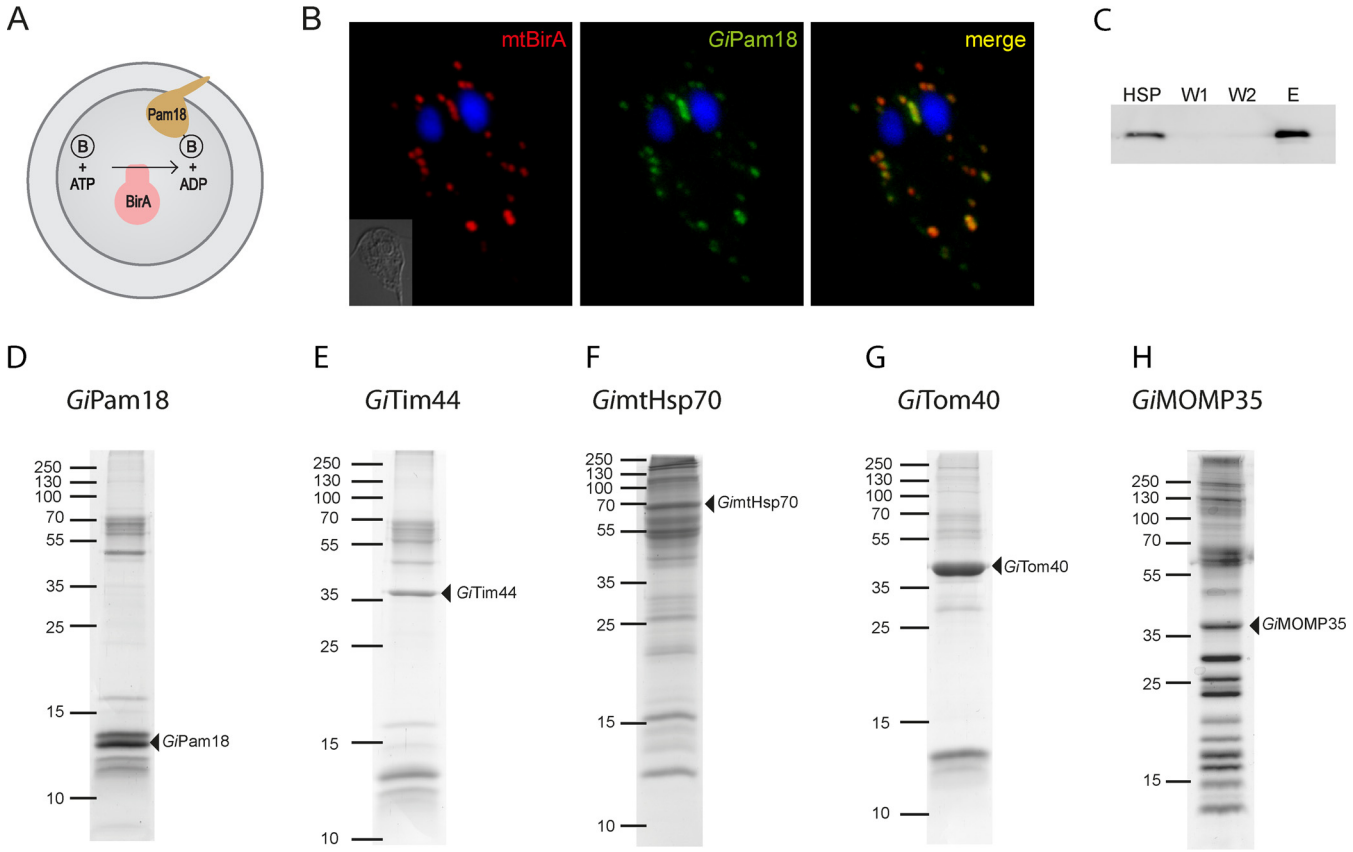

FIG 1 *Gi*Pam18 is biotinylated within mitosomes. (A) Schematic representation of mitosome-specific *in vivo* enzymatic tagging. *E. coli* biotin ligase (BirA) specifically biotinylates the biotin acceptor peptide when present in the same compartment. B, biotin. (B) BAP-tagged *Gi*Pam18 was successfully biotinylated by mtBirA. Cells were stained with an anti-HA tag antibody (red) and streptavidin-conjugated Alexa Fluor 488 (green) to detect mtBirA. Nuclei were stained with DAPI (blue). (C) Example of the purification steps (*Gi*Pam18) as analyzed on the Western blot by Alexa Fluor Fluor 488-streptavidin conjugate. (D to H) Protein profiles of the particular eluates from the streptavidin-coupled magnetic beads resolved by SDS-PAGE. The triangles indicate the proteins carrying the BAP tag.

proach involving highly specific protein pulldown assays followed by mass spectrometry analyses. To this end, an *in vivo* enzymatic tagging technique based on the biotin-avidin interaction was introduced into *Giardia*. This tagging relies on the highly specific *E. coli* biotin ligase (BirA), which uses one ATP molecule to catalyze the covalent attachment of biotin to the side chain of lysine within a biotin acceptor peptide (BAP) (27). A chimeric construct composed of *E. coli* BirA preceded by the N-terminal region of mitosomal *Gi*Mge1 and followed by a double HA tag was expressed in *Giardia*. The resulting strain contained mitosomally localized BirA (mtBirA). This construct was cotransformed with a second plasmid carrying a gene encoding mitosomal *Gi*Pam18 with the C-terminal BAP (Fig. 1A). Detection using a fluorescent streptavidin conjugate revealed the specific biotinylation of BAP (Fig. 1B). *Gi*Pam18-BAP-specific biotinylation was confirmed by Western blotting of a *Giardia* trophozoite lysate, which produced a single band of approximately 13 kDa, which corresponded to *Gi*Pam18-BAP. These results demonstrated that BirA remained active when delivered to *Giardia* mitosomes and that no nonspecific biotinylation was detected. Moreover, the use of mitosomal ATP during the biotinylation of the BAP had no apparent effects on mitosomal morphology, mitosomal distribution, or parasite growth.

Search for the TIM components. *Gi*Pam18-BAP was further used to identify putative components of the mitosomal TIM complex. As a part of the PAM complex at the inner mitochondrial membrane, Pam18 interacts with the translocation channel via Tim44 (28). HSPs, which were enriched for mitosomes, were obtained from *Giardia* trophozoites expressing mtBirA and *Gi*Pam18-BAP. The purification of the biotinylated proteins was initially performed under native conditions; however, the resulting eluates contained numerous contaminating proteins (data not shown). Thus, chemical cross-linking and denaturation conditions were used instead. The HSP was treated with a low concentration of the membrane-permeable reversible cross-linker DSP, which is commonly used to identify interacting proteins in various cellular compartments, including mitochondria (29, 30).

Upon cross-linking, the detergent-solubilized samples were passed over streptavidin-coupled magnetic beads, and the resulting protein fractions were analyzed via SDS-PAGE and Western blotting (Fig. 1C and D). The samples were then trypsin cleaved and analyzed by mass spectrometry. Analogous purification experiments were performed in parallel using HSPs isolated from wild-type *Giardia* cells and from *Giardia* cells expressing mtBirA only. These two samples were used as negative controls for the mass spectrometry protein identification. After the results of the negative controls were subtracted, the identified proteins were ordered according to their Mascot score. Although none of the

known mitosomal proteins were present in the negative controls, these proteins were abundant among the hits derived from the *Gi*Pam18-BAP samples. The high specificity of the purification procedures suggests that *Gi*Pam18-interacting partners were present among the top identified proteins. The remainder of the refined data set largely represented proteins of unknown function, and their amino acid sequences were analyzed using homology and topology detection software.

Mitosomes contain highly diverged Tim44. Of the proteins that copurified with *Gi*Pam18-BAP, GL50803_14845 had the highest Mascot score of the unknown proteins (see Fig. S3 in the supplemental material). Although pairwise sequence analyses of GL50803_14845 showed no obvious homology to known protein families, profile-sequence comparisons conducted with HHpred showed clear homology to Tim44, a key component of the TIM complex (Fig. 2A). The mitosomal localization of GL50803_14845, here referred to as *Gi*Tim44, was confirmed by its episomal expression in *Giardia* (Fig. 2B). Further comparisons with mitochondrial and hydrogenosomal Tim44 proteins revealed that *Gi*Tim44 is one of the most divergent Tim44 orthologs identified and that it consists of the C-terminal domain of Tim44, which has been suggested to interact with mitochondrial lipids. However, *Gi*Tim44 lacks recognizable N-terminal domain of Tim44 (Fig. 2C), which binds the import motor molecule mtHsp70 and the core subunit of the protein-conducting channel, Tim23 (31, 32).

The homology model of the C-terminal domain of *Gi*Tim44 indicated that this protein was capable of forming a conserved Tim44 structure containing a hydrophobic cavity, indicating its possible attachment to the mitosomal membrane (Fig. 2F). To test whether mitosomal *Gi*Tim44 interacts with its putative mitochondrial partner, *Gi*mtHsp70, *Giardia* trophozoites coexpressing mtBirA and *Gi*Tim44-BAP were generated. Following chemical cross-linking and purification, the proteins that copurified with *Gi*Tim44-BAP were analyzed by mass spectrometry. Similar to what was seen in the initial experiment, the purified sample was highly enriched for known mitosomal proteins (see Fig. S3 in the supplemental material). The five most highly enriched identified proteins included mitosomal *Gi*mtHsp70 and its nucleotide exchange factor, *Gi*Mge1, which strongly supports the hypothesis that Tim44 and Hsp70 interact within mitosomes.

Distant Tim44 orthologs in eukaryotes. The discovery of a divergent Tim44 in *Giardia* led us to search for other Tim44 orthologs in eukaryotes. Using Tim44-specific HMMs, we identified Tim44 orthologs in two free-living metamonads, *Carpediemonas membranifera* and *Ergobibamus cyprinoides*. However, no Tim44 orthologs were identified in the fish parasite *Spironucleus salmonicida* or in the group Euglenozoa, which includes medically important trypanosomes and leishmania.

Surprisingly, the HMMs identified two mitochondrial proteins, MRLP45 and Mba1, as belonging to the Tim44 protein family (Fig. 2C and D). Whereas MRLP45 is a subunit of the mitochondrial ribosome (33), Mba1 serves as a mitochondrial ribosome receptor during the membrane insertion of mitochondrially translated proteins (34). Their distribution in eukaryotes suggests that both proteins represent independent paralogs of Tim44 that are specialized for mitochondrial protein translation (Fig. 2D).

Search for the translocase of the TOM components. To identify outer mitosomal membrane components, *Gi*Tom40-BAP was coexpressed with the cytosolic version of BirA (cytBirA). As a result, mitosome-specific biotinylation was observed (see Fig. S1 in the supplemental material). Employing the same strategy as the one used for *Gi*Pam18 and *Gi*Tim44, the proteins obtained by *Gi*Tom40-BAP purification were identified using mass spectrometry. The proteins obtained from wild-type *Giardia* cells and *Giardia* cells expressing cytBirA only were subtracted from the data set.

Because *Gi*Tom40 is the only known outer mitosomal membrane protein, the specificity of the purification procedure could not be determined. Nevertheless, the absence of mitosomal matrix proteins among the most significant hits (see Fig. S3 in the supplemental material) indicated that a distinct subset of mitosomal proteins was obtained. However, the previously identified mitosomal protein GL50803_14939 was found among the hits (7) (see Fig. S3 in the supplemental material). According to transmembrane topology predictors, GL50803_14939 contains two transmembrane domains in its N-terminal region. To determine whether the protein is embedded in the outer or inner mitosomal membrane, an HSP isolated from *Giardia* expressing C-terminally HA-tagged GL50803_14939 was subjected to a protease protection assay. Similar to *Gi*Tom40, GL50803_14939 was sensitive to protease activity even without the addition of detergent, which suggests that GL50803_14939 is inserted into the outer membrane (Fig. 3A). Taken together, these data suggest that GL50803_14939, here referred to as mitosomal outer membrane protein 35 (*Gi*MOMP35), is anchored by two N-terminal transmembrane domains in the outer mitosomal membrane and that its C-terminal domain is in the cytosol. Whether the transmembrane domains of *Gi*MOMP35 are also responsible for its mitosomal targeting was tested by analyzing the expression of an N-terminally truncated version of the protein. Indeed, the removal of the transmembrane domains resulted in the cytosolic localization of the truncated *Gi*MOMP35 (see Fig. S2A in the supplemental material).

The function of the exposed soluble domain could not be predicted using bioinformatic analyses, which revealed no significant similarity of the domain to any known protein families. To examine the function of *Gi*MOMP35, we attempted to overexpress the full-length protein using a strong promoter (ornithine carbamoyltransferase) (35). However, a stable *Giardia* line could not be established after numerous attempts, indicating that the overexpression of *Gi*MOMP35 was lethal. Milder *Gi*MOMP35 overexpression (using the 5′ untranslated region [5′UTR] of glutamate dehydrogenase as a promoter) allowed a stable line of *Giardia* transformants to be established and inspected for mitosome-related defects. Approximately one half of the cells retained typical mitosomal distribution and morphology (Fig. 3B), whereas the other half exhibited dramatic membrane protrusions and aggregation (Fig. 3C to E).

Further analyses indicated that *Gi*Tom40 colocalized with these elongated structures (Fig. 3C). However, these structures were largely devoid of the mitosomal protein GL50803_9296, which localized to the mitosomal matrix (see Fig. S2B in the supplemental material). When examined with a transmission electron microscope, the structures were observed as tightly packed multimembrane complexes (Fig. 3F). These data suggest that the membrane protrusions corresponded to the enlarged and aggregated outer mitosomal membrane. In contrast, the overexpression of *Gi*MOMP35 did not result in an ER-related phenotype, as illus-

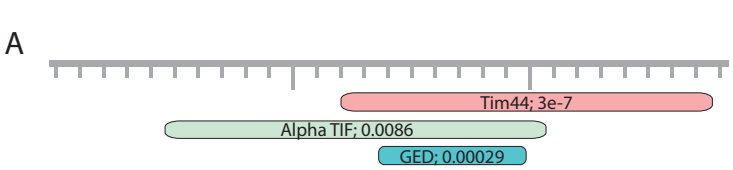

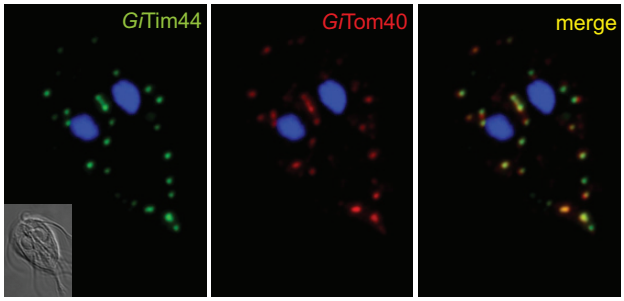

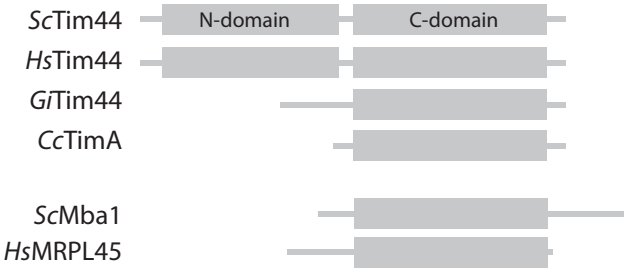

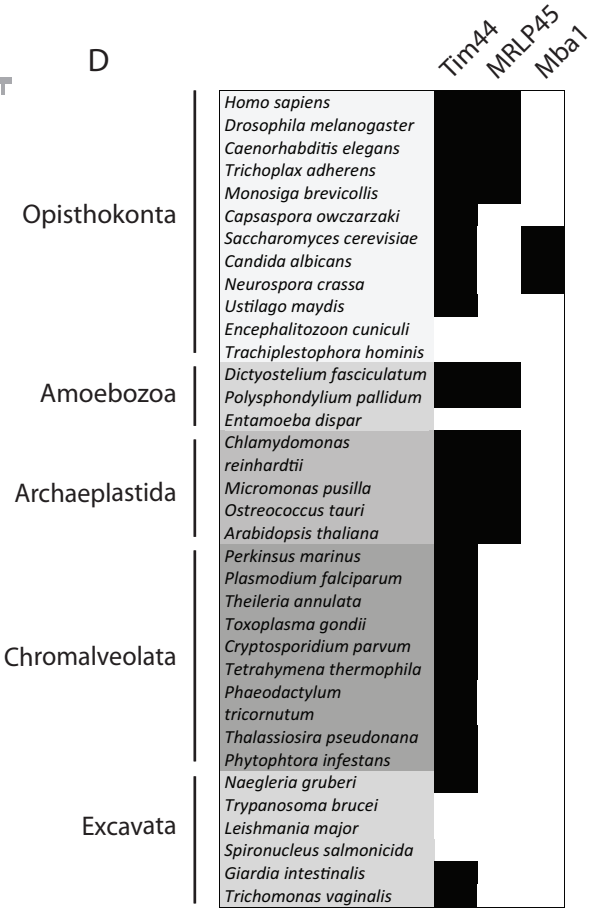

E

```
G.intestinalis     119 ---------- -----LALDF RRLR-SLLPS FDLPHFTENY GIDTLVAILG GYLNIFNTYN PQSYPRQTIA YLLDNCTSKL QKQ-LLEGIQ EHIRKDVDTH FRLHHIRGVK CTGLDLH---  219
C.membranifera     133 -------SQW GKGTELGINV GLVS-AWIP- ---------- --QFVAQIM- ---------- -EAYFMNDVA TLRECCADGA LSI-LLQGLK EQRDKHLSVQ GSTYRIGTTD LARVGG---D  216
E.cyprinoides      135 -----MACDL IGRDTQAAVA AARA-HFDRD FDLHQLQDSA A-AITGELM- ---------- -DAFFAGDVE TVAGLTAEVP RRL-LLDAMR QFLNARIEVT GWTYWAGEPA LRSADVSE-E  234
B.naejangsanensis  56 ---------- --DPALTAAI AGLK-ARDPN FDPHRFLEGA RQAY-ETIV- ---------- -GAYAKGDRE ALRPLLLDKV MGS-FEAGIA AREARGDIES AELVHPPRAD LELATAE--G  147
H.sapiens          281 DKVTDLLGGL FSKTEMSEVL TELL-RVDPA FDKDRFLKQC ENDIIPNVLL ---------- -EAMISGELD ILKDWQYEAT YSQ-LAHPIQ QAKALGLQFH SRILDIDNVD LAMGKMM--E  384
S.cerevisiae       259 NKV----GGF FAETESSRVY SQFK-LMDPT FSNESFTRHL REYIVPEILL ---------- -EAYVKGDVK VLKKWFSEAP FNV-YAAQQK IFKEQDVYAD GRILDIRGVE IVSAKLLAPQ  360
A.thaliana         301 --IQDMNEKF LKETDSASTY KELR-SRDPS FSLPDEAAEI EEVIKF-VLL ---------- -NAYSEGDVE TLKKYCSKEV IER-CTAERT AVQTHGVLFD NKLLHISEVS VSVTKMM--G  402
N.gruberi          348 EDIPDTEADI SSTSENALAM GAFK-KRDPR FDLDLLLVTM ETLTIPEIM- ---------- -SAYFNDDAH TLKKFVSESC YRQVFFPRIQ EFVHTKIKYD AKLLHVEDVM LYTTRYD--A  452
P.falciparum       302 -------GKL FGETELAAAL REMK-MIDKN FKLSELMYLF EYVISKHIV- ---------- -ESYLIGDEF TLRLHCGSSA FNS-LNASIT LKKKKVFLD TNVLIYKNHF LKGAQRME-E  400
T.vaginalis        156 NASSVVVSKL TQPSKEQLVQ MSIQ-MYYPT FTISEFKQWI EKSFLPVLL- ---------- -ERYLRGNIK QLEELTSQQV AKE-RQLAVV QFLSNRLIIR TKLLSITDVD IMGFDFT--N  259
D.fasciculatum     362 GTIAGFVGGY TSSPALTKFY FDYRDLIMPG FFFNKFLPIA KSKFIPEFL- ---------- -EIVFANDVD GLEDFCGETL HKM-LSGIIA ANEAGHKVFD GKIVKIDTLD FMGINES--E  466

G.intestinalis     219 ---SMELHFT AILTGAYAVT NRS---GQTV NGGYNKSRD- -YLVDYSYRY YNGK------ ---------- WLLSALKMSI LSISAKPTYF Y 286
C.membranifera     217 DRPTLTVNET --LSHFFRVN LPR---GHCL HGS-KKGRDY TYTATISPEK GQWVDLTEGD AKIEVR---- WMLTDIHAET VDYVANKEE- - 295
E.cyprinoides      235 GVPSFFEAVT --LSQLYAAT RAGEHGPELL HGSLRRGTDF EYVFKLRPAG EPRAIVGRG- -NQGPTR--- WIVSALLAPT LDATLEPRGA T 318
B.naejangsanensis  148 DRALAKVREL --AEVRGSLT PSG---GETV TEE----RRT AEIWTFERRL G--------- -TSDPN---- WALARVEPAA A--------- - 205
H.sapiens          385 QGFVLTITFQ --AQLVMVVR NPK---GEVV EGDPDKYLRM LYVWAIGRGQ DEL------- -NPYAA---- WRLLDISASS TEQIL----- - 452
S.cerevisiae       361 DIEVLVVGCR --AQEINLYR KKKT--GEIA AGDEANILMS SYAMVFIRDP EQIDD----- -DETEG---- WKILEFVRGG SRQFT----- - 431
A.thaliana         403 DSPIITAKFQ --TQEIYCVR DEN---GEIQ EGGQDTIHTV YHEWAMQGVE T----TELGE DAIYPI---- WRLREMCRNG VQALI----- - 474
N.gruberi          453 GNPALVISCA --VQYIHCMK NEA---GEIV EGGPKDIRKE NQMWIIKQDE S--------- -QETDD---- WYVSEVSMLN ADAVK----I V 520
P.falciparum       401 SSPWFIFTFH --TQQINCLK NKN---DEII EGKIDDIREV VYTIALSEHP E--------- -PCKEGLLYP YIVREFAIIG NTPSW----- - 470
T.vaginalis        260 RMPSILVRCS --ADHTNEVI TMNS--GTIV EGGPQDICHT DFIVVLTIDA S--------- -KQTPR---- WIASELRPDS TSNRI----- - 326
D.fasciculatum     467 NREETYFSFL VVVHHTYCIR IYQ---FEIV EGGDHEIIKT QMIVHMSVDT D--------- -LNEFG---- WCVSKLDVHP SESIY----- L 535
```

F

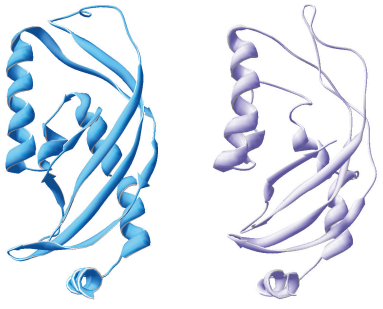

ScTim44 GiTim44

trated by the lack of colocalization between the ER and the enlarged mitosomes (Fig. 3E).

As an alternate means of investigating the function of *Gi*MOMP35, the cross-linked BAP-tagged protein was purified and subjected to mass spectrometry. As expected, *Gi*Tom40 was included in the significant hits; however, the obtained data set contained no clear indication of the function of *Gi*MOMP35 (see Fig. S3 in the supplemental material).

Newly identified mitosomal proteins. In addition to *Gi*Tim44 and *Gi*MOMP35, a number of other proteins of unknown function were identified from the pulldown experiments. The proteins that coprecipitated with BAP-tagged mitosomal Hsp70 (*Gi*mtHsp70) were added to the data sets derived from the *Gi*Pam18, *Gi*Tim44, *Gi*Tom40, and *Gi*MOP35 coimmunoprecipitations, and the data were analyzed together (Fig. 1D to H). *Gi*mtHsp70 is thought to be a central component of mitosomal metabolism and to participate in protein import and iron-sulfur cluster assembly.

Seventeen proteins (see Table S2 in the supplemental material) were subcloned into *Giardia* expression vectors to verify their mitosomal localization. These proteins were selected according to three criteria: (i) the protein copurified with more than one target molecule, (ii) the identification of the protein was highly significant, or (iii) homology predictors showed an affiliation with a particular protein family. Using this approach, mitosomal localization was confirmed for 13 of the proteins, including 3 with dual localization (Fig. 4). The localization of one protein (GL50803_92741) could not be confirmed because no viable transformants were obtained after three independent transfections. Particular attention was paid to GL50803_27910 and GL50803_16424. The first represents an ortholog of rhodanese, a protein involved in various aspects of sulfur metabolism (36), including the repair of iron-sulfur clusters (37). The latter was the only protein identified in all the pulldown experiments performed in this study (see Fig. S3 in the supplemental material); i.e., GL50803_16424 coprecipitated with the outer membrane, the inner membrane, and the matrix proteins, which might indicate its complicated topology. Moreover, the episomal expression of GL50803_16424 often but not always resulted in the formation of enlarged structures at the mitosomal sites (Fig. 4). Strikingly, this protein appears to be a member of the myelodysplasia-myeloid leukemia factor 1-interacting protein (Mlf1IP) family, which has been considered exclusive to metazoans (38). For the remainder of the confirmed mitosomal proteins, no recognizable homology could be identified. Moreover, with the exception of GL50803_27910, GL50803_3491, and GL50803_16424, these proteins appear to lack orthologs, even in other metamonad species; thus, they currently represent *Giardia*-specific molecules (see Table S3 in the supplemental material).

Mode of mitosomal protein import. Compartment-specific biotinylation allows one to determine whether a given protein is transported into an organelle co- or posttranslationally. To this end, we generated a *Giardia* strain expressing a cytosolic version of BirA (cytBirA) (Fig. 5). The ability of cytBirA to biotinylate the BAP on a mitosomal protein indicates that the protein is transported posttranslationally. Indeed, the biotinylation of *Gi*Tim44-BAP was observed upon coexpression with cytBirA (Fig. 5A). Similarly, the use of compartment-specific biotinylation allowed us to assess whether the reported presence of a SNARE protein, Sec20, in the mitosomes (39) indicated the fusion of secretory vesicles with the mitosomal surface. However, because no biotinylation of the mitosomal proteins was observed when BirA was targeted to the ER (data not shown), the integration of mitosomes into the secretory pathway could not be confirmed. The posttranslational transport of mitosomal proteins raised the question of whether these proteins are required to retain their unfolded state during import. To address that question, a chimeric construct encoding mitosomal *Gi*Mge1, mouse dihydrofolate reductase (DHFR), and a C-terminal HA tag was expressed in *Giardia*. The DHFR domain is a classical experimental substrate used in protein translocation studies due to its ability to fold upon the addition of a folate analog (40). Usually, the use of folate analogs requires the experiment to be performed *in vitro* on isolated organelles due to the effect of these analogs to the endogenous enzyme (40). However, *Giardia* lacks DHFR and instead relies on the purine salvage pathway (41), which allows for the *in vivo* use of DHFR-containing constructs. The localization of the chimeric protein was examined in cells incubated with or without the folate analog pyrimethamine (PM). As expected, in the absence of the folate analog, the targeting information on *Gi*Mge1 mediated the efficient delivery of this protein to the mitosomes (Fig. 5B). In contrast, the addition of PM resulted in an entirely cytosolic localization (Fig. 5C). These results demonstrate that the protein must remain unfolded before and during its import into mitosomes.

DISCUSSION

The *Giardia* mitosome remains one of the least well characterized forms of mitochondria. This is especially true for its biogenesis pathways, which ensure that the organelle maintains its integrity and functions. The aim of this study was to identify new mitosomal proteins, which might have diverged from known proteins beyond the sensitivity of homology detection algorithms or have been replaced by lineage-specific components. Because mitosomes represent one of the smallest membrane-bound cellular compartments of eukaryotes (42), biochemical approaches using cell fractionation techniques are highly challenging (7). The *in vivo* enzymatic tagging approach utilizing *E. coli* BirA introduced in this study allows proteins of interest to be purified and their transport through cellular organelles and their subcompartments to be monitored.

First, two key proteins involved in mitosomal protein import, which reside in different mitosomal membranes, were used to

FIG 2 A Tim44 homolog is present in giardial mitosomes. (A) HHpred analysis of GL50803_14845 shows the presence of a Tim44 domain. (B) HA-tagged *Giardia* Tim44 (*Gi*Tim44) localizes to mitosomes. Green, anti-HA antibody; red, anti-*Gi*Tom40 antibody; blue, nuclei stained with DAPI. (C) Domain structure of Tim44 orthologs in eukaryotes and bacteria. *Sc*, *Saccharomyces cerevisiae*; *Hs*, *Homo sapiens*; *Gi*, *Giardia intestinalis*; *Cc*, *Caulobacter crescentus*. (D) Distribution of Tim44 paralogs in eukaryotes. (E) Protein sequence alignment of *Gi*Tim44 with the C-terminal domains of Tim44 orthologs from *Carpediemonas membranifera*, *Ergobibamus cyprinoides*, *Brevundimonas naejangsanensis*, *Homo sapiens*, *Saccharomyces cerevisiae*, *Arabidopsis thaliana*, *Naegleria gruberi*, *Plasmodium falciparum*, *Trichomonas vaginalis*, and *Dictyostelium discoideum*. The sequences were aligned using MAFFT at http://mafft.cbrc.jp/alignment/server/. The residues involved in forming a hydrophobic pocket are framed in red (57). (F) Model of the C-terminal domain of *Gi*Tim44 obtained by Swiss-Model (58) using human Tim44 as a template (48).

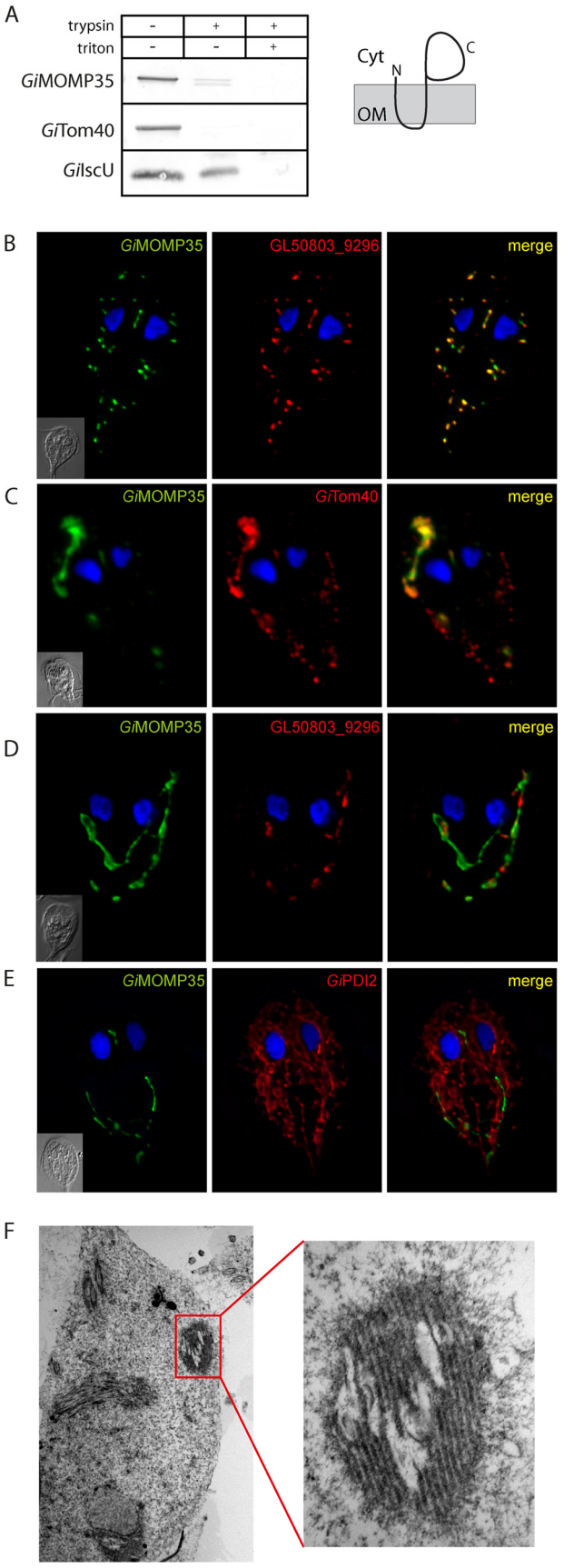

search for new mitosomal components. *Gi*Pam18 was the best available candidate to identify putative TIM components in mitosomes. The protein identified with this approach, *Gi*Tim44, represents one of the most diverged eukaryotic Tim44 proteins. The homology of *Gi*Tim44 is limited to the C-terminal membrane interaction domain, an arrangement reminiscent of the distant Tim44 ortholog found exclusively in alphaproteobacteria (43). However, despite the absence of the N-terminal domain, which has been shown to mediate an interaction with mtHsp70 (31), *Gi*mtHsp70 was found among the most significant proteins that copurified with *Gi*Tim44. This finding may indicate that the interaction between these proteins is conserved in mitosomes, although it is mediated by different amino acid residues. Unfortunately, no protein translocase candidate was found among the obtained data set, which lacked polytopic membrane proteins. This absence was likely due to the experimental conditions used, particularly the cross-linking chemistry and the preparation of samples for mass spectrometry (44). A customized procedure will be necessary to identify such proteins.

Using *Gi*Tim44 as a query, related sequences were found in metamonads such as *C. membranifera* and *E. cyprinoides*. Surprisingly, no Tim44 ortholog was identified in the recently published genome of the hydrogenosome-bearing fish parasite *S. salmonicida* (45). According to further HMM-based searches, Tim44 has been lost several times in the evolution of eukaryotes. Previous reports have shown that this protein is absent from Entamoeba (46) and microsporidian species (47), which also carry highly adapted mitosomes. Strikingly, the Tim44 protein is also missing from the entire group of kinetoplastida, which contain complex aerobic mitochondria. However, our Tim44-specific HMM identified additional new Tim44 paralogs in the mitochondria of opisthokonts, amoebozoa, and plants. Specifically, the mitochondrial proteins MRLP45 and Mba1 participate in mitochondrial translation and membrane protein insertion, respectively (33, 34). MRLP45 is a component of the large subunit of the mitoribosome, the structure of which was recently been resolved (33). The structure of MRLP45 clearly demonstrates its homology to the C-terminal domain of Tim44 (48). Although Mba1 is not a mitoribosome component, it binds the large subunit of the mitoribosome and cooperates with OxaI in the membrane insertion of mitochondrially translated proteins (34). Despite the differences in the molecular architecture of the complexes containing MRLP45 and Mba1, it is likely that these proteins perform analogous functions.

FIG 3 *Gi*MOMP35 is an outer mitosomal membrane protein. (A) Protease protection assay of high-speed pellets isolated from *Giardia* expressing HA-tagged *Gi*MOMP35. After incubation with trypsin, the samples were immunolabeled with antibodies against the HA tag, the outer membrane protein *Gi*Tom40, and the matrix protein *Gi*IscU. The sensitivity of *Gi*MOMP35 to the protease indicates its outer membrane localization. The drawing shows the suggested topology of *Gi*MOMP35. Cyt, cytosol; OM, outer mitosomal membrane. (B) Cells expressing HA-tagged *Gi*MOMP35 were stained with an anti-HA tag antibody (green) and an anti-GL50803_9296 antibody (red). Nuclei were stained with DAPI (blue). In addition to exhibiting typical mitosomal morphology (B), approximately 50% of the observed trophozoites contained elongated tubular structures (C to E). These structures colocalized with *Gi*Tom40 (red) (C); however, only a small fraction exhibited costaining for GL50803_9296 (red) (D). The structures were devoid of the ER marker *Gi*PDI2 (red) (E). These data indicate that the elongated tubular structures represent an enlarged outer mitosomal membrane. Under transmission electron microscopy, the structures appeared as organized membrane layers (F).

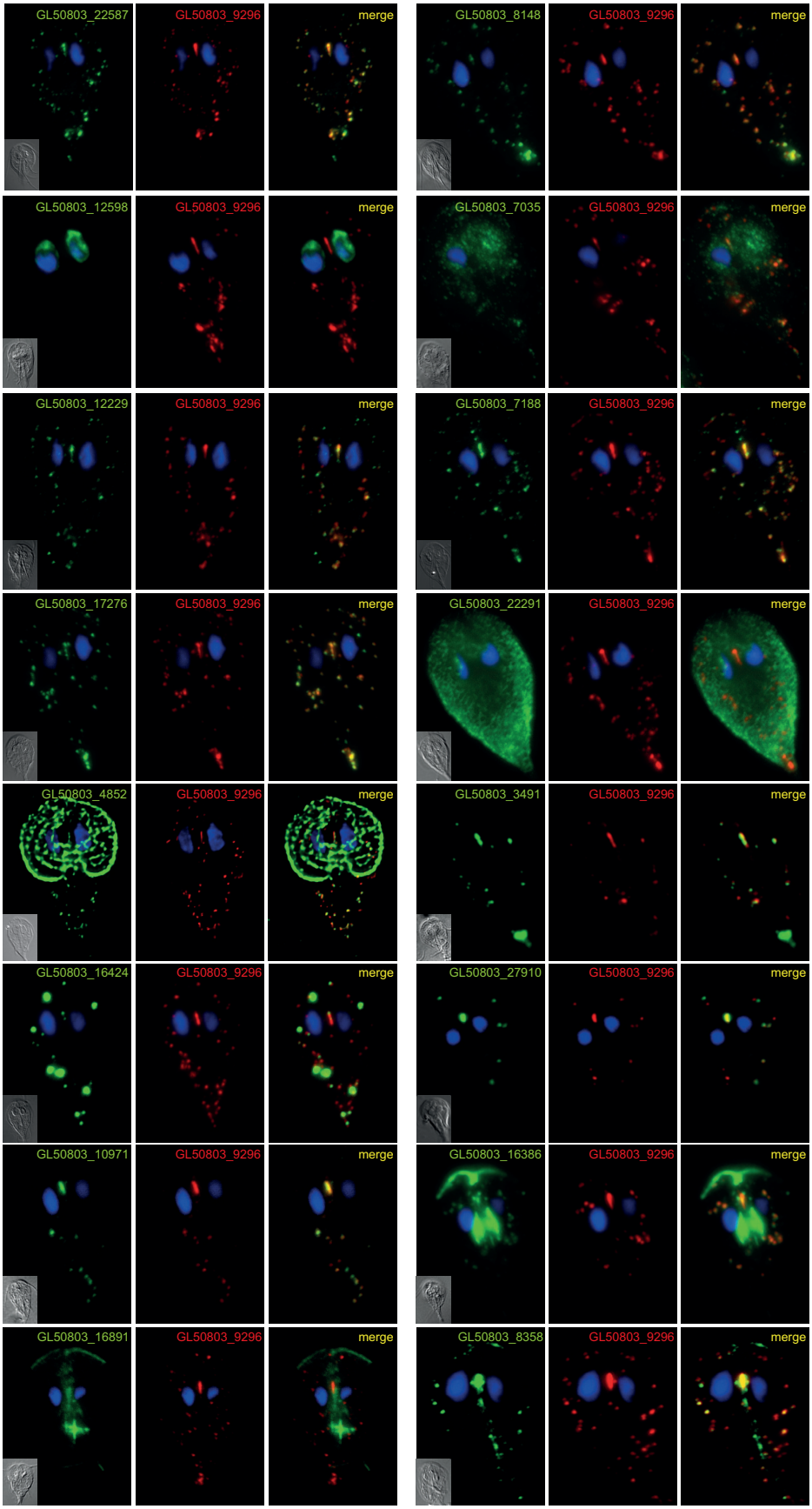

FIG 4 Localization of putative mitosomal proteins. Selected HA-tagged proteins were expressed in *Giardia*, and their cellular localization was determined using immunofluorescence microscopy. The cells were stained with anti-HA tag (green) and anti-GL50803_9296 (red) antibodies. Nuclei were stained with DAPI (blue).

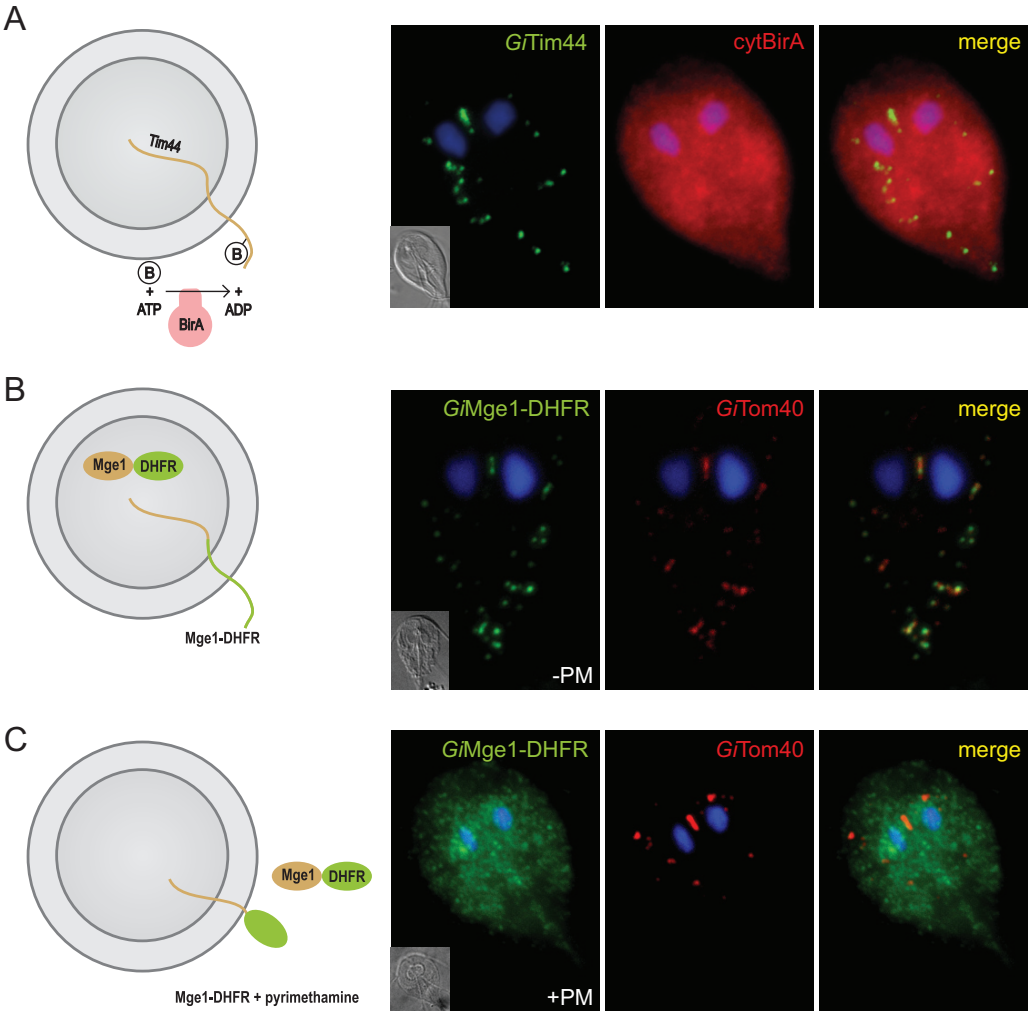

FIG 5 Mitosomal proteins are transported posttranslationally and in an unfolded state. BAP-tagged *Gi*Tim44 was coexpressed with cytosolic BirA (cytBirA), and the biotinylation of the tag was observed using fluorescence microscopy. Cells were stained with an anti-HA tag antibody (red) to detect cytBirA and with streptavidin-conjugated Alexa Fluor 488 (green) to detect the biotinylation of the BAP tag. Nuclei were stained with DAPI (blue). (A) A fusion protein of mouse DHFR, mitosomal *Gi*Mge1, and a C-terminal HA tag was expressed in *Giardia*. (B and C) The localization of the chimeric construct was assessed in the absence (B) or presence (C) of 100 μM pyrimethamine (+PM), which induces the folding of the DHFR domain. The cells were stained with anti-HA (green) and anti-*Gi*Tom40 antibodies (red). Nuclei were stained with DAPI (blue).

The only known outer mitosomal membrane protein has been *Gi*Tom40. This eukaryotic porin is a hallmark of all mitochondria (49), in which it constitutes the general import pore (18, 50) and interacts with the components of the SAM and ERMES complexes (51). The purification of *Gi*Tom40 led to the identification of *Gi*MOMP35. The protein had already been identified in giardial mitosomes, but neither its localization within the mitosome nor its topology had been determined (7). According to our results, the *Gi*MOMP35 protein is anchored in the outer mitosomal membrane with its C-terminal domain exposed to the cytosol. The phenotype of mitochondrial aggregation triggered by the overexpression of *Gi*MOMP35 is reminiscent of the overexpression of some of the outer membrane proteins involved in protein import (52) or mitochondrial dynamics (53). However, without further characterization of its C-terminal domain, the exact function of *Gi*MOMP35 in mitosome biology will remain unknown. This protein is exclusive to *Giardia*; no related sequences have been found in *S. salmonicida* or in other parasitic or free-living metamonads.

Due to the presence of Tom40 in the outer mitosomal membrane, the occurrence of Sam50 was expected (54). Sam50 is an essential component of the SAM complex, the β-barrel protein folding machine (55) that is considered an important evolutionary feature linking mitochondria to Gram-negative bacteria (56). Despite the omnipresence of Sam50 in eukaryotes, no ortholog has been identified in the *Giardia* genome (18) or among the proteins that copurified with *Gi*Tom40 or *Gi*MOMP35 in the present work. Surprisingly, while missing in the *G. intestinalis* and *S. salmonicida* genomes, Sam50 orthologs are present in the expressed sequence tag (EST) data of *C. membranifera* and *E. cyprinoides* (M. Kolísko and A. J. Roger, unpublished results). This strongly suggests that the unique loss of Sam50 in the evolution of eukaryotes occurred in the common ancestor of diplomonads.

However, 5 of the 13 novel mitosomal proteins seem to be

specific to the outer mitosomal membrane, as these were exclusive to *Gi*Tom40- and *Gi*MOMP35-derived data sets. Further investigation of these proteins may bring more information on the biogenesis of the outer mitosomal membrane as well as on the interaction between the mitosomes and other cellular organelles.

In general, the identification of novel mitosomal proteins, the vast majority of which are specific to *Giardia*, demonstrates that metabolic processes other than the formation of iron-sulfur clusters occur in mitosomes. The presence of a rhodanese ortholog indicates the existence of additional sulfur metabolism at a minimum. In addition, the striking presence of an Mlf1IP ortholog in mitosomes may shed light on the exact function of the protein, for which a precise role has not been assigned in the Metazoa.

In addition to the identification of new proteins, the techniques used in this study enabled us to demonstrate that proteins maintain an unfolded state while traveling to mitosomes posttranslationally. However, no sign of mixing of the ER and mitosome lumina was detected. The reported mitosomal localization of *Giardia* Sec20 ortholog indicated that a vesicular transport may play a role in mitosomal protein import (39). Our data on the localization of the endogenous Sec20 (not shown in this work) using specific polyclonal antibody indicate that its mitosomal localization is a result of experimental artifact, a phenomenon often observed for the overexpression of tail-anchored proteins. These results provide new evidence that mitosomal biogenesis follows the same rules as mitochondrial biogenesis despite the absence of some of the core components.

Taken together, the data presented here demonstrate that techniques such as *in vivo* enzymatic tagging are extremely valuable tools to investigate the biology of organelles as small as *Giardia* mitosomes. The identification of *Giardia*-specific proteins also demonstrates that our current concept of mitosomes as highly simplified mitochondria may not entirely reflect the true biology of these organelles. Future studies will likely reveal yet-unknown mitosomal functions.

ACKNOWLEDGMENTS

We thank Veronika Klápštová, Vladimíra Najdrová, and Zuzana Drašnarová for valuable technical assistance.

This work was funded by a grant from the Czech Science Foundation (P305-10-0651), by the European Regional Development Fund to the Biomedicine Center of the Academy of Sciences and Charles University (CZ.1.05/1.1.00/02.0109), and by a grant from Charles University Grant Agency (98214).

REFERENCES

1. **Adam RD.** 2001. Biology of Giardia lamblia. Clin Microbiol Rev **14:**447–475. http://dx.doi.org/10.1128/CMR.14.3.447-475.2001.
2. **Ankarklev J, Jerlström-Hultqvist J, Ringqvist E, Troell K, Svärd SG.** 2010. Behind the smile: cell biology and disease mechanisms of Giardia species. Nat Rev Microbiol **8:**413–422. http://dx.doi.org/10.1038/nrmicro2317.
3. **Hehl AB, Marti M.** 2004. Secretory protein trafficking in Giardia intestinalis. Mol Microbiol **53:**19–28. http://dx.doi.org/10.1111/j.1365-2958.2004.04115.x.
4. **Lanfredi-Rangel A, Attias M, de Carvalho TM, Kattenbach WM, De Souza W.** 1998. The peripheral vesicles of trophozoites of the primitive protozoan Giardia lamblia may correspond to early and late endosomes and to lysosomes. J Struct Biol **123:**225–235. http://dx.doi.org/10.1006/jsbi.1998.4035.
5. **Konrad C, Spycher C, Hehl AB.** 2010. Selective condensation drives partitioning and sequential secretion of cyst wall proteins in differentiating Giardia lamblia. PLoS Pathog **6:**e1000835. http://dx.doi.org/10.1371/journal.ppat.1000835.
6. **Dolezal P, Smíd O, Rada P, Zubácová Z, Bursać D, Suták R, Nebesárová J, Lithgow T, Tachezy J.** 2005. Giardia mitosomes and trichomonad hydrogenosomes share a common mode of protein targeting. Proc Natl Acad Sci U S A **102:**10924–10929. http://dx.doi.org/10.1073/pnas.0500349102.
7. **Jedelský PL, Doležal P, Rada P, Pyrih J, Smíd O, Hrdý I, Sedinová M, Marcinčiková M, Voleman L, Perry AJ, Beltrán NC, Lithgow T, Tachezy J.** 2011. The minimal proteome in the reduced mitochondrion of the parasitic protist Giardia intestinalis. PLoS One **6:**e17285. http://dx.doi.org/10.1371/journal.pone.0017285.
8. **Regoes A, Zourmpanou D, León-Avila G, van der Giezen M, Tovar J, Hehl AB.** 2005. Protein import, replication, and inheritance of a vestigial mitochondrion. J Biol Chem **280:**30557–30563. http://dx.doi.org/10.1074/jbc.M500787200.
9. **Roger AJ, Svärd SG, Tovar J, Clark CG, Smith MW, Gillin FD, Sogin ML.** 1998. A mitochondrial-like chaperonin 60 gene in Giardia lamblia: evidence that diplomonads once harbored an endosymbiont related to the progenitor of mitochondria. Proc Natl Acad Sci U S A **95:**229–234. http://dx.doi.org/10.1073/pnas.95.1.229.
10. **Tachezy J, Sánchez LB, Müller M.** 2001. Mitochondrial type iron-sulfur cluster assembly in the amitochondriate eukaryotes Trichomonas vaginalis and Giardia intestinalis, as indicated by the phylogeny of IscS. Mol Biol Evol **18:**1919–1928. http://dx.doi.org/10.1093/oxfordjournals.molbev.a003732.
11. **Likic VA, Dolezal P, Celik N, Dagley M, Lithgow T.** 2010. Using hidden markov models to discover new protein transport machines. Methods Mol Biol **619:**271–284. http://dx.doi.org/10.1007/978-1-60327-412-8_16.
12. **Sickmann A, Reinders J, Wagner Y, Joppich C, Zahedi R, Meyer HE, Schönfisch B, Perschil I, Chacinska A, Guiard B, Rehling P, Pfanner N, Meisinger C.** 2003. The proteome of Saccharomyces cerevisiae mitochondria. Proc Natl Acad Sci U S A **100:**13207–13212. http://dx.doi.org/10.1073/pnas.2135385100.
13. **Schneider RE, Brown MT, Shiflett AM, Dyall SD, Hayes RD, Xie Y, Loo JA, Johnson PJ.** 2011. The Trichomonas vaginalis hydrogenosome proteome is highly reduced relative to mitochondria, yet complex compared with mitosomes. Int J Parasitol **41:**1421–1434. http://dx.doi.org/10.1016/j.ijpara.2011.10.001.
14. **Panigrahi AK, Ogata Y, Zíková A, Anupama A, Dalley RA, Acestor N, Myler PJ, Stuart KD.** 2009. A comprehensive analysis of Trypanosoma brucei mitochondrial proteome. Proteomics **9:**434–450. http://dx.doi.org/10.1002/pmic.200800477.
15. **Wampfler PB, Tosevski V, Nanni P, Spycher C, Hehl AB.** 2014. Proteomics of secretory and endocytic organelles in Giardia lamblia. PLoS One **9:**e94089. http://dx.doi.org/10.1371/journal.pone.0094089.
16. **Keister DB.** 1983. Axenic culture of Giardia lamblia in TYI-S-33 medium supplemented with bile. Trans R Soc Trop Med Hyg **77:**487–488. http://dx.doi.org/10.1016/0035-9203(83)90120-7.
17. **Martincová E, Voleman L, Najdrová V, De Napoli M, Eshar S, Gualdron M, Hopp CS, Sanin DE, Tembo DL, Van Tyne D, Walker D, Marcinčiková M, Tachezy J, Doležal P.** 2012. Live imaging of mitosomes and hydrogenosomes by HaloTag technology. PLoS One **7:**e36314. http://dx.doi.org/10.1371/journal.pone.0036314.
18. **Dagley MJ, Dolezal P, Likic VA, Smid O, Purcell AW, Buchanan SK, Tachezy J, Lithgow T.** 2009. The protein import channel in the outer mitosomal membrane of Giardia intestinalis. Mol Biol Evol **26:**1941–1947. http://dx.doi.org/10.1093/molbev/msp117.
19. **Howarth M, Takao K, Hayashi Y, Ting AY.** 2005. Targeting quantum dots to surface proteins in living cells with biotin ligase. Proc Natl Acad Sci U S A **102:**7583–7588. http://dx.doi.org/10.1073/pnas.0503125102.
20. **Gehde N, Hinrichs C, Montilla I, Charpian S, Lingelbach K, Przyborski JM.** 2009. Protein unfolding is an essential requirement for transport across the parasitophorous vacuolar membrane of Plasmodium falciparum. Mol Microbiol **71:**613–628. http://dx.doi.org/10.1111/j.1365-2958.2008.06552.x.
21. **Rada P, Doležal P, Jedelský PL, Bursac D, Perry AJ, Šedinová M, Smíšková K, Novotný M, Beltrán NC, Hrdý I, Lithgow T, Tachezy J.** 2011. The core components of organelle biogenesis and membrane transport in the hydrogenosomes of Trichomonas vaginalis. PLoS One **6:**e24428. http://dx.doi.org/10.1371/journal.pone.0024428.
22. **Söding J, Biegert A, Lupas AN.** 2005. The HHpred interactive server for protein homology detection and structure prediction. Nucleic Acids Res **33:**W244–W248. http://dx.doi.org/10.1093/nar/gki408.
23. **Eddy SR.** 2011. Accelerated profile HMM searches. PLoS Comput Biol **7:**e1002195. http://dx.doi.org/10.1371/journal.pcbi.1002195.

24. **Zhang Y.** 2008. I-TASSER server for protein 3D structure prediction. BMC Bioinformatics **9:**40. http://dx.doi.org/10.1186/1471-2105-9-40.
25. **Krogh A, Larsson B, von Heijne G, Sonnhammer EL.** 2001. Predicting transmembrane protein topology with a hidden Markov model: application to complete genomes. J Mol Biol **305:**567–580. http://dx.doi.org/10.1006/jmbi.2000.4315.
26. **Käll L, Krogh A, Sonnhammer ELL.** 2007. Advantages of combined transmembrane topology and signal peptide prediction—the Phobius web server. Nucleic Acids Res **35:**W429–W432. http://dx.doi.org/10.1093/nar/gkm256.
27. **Howarth M, Ting AY.** 2008. Imaging proteins in live mammalian cells with biotin ligase and monovalent streptavidin. Nat Protoc **3:**534–545. http://dx.doi.org/10.1038/nprot.2008.20.
28. **Chacinska A, van der Laan M, Mehnert CS, Guiard B, Mick DU, Hutu DP, Truscott KN, Wiedemann N, Meisinger C, Pfanner N, Rehling P.** 2010. Distinct forms of mitochondrial TOM-TIM supercomplexes define signal-dependent states of preprotein sorting. Mol Cell Biol **30:**307–318. http://dx.doi.org/10.1128/MCB.00749-09.
29. **Tieu Q, Okreglak V, Naylor K, Nunnari J.** 2002. The WD repeat protein, Mdv1p, functions as a molecular adaptor by interacting with Dnm1p and Fis1p during mitochondrial fission. J Cell Biol **158:**445–452. http://dx.doi.org/10.1083/jcb.200205031.
30. **Yoon Y, Krueger EW, Oswald BJ, McNiven MA.** 2003. The mitochondrial protein hFis1 regulates mitochondrial fission in mammalian cells through an interaction with the dynamin-like protein DLP1. Mol Cell Biol **23:**5409–5420. http://dx.doi.org/10.1128/MCB.23.15.5409-5420.2003.
31. **Merlin A, Voos W, Maarse AC, Meijer M, Pfanner N, Rassow J.** 1999. The J-related segment of tim44 is essential for cell viability: a mutant Tim44 remains in the mitochondrial import site, but inefficiently recruits mtHsp70 and impairs protein translocation. J Cell Biol **145:**961–972. http://dx.doi.org/10.1083/jcb.145.5.961.
32. **Ting S-Y, Schilke BA, Hayashi M, Craig EA.** 2014. Architecture of the TIM23 inner mitochondrial translocon and interactions with the matrix import motor. J Biol Chem **289:**28689–28696. http://dx.doi.org/10.1074/jbc.M114.588152.
33. **Brown A, Amunts A, Bai X-C, Sugimoto Y, Edwards PC, Murshudov G, Scheres SHW, Ramakrishnan V.** 2014. Structure of the large ribosomal subunit from human mitochondria. Science **346:**718–722. http://dx.doi.org/10.1126/science.1258026.
34. **Ott M, Prestele M, Bauerschmitt H, Funes S, Bonnefoy N, Herrmann JM.** 2006. Mba1, a membrane-associated ribosome receptor in mitochondria. EMBO J **25:**1603–1610. http://dx.doi.org/10.1038/sj.emboj.7601070.
35. **Lauwaet T, Davids BJ, Torres-Escobar A, Birkeland SR, Cipriano MJ, Preheim SP, Palm D, Svärd SG, McArthur AG, Gillin FD.** 2007. Protein phosphatase 2A plays a crucial role in Giardia lamblia differentiation. Mol Biochem Parasitol **152:**80–89. http://dx.doi.org/10.1016/j.molbiopara.2006.12.001.
36. **Cipollone R, Ascenzi P, Visca P.** 2007. Common themes and variations in the rhodanese superfamily. IUBMB Life **59:**51–59. http://dx.doi.org/10.1080/15216540701206859.
37. **Bonomi F, Pagani S, Cerletti P, Cannella C.** 1977. Rhodanese-mediated sulfur transfer to succinate dehydrogenase. Eur J Biochem **72:**17–24. http://dx.doi.org/10.1111/j.1432-1033.1977.tb11219.x.
38. **Ohno K, Takahashi Y, Hirose F, Inoue YH, Taguchi O, Nishida Y, Matsukage A, Yamaguchi M.** 2000. Characterization of a Drosophila homologue of the human myelodysplasia/myeloid leukemia factor (MLF). Gene **260:**133–143. http://dx.doi.org/10.1016/S0378-1119(00)00447-9.
39. **Elias EV, Quiroga R, Gottig N, Nakanishi H, Nash TE, Neiman A, Lujan HD.** 2008. Characterization of SNAREs determines the absence of a typical Golgi apparatus in the ancient eukaryote Giardia lamblia. J Biol Chem **283:**35996–36010. http://dx.doi.org/10.1074/jbc.M806545200.
40. **Eilers M, Schatz G.** 1986. Binding of a specific ligand inhibits import of a purified precursor protein into mitochondria. Nature **322:**228–232.
41. **Wang CC, Aldritt S.** 1983. Purine salvage networks in Giardia lamblia. J Exp Med **158:**1703–1712. http://dx.doi.org/10.1084/jem.158.5.1703.
42. **van der Giezen M, Tovar J.** 2005. Degenerate mitochondria. EMBO Rep **6:**525–530. http://dx.doi.org/10.1038/sj.embor.7400440.
43. **Clements A, Bursac D, Gatsos X, Perry AJ, Civciristov S, Celik N, Likic VA, Poggio S, Jacobs-Wagner C, Strugnell RA, Lithgow T.** 2009. The reducible complexity of a mitochondrial molecular machine. Proc Natl Acad Sci U S A **106:**15791–15795. http://dx.doi.org/10.1073/pnas.0908264106.
44. **Schey KL, Grey AC, Nicklay JJ.** 2013. Mass spectrometry of membrane proteins: a focus on aquaporins. Biochemistry **52:**3807–3817. http://dx.doi.org/10.1021/bi301604j.
45. **Xu F, Jerlström-Hultqvist J, Einarsson E, Astvaldsson A, Svärd SG, Andersson JO.** 2014. The genome of Spironucleus salmonicida highlights a fish pathogen adapted to fluctuating environments. PLoS Genet **10:**e1004053. http://dx.doi.org/10.1371/journal.pgen.1004053.
46. **Dolezal P, Dagley MJ, Kono M, Wolynec P, Likić VA, Foo JH, Sedinová M, Tachezy J, Bachmann A, Bruchhaus I, Lithgow T.** 2010. The essentials of protein import in the degenerate mitochondrion of Entamoeba histolytica. PLoS Pathog **6:**e1000812. http://dx.doi.org/10.1371/journal.ppat.1000812.
47. **Waller RF, Jabbour C, Chan NC, Celik N, Likic VA, Mulhern TD, Lithgow T.** 2009. Evidence of a reduced and modified mitochondrial protein import apparatus in microsporidian mitosomes. Eukaryot Cell **8:**19–26. http://dx.doi.org/10.1128/EC.00313-08.
48. **Handa N, Kishishita S, Morita S, Akasaka R, Jin Z, Chrzas J, Chen L, Liu Z-J, Wang B-C, Sugano S, Tanaka A, Terada T, Shirouzu M, Yokoyama S.** 2007. Structure of the human Tim44 C-terminal domain in complex with pentaethylene glycol: ligand-bound form. Acta Crystallogr D Biol Crystallogr **63:**1225–1234. http://dx.doi.org/10.1107/S0907444907051463.
49. **Zarsky V, Tachezy J, Dolezal P.** 2012. Tom40 is likely common to all mitochondria. Curr Biol **22:**R479–R481; author reply, R481–R482. http://dx.doi.org/10.1016/j.cub.2012.03.057.
50. **Baker KP, Schaniel A, Vestweber D, Schatz G.** 1990. A yeast mitochondrial outer membrane protein essential for protein import and cell viability. Nature **348:**605–609. http://dx.doi.org/10.1038/348605a0.
51. **Yamano K, Tanaka-Yamano S, Endo T.** 2010. Mdm10 as a dynamic constituent of the TOB/SAM complex directs coordinated assembly of Tom40. EMBO Rep **11:**187–193. http://dx.doi.org/10.1038/embor.2009.283.
52. **Yano M, Kanazawa M, Terada K, Namchai C, Yamaizumi M, Hanson B, Hoogenraad N, Mori M.** 1997. Visualization of mitochondrial protein import in cultured mammalian cells with green fluorescent protein and effects of overexpression of the human import receptor Tom20. J Biol Chem **272:**8459–8465. http://dx.doi.org/10.1074/jbc.272.13.8459.
53. **Rojo M, Legros F, Chateau D, Lombès A.** 2002. Membrane topology and mitochondrial targeting of mitofusins, ubiquitous mammalian homologs of the transmembrane GTPase Fzo. J Cell Sci **115:**1663–1674.
54. **Dolezal P, Likic V, Tachezy J, Lithgow T.** 2006. Evolution of the molecular machines for protein import into mitochondria. Science **313:**314–318. http://dx.doi.org/10.1126/science.1127895.
55. **Kozjak V, Wiedemann N, Milenkovic D, Lohaus C, Meyer HE, Guiard B, Meisinger C, Pfanner N.** 2003. An essential role of Sam50 in the protein sorting and assembly machinery of the mitochondrial outer membrane. J Biol Chem **278:**48520–48523. http://dx.doi.org/10.1074/jbc.C300442200.
56. **Gentle I, Gabriel K, Beech P, Waller R, Lithgow T.** 2004. The Omp85 family of proteins is essential for outer membrane biogenesis in mitochondria and bacteria. J Cell Biol **164:**19–24. http://dx.doi.org/10.1083/jcb.200310092.
57. **Josyula R, Jin Z, Fu Z, Sha B.** 2006. Crystal structure of yeast mitochondrial peripheral membrane protein Tim44p C-terminal domain. J Mol Biol **359:**798–804. http://dx.doi.org/10.1016/j.jmb.2006.04.020.
58. **Biasini M, Bienert S, Waterhouse A, Arnold K, Studer G, Schmidt T, Kiefer F, Cassarino TG, Bertoni M, Bordoli L, Schwede T.** 2014. SWISS-MODEL: modelling protein tertiary and quaternary structure using evolutionary information. Nucleic Acids Res **42:**W252–W258. http://dx.doi.org/10.1093/nar/gku340.

Molecular Microbiology (2016) 102(4), 701–714 ■
doi:10.1111/mmi.13487
First published online 6 September 2016

Minimal cytosolic iron-sulfur cluster assembly machinery of *Giardia intestinalis* is partially associated with mitosomes

Jan Pyrih,[1†] Eva Pyrihová,[1] Martin Kolísko,[2‡] Darja Stojanovová,[1] Somsuvro Basu,[3§] Karel Harant,[1] Alexander C. Haindrich,[3,4] Pavel Doležal,[1] Julius Lukeš,[3,4,5] Andrew Roger[2,5] and Jan Tachezy[1]*

[1]*Department of Parasitology, Charles University in Prague, Vestec 252 42, Czech Republic.*
[2]*Centre for Comparative Genomics and Evolutionary Bioinformatics, Department of Biochemistry and Molecular Biology, Dalhousie University, Halifax, NS B3H 4R2, Canada.*
[3]*Institute of Parasitology, Biology Centre, České Budějovice, Budweis 37005, Czech Republic.*
[4]*Faculty of Sciences, University of South Bohemia, České Budějovice, Budweis 37005, Czech Republic.*
[5]*Canadian Institute for Advanced Research, Toronto, ON M5G 1Z8, Canada.*

Summary

Iron-sulfur (Fe-S) clusters are essential cofactors that enable proteins to transport electrons, sense signals, or catalyze chemical reactions. The maturation of dozens of Fe-S proteins in various compartments of every eukaryotic cell is driven by several assembly pathways. The ubiquitous cytosolic Fe-S cluster assembly (CIA) pathway, typically composed of eight highly conserved proteins, depends on mitochondrial Fe-S cluster assembly (ISC) machinery. *Giardia intestinalis* contains one of the smallest eukaryotic genomes and the mitosome, an extremely reduced mitochondrion. Because the only pathway known to be retained within this organelle is the synthesis of Fe-S clusters mediated by ISC machinery, a likely function of the mitosome is to cooperate with the CIA pathway. We investigated the cellular localization of CIA components in *G. intestinalis* and the origin and distribution of CIA-related components and Tah18-like proteins in other Metamonada. We show that orthologs of Tah18 and Dre2 are missing in these eukaryotes. In *Giardia*, all CIA components are exclusively cytosolic, with the important exception of Cia2 and two Nbp35 paralogs, which are present in the mitosomes. We propose that the dual localization of Cia2 and Nbp35 proteins in *Giardia* might represent a novel connection between the ISC and the CIA pathways.

Accepted 21 August, 2016. *For correspondence E-mail tachezy@natur.cuni.cz; Tel. (+420) 325 873 144. Present addresses: †School of Biosciences, University of Kent, CT2 7NJ, United Kingdom; ‡Department of Botany, University of British Columbia, Vancouver, V6T 1Z4, Canada §Institut für Zytobiologie, Philipps-Universität Marburg, Marburg, 35032, Germany.

Introduction

Iron-sulfur (Fe-S) clusters are important cofactors found in a variety of proteins in each and every extant cell. The ability of these ancient cofactors to transfer electrons is essential for near-ubiquitous processes such as respiration, photosynthesis, isoprenoid biosynthesis, DNA metabolism and translation (Netz *et al.*, 2014; Tanaka *et al.*, 2015). The Fe-S cluster assembly is performed by dedicated machineries in several cellular compartments. The iron sulfur cluster (ISC) pathway is present in mitochondria, the sulfur mobilization pathway is confined to plastids, and the cytosolic iron-sulfur cluster assembly (CIA) is found in the cytosol. The CIA pathway is required for the maturation of all cytosolic and nuclear Fe-S cluster-containing proteins (Stehling *et al.*, 2012; Stehling *et al.*, 2013; Netz *et al.*, 2014). All eight components of this pathway identified thus far (Tah18, Dre2, Nbp35, Cfd1, Nar1, Cia1, Cia2 and MMS19) appear to be present in most eukaryotes. Initially, a transient [4Fe-4S] cluster is assembled on a cytosolic hetero-tetrameric scaffold complex composed of Cfd1 and Nbp35 (Hausmann *et al.*, 2005; Netz *et al.*, 2007, 2012), where it is coordinated by the bridging of two cysteine residues of Nbp35 to another two cysteines on Cfd1. In addition, Nbp35 binds another stable [4Fe-4S] cluster at its N terminus (Netz *et al.*, 2012). The transient cluster is then transferred to apoproteins with

the assistance of the hydrogenase-like protein Nar1 (Balk *et al*., 2004) and the CIA targeting complex formed by Cia1, Cia2 and MMS19 (Balk *et al*., 2005; Gari *et al*., 2012; Luo *et al*., 2012; Stehling *et al*., 2012). Coprecipitations and functional studies have revealed that the Cia1, Cia2 and MMS19 components are dedicated to the maturation of cytosolic and nuclear FeS proteins involved mainly in DNA metabolism (Stehling *et al*., 2012). Although a role of Cia2, a small protein containing the DUF59 domain with a highly conserved reactive cysteine residue (Weerapana *et al*., 2010), in cluster loading on a subset of cytosolic and nuclear Fe-S proteins has been described (Stehling *et al*., 2012), its precise function remains unknown.

Furthermore, an electron transfer chain composed of the NADPH-dependent diflavin oxidoreductase Tah18 and the Fe-S carrying Dre2 is required for the assembly of the [4Fe-4S] cluster on Nbp35 (Zhang *et al*., 2008; Netz *et al*., 2010). It was demonstrated that Tah18 enables electron transfer from NADPH to Dre2, from which electrons are then transferred to Nbp35 (Netz *et al*., 2010). Interestingly, several other alternative functions unrelated to Fe-S cluster synthesis, such as the control of mitochondrial integrity and cellular death (Vernis *et al*., 2009), and nitric oxide synthesis (Nishimura *et al*., 2013), as well as involvement in the synthesis of the diferric-tyrosyl radical cofactor of ribonucleotide reductase (Zhang *et al*., 2014), were suggested for the Tah18 and Dre2 proteins in yeast. It is noteworthy that Tah18 is highly similar to cytochrome p450 reductase and methionine synthase reductase, the shared features being similar length, an $NADP^+$ binding site and FMN and FAD redox centers, with the latter containing the CPR domain derived from the cytochrome p450 reductase-like domain (Netz *et al*., 2010; Jedelsky *et al*., 2011). Moreover, this domain is also part of several fusion proteins, such as nitric oxide synthase in metazoans and pyruvate:NADP+ oxidoreductase (PNO) in various protists (Rotte *et al*., 2001; Iyanagi *et al*., 2012).

In yeasts, human and plants, it has been shown that Fe-S cluster formation via the CIA pathway is dependent on the export of a still unknown sulfur-containing compound likely generated in mitochondria by the ISC machinery (Leighton and Schatz, 1995; Kispal *et al*., 1999; Lange *et al*., 2001; Mühlenhoff *et al*., 2004; Netz *et al*., 2014). The Atm1 and Erv1 proteins located in the inner mitochondrial membrane and the intermembrane space, respectively, were implicated in the export of this compound from the organelle (Kispal *et al*., 1999; Lange *et al*., 2001). Additionally, thiol-containing glutathione, an indispensable connection between the ISC and CIA pathways (Sipos *et al*., 2002; Srinivasan *et al*., 2014), is bound to Atm1 in the form of a cofactor and stimulates its ATPase activity (Kuhnke *et al*., 2006; Srinivasan *et al*., 2014). However, the exact mechanism of the export across the two mitochondrial membranes of this elusive sulfur-containing precursor required by the CIA pathway remains unknown (Lill *et al*., 2015).

Although our understanding of the CIA machinery in yeast, human and plant cells is increasing (Netz *et al*., 2014), only very limited information is available about how Fe-S clusters are assembled in the cytosol of anaerobic protists. Several components of the CIA machinery, such as Nbp35, Nar1, Cia1 and Cia2, are highly conserved across eukaryotes (Basu *et al*., 2013; Tsaousis *et al*., 2014), whereas Dre2 and Erv1 have been proposed to be absent in anaerobes (Basu *et al*., 2013). Moreover, although various anaerobic protists possess proteins with a CPR domain, similar to Tah18, their classification and functional characterization are challenging, because knock-down techniques have not typically been established for these organisms. Furthermore, human Tah18 protein was shown to interact with cytochromes *in vitro* similarly to cytochrome p450 reductase (Olteanu and Banerjee, 2003), casting doubt over the suitability of knock-in techniques to distinguish between these two proteins. To identify the Tah18 homologs, phylogenetic analysis was used to classify the CPR domain-containing proteins, although in anaerobes such as *Blastocystis* and *Giardia* resolution was limited due to their extensive divergence (Tsaousis *et al*., 2014).

As an adaptation to anaerobic environments and a parasitic lifestyle, *Giardia intestinalis*, a member of the phylum Metamonada, has reduced its mitochondria into mitosomes (Tovar *et al*., 2003; Doležal *et al*., 2005). The only pathway identified within this organelle to date is ISC-mediated Fe-S cluster synthesis (Jedelsky *et al*., 2011; Martincová *et al*., 2015). Furthermore, *G. intestinalis* possesses a minimalistic nuclear genome with only a few introns (Morrison *et al*., 2007), as well as simplified machineries for DNA replication, transcription, RNA processing, and most metabolic pathways (Morrison *et al*., 2007). The Atm1, Erv1 and Dre2 proteins are prominently absent from the *G. intestinalis* genome, whereas Nbp35, Nar1, Cia1 and Cia2 have been identified (Tsaousis *et al*., 2014). The CPR domain-containing GiOR-1 and GiOR-2 proteins are putative orthologs of Tah18 (Jedelsky *et al*., 2011; Basu *et al*., 2013; Tsaousis *et al*., 2014). Interestingly, GiOR-1, a possible reductase of cytosolic b_5 cytochromes (Pyrih *et al*., 2014), was previously identified in the mitosome, whereas GiOR-2 is associated with heretofore unidentified vesicles (Jedelsky *et al*., 2011).

It is noteworthy that in *G. intestinalis* many proteins are highly divergent (Morrison *et al*., 2007; Dagley *et al*., 2009), which limits or even hinders homology searches (Dagley *et al*., 2009; Martincová *et al*., 2015). However,

related free-living metamonads, such as *Trimastix* or *Carpediemonas*, tend to constitute shorter branches in molecular phylogenies and consequently appear to be less diverged and more suitable for this approach (Kolísko *et al*., 2010; Takishita *et al*., 2012).

Here, we show that Tah18, Dre2, Erv1, Atm1 and MMS19 are likely absent from metamonads, whereas Cfd1 could not be identified by homology searches in *G. intestinalis* and *Spironucleus* but is present in *Carpediemonas* and *Trichomonas vaginalis*. Moreover, we provide evidence that GiOR-1 and GiOR-2 likely perform cellular roles unrelated to those of Tah18. The cytosolic localization of Cia1, Nar1 and one paralog of Nbp35 was anticipated; however, the dual mitosomal and cytosolic localization of the other paralogs of Nbp35 and Cia2 was surprising.

Results

CIA components in metamonads

We performed homology searches for the CIA components in the genomes of metamonads *G. intestinalis*, *T. vaginalis* and *Spironucleus salmonicida* and in the EST data of other metamonads for which genomes are not available. The Nbp35, Nar1, Cia1 and Cia2 genes were present in all these protists (Fig. 1). The absence of some of core components in *Trimastix marina* (isolate PCT), *Spironucleus vortens*, *Ergobibamus cyprinoides* and *Carpediemonas*-like organism (CLO NY171) is most likely caused by insufficient sequence data coverage. Dre2 and MMS19 are most likely absent in metamonads, with the exception of a putative divergent MMS19 homolog in *T. marina* (Fig. 1). The Cfd1 protein is the only CIA component that showed a varied distribution across metamonads, as it was identified in *T. vaginalis*, *C. membranifera*, CLO NY171 and *Chilomastix cuspidata*, whereas it could not be identified by homology searches in *G. intestinalis* and *S. salmonicida* (Fig. 1). Because the latter two genera are more derived (Takishita *et al*., 2012), we propose that Cfd1 was present in the ancestor of all metamonads and was possibly lost only secondarily. Next, we searched for the CPR domain-containing proteins, possible Tah18 homologs. In addition to the GiOR proteins in *G. intestinalis*, similar Tah18-like proteins were identified in *Trepomonas* sp. (isolate PC1), *Dysnectes brevis*, and CLO NY171 (Fig. 1). Interestingly, in *T. vaginalis*, *C. membranifera*, *T. marina*, and *C. cuspidata*, we were able to identify only fusion genes of the CPR domain with hydrogenase. In *D. brevis*, both genes carrying the fusion hydrogenase and only the CPR domain are present. Although the presence of ABC transporters similar to the ISC and

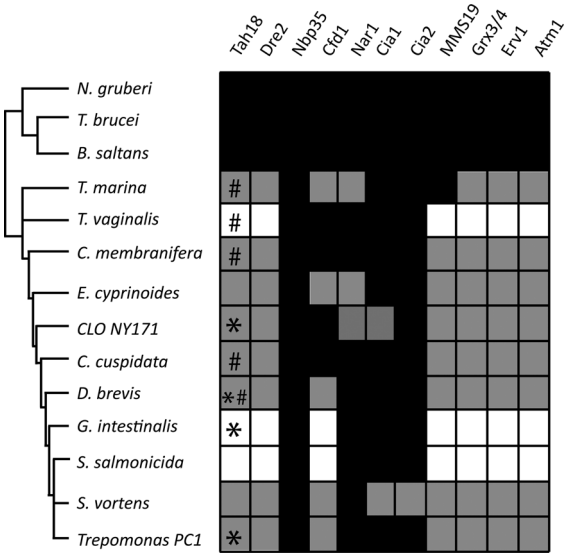

Fig. 1. Distribution of CIA machinery components in metamonads
The complete CIA pathway is present in selected members of the Kinetoplastea (*Trypanosoma brucei*, *Bodo saltans*) and Heterolobosea (*Naegleria gruberi*) groups. In metamonads, this pathway is reduced to a minimal set of proteins: Nbp35, Cfd1, Nar1, Cia1 and Cia2. The presence of an ortholog in the genome is denoted by black shading. The absence is indicated in white. Gray indicates that the gene is absent in the available EST database. For Tah18-like orthologs, the presence of similarly organized proteins or fusion with a hydrogenase-like domain is indicated by an asterisk or hash sign, respectively. Relationships between different eukaryotic groups is based on the current consensus (Takishita *et al*., 2012).

CIA linking proteins Erv1 and Atm1 was previously suggested in the *G. intestinalis* mitosome (Jedelsky *et al*., 2011), we were unable to identify any putative homologs of these two proteins.

Localization of CIA pathway components in Giardia

In the *G. intestinalis* genome, Nar1, Cia1 and Cia2 are encoded by single-copy genes, whereas Nbp35 is present in three similar copies, herein labeled Nbp35-1, Nbp35-2 and Nbp35-3. To investigate their subcellular localization, all these CIA components were expressed with a C-terminal HA-tag. In parallel, specific antibodies against the HA-tag or target proteins were used for immunofluorescence microscopy and probing of subcellular fractions.

To corroborate the previously observed mitosomal localization of the HA-tagged GiOR-1 (Jedelsky *et al*., 2011), polyclonal antibody was raised against this protein. Indeed, all specific signals were localized in the mitosomes (Fig. 2). Both immunofluorescence microscopy and western blot analysis of subcellular fractionation indicated cytosolic localization of Nar1, Cia1 and Nbp35-3 (Fig. 2). Interestingly, immunofluorescence

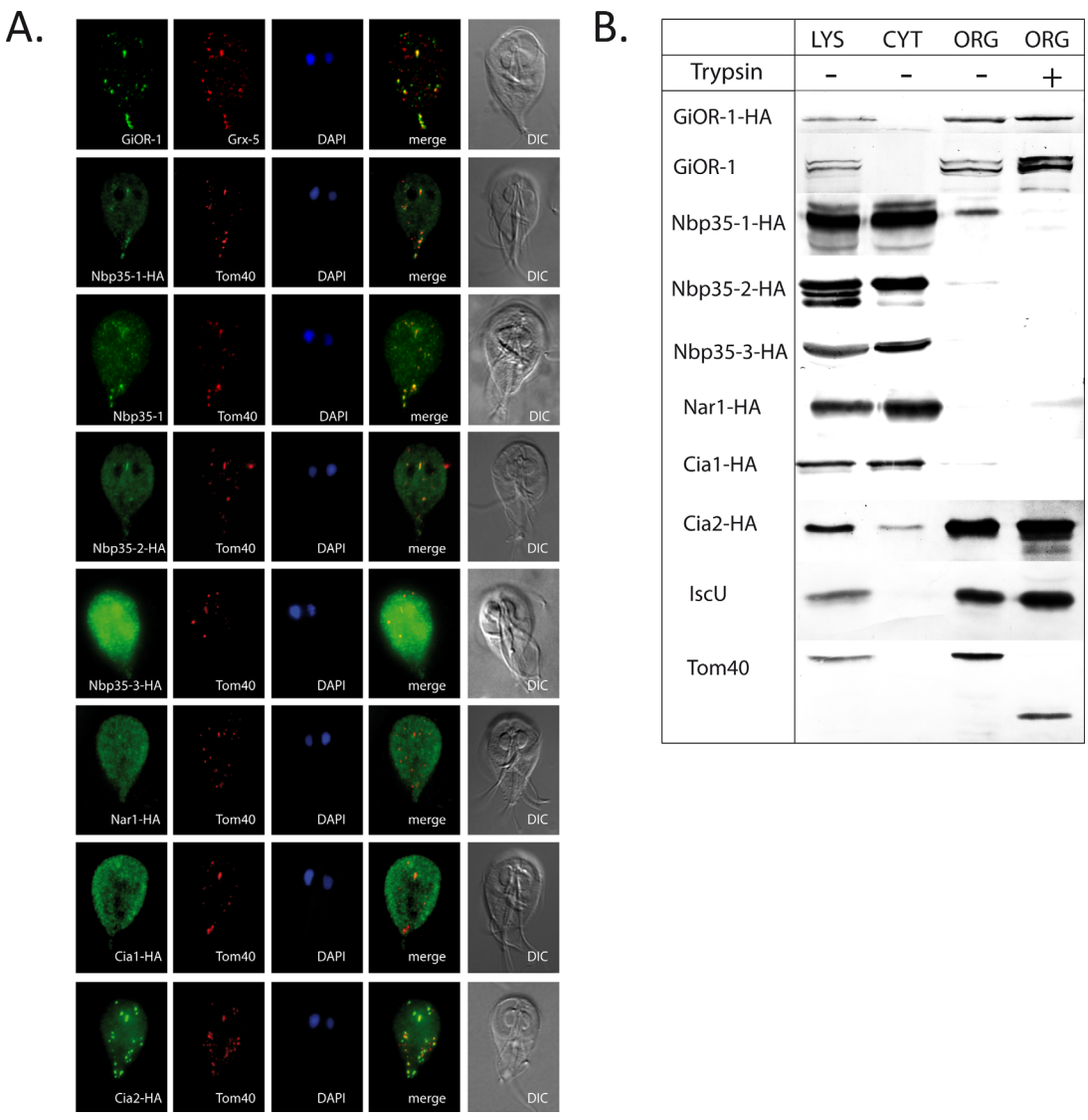

Fig. 2. Subcellular distribution of CIA pathway components in *G. intestinalis*
A. Localization of proteins of CIA pathway in *G. intestinalis* using immunofluorescence microscopy. α-HA rat antibody was used to detect HA-tagged proteins (green signal). Specific α-GiOR-1 rabbit and anti-Nbp35-1 rat polyclonal antibodies were used to detect GiOR-1 and Nbp35-1, respectively, in wild-type cells. Grx5, Tom40 and IscU were used as markers for the mitosomal outer membrane and matrix, respectively. The proteins were detected by polyclonal rabbit α-Tom40 and α-IscU antibodies. Nuclei were stained with DAPI (blue). DIC, differential interference contrast.
B. Western blot analysis of subcellular fractions. The same primary antibodies indicated above were used. Trypsin treatment of the organellar fraction is indicated by "+" (protein protection assay). LYS, cell lysate; CYT, cytosol; ORG, mitosome-containing organellar fraction.

analysis of Cia2 revealed its partial association with the mitosomes (Fig. 2A), an observation further confirmed by subcellular fractionation, which clearly localized a portion of the Cia2 signal within the organellar fraction (Fig. 2B). Moreover, protein protection assay using trypsinization of the organellar sample revealed that Cia2 is present inside of the organelles. Similarly, Nbp35-1 and Nbp35-2 possess dual cytosolic and mitosomal localization, as observed by immunofluorescence. Moreover, a faint band and a barely detectable band corresponding to Nbp35-1 and Nbp35-2, respectively, were associated with the organellar fraction. However, following trypsinization of the samples, both Nbp35-1 and Nbp35-2 bands were lost (Fig. 2B), similarly to the integral outer mitosomal membrane marker protein Tom40, the cytosolic part of which was digested upon the addition of trypsin (Martincová *et al.*, 2015; Fig. 2B). This finding suggests that both Nbp35-1 and Nbp35-2 most likely have dual localization, being distributed in the cytosol and associated with the outer mitosomal membrane.

The dual localization of Nbp35-1 was further confirmed using the α-Nbp35-1 antibody (Fig. 2A). To address the possibility of its interaction with mitosome-associated CIA components, the localization of GiOR-1 was investigated in greater detail. Together with the results from immunofluorescence, a protease protection assay performed using the α-GiOR-1 antibody convincingly showed that GiOR-1 is an inner mitosomal protein (Fig. 2A and B).

Intramitosomal distribution of Cia2 and GiOR-1

No technique for mitosome subfractionation is currently available. To better understand the exact topology of Cia2 and GiOR-1 within the mitosome, an *in vivo* biotinylation assay followed by precipitation of interacting proteins, a technique recently established for *G. intestinalis* (Martincová *et al*., 2015), was performed. Briefly, the protein of interest is expressed as a fusion protein with a biotin acceptor peptide (BAP) in a cell line coexpressing cytosolic biotin ligase (cBirA). cBirA biotinylates BAP-tagged proteins that are in the cytosol as well as proteins that are post-translationally targeted to mitosomes (Martincová *et al*., 2015). Thus, the protein of interest is biotinylated *in vivo*; the sample is treated with dithiobis succinimidyl propionate (DSP), a membrane-permeable cross-linking reagent; and the complex composed of the protein of interest and its interacting partners is purified using streptavidin-coupled magnetic beads. The samples are washed under highly stringent condition of 2% sodium dodecyl sulfate and analyzed by mass spectrometry. The same procedure is performed with wild-type *Giardia* and cells overexpressing BirA protein only, and proteins identified in these negative controls are subtracted from the dataset that was obtained with the lineage expressing BAP-tagged proteins (Supporting Infromation Table S1).

The majority of the proteins identified upon the purification of putative interacting partners of GiOR-1 are homologs of mitochondrial matrix proteins (Fig. 3A). These proteins are involved in mitochondrial protein import and maturation (Hsp70, Hsp60, Tim44 and giardial processing peptidase) or the ISC machinery (IscS, Nfu and glutaredoxin 5).

In contrast, coprecipitation of Cia2 from the mitosome-containing fraction did not reveal any known mitosomal matrix proteins among its putative interaction partners (Fig. 3B). However, all identified proteins were previously found to coprecipitate with integral outer mitosomal membrane proteins Tom40 and GiMOMP35 (Martincová *et al*., 2015; Fig. 3B). Together with the finding that Cia2 is present within the mitosome (Fig. 2B), the identification of its interacting partners strongly points toward localization of the mitosomal fraction of Cia2 in the intermembrane space.

Functional characterization of GiOR-1 and GiOR-2 in Trypanosoma brucei

To functionally address the putative relatedness between the GiOR and Tah18 proteins (GiOR-1, and GiOR-2 displayed 17.5%, and 19% amino acid sequence identities when compared with *T. brucei* Tah18, respectively), the ability of both GiOR proteins to rescue the Tah18-dependent activity in the CIA pathway of *T. brucei* was tested. In the procyclic stage of *T. brucei*, RNAi-mediated depletion of either *Tb*Tah18 or *Tb*Dre2 did not result in a growth phenotype, likely because of the insufficient downregulation of the target protein (Basu *et al*., 2014). Nevertheless, the essentiality of these proteins in the CIA machinery was demonstrated by the RNAi double knock-down of *Tb*Tah18 and *Tb*Dre2 (Basu *et al*., 2014). The expression of HA-tagged GiORs in *T. brucei* lacking both *Tb*Tah18 and *Tb*Dre2 resulted in a slight rescue of the growth phenotype (Fig. 4A.). Taken together, growth of both rescue cell-lines is ameliorated compared with that of the *Tb*Tah18-*Tb*Dre2 double RNAi mutant line (the cumulative density of the *Tb*Tah18-*Tb*Dre2 double RNAi-non-induced strain was below 10 log cells/ml after 10 days of RNAi induction, but for the GiOR-1 or GiOR-2 rescue strains the growth attained 10 log cells/ml or above, respectively) (Fig. 4A). Next, we wondered whether the Fe-S cluster-dependent activity of a cytosolic enzyme has been rescued by expression of the heterologous protein from *Giardia*. For this purpose, the activity of the cytosolic enzyme aconitase that carries [4Fe-4S] clusters was measured following a protocol described elsewhere (Long *et al*., 2011). Indeed, a strong rescue of its activity was observed in trypanosomes expressing either GiOR-1 or GiOR-2, where >50 or 40% revival was achieved, respectively (Fig. 4B). As an internal control, the measurement of mitochondrial aconitase activity showed that in this cellular compartment it remained unaffected (Fig. 4B).

The function of Tah18 is dependent on the interaction with Dre2 within the same cellular compartment (cytosol); however, in Giardia, GiOR-1 is present in mitosomes, whereas GiOR-2 is in multiple vesicles of unclear character (Jedelsky *et al*., 2011). Therefore, we investigated localization of HA-tagged GiOR proteins in *T. brucei*. Both proteins were present exclusively in the cytosolic cellular fraction (Fig. 4C), which is in agreement with their ability to partially complement the *Tb*Tah18-*Tb*Dre2 double RNAi knock down. However, the difference in the cellular localization of GiOR

A.

Name of the protein	G.I. number	TM	UP	Pam 18	Tim 44	Hsp 70	Tom 40	Momp 35	Cia 2
GiOR-1	GL50803_91252	0	7			■			
Hsp70	GL50803_14581	0	9	■	■	■	■	■	
Cpn60	GL50803_103891	0	8	■	■	■	■	■	
IscS	GL50803_14519	0	4		■	■	■	■	
GPP	GL50803_9478	0	3	■	■	■	■		
Glutaredoxin 5	GL50803_2013	0	3	■	■	■	■		
Tim44	GL50803_14845	0	2	■	■	■			
Hypothetical	GL50803_3491	0	2		■	■			
Nfu	GL50803_32838	0	2	■				■	
Ferredoxin	GL50803_27266	0	2		■	■		■	
Rhodanese like	GL50803_27910	0	2	■		■			
Hypothetical	GL50803_3582	0	2			■	■		

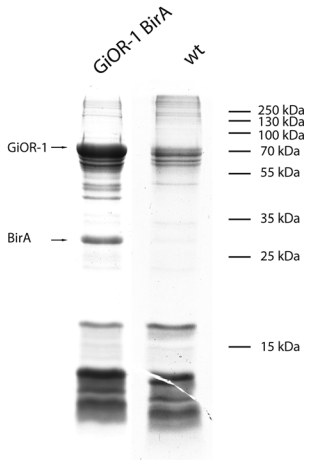

B.

Name of the protein	G.I. number	TM	UP	Pam 18	Tim 44	Hsp 70	Tom 40	Momp 35	GiOR 1
Cia2	GL50803_8819	0	7						
Hypothetical	GL50803_17249	0	7				■		
Hypothetical	GL50803_113603	0	4			■		■	
Carboxy peptidase (putative)	GL50803_10976	0	3					■	
Multidrug MFS transporter	GL50803_8444	11	3			■		■	
Hypothetical	GL50803_94542	1	2			■	■		
Hypothetical	GL50803_7723	0	2			■		■	
Myeloid leukemia factor	GL50803_16424	0	2	■	■	■			
Hypothetical	GL50803_16648	0	2			■	■	■	

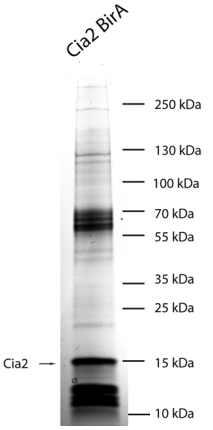

Fig. 3. Identification of GiOR-1 and Cia2 interacting proteins in mitosome.
A1. List of proteins coprecipitated with GiOR-1. GPP, *Giardia* processing peptidase; IscS, cysteine desulfurase; Thioredoxin red, Thioredoxin reductase; S/T kinase, Serine/Threonine kinase. A2. A representative SDS-PAGE analysis of proteins coprecipitated with GiOR-1 is displayed. GiOR-1 was biotinylated by cytosolic BirA (GiOR-1 BirA). wt, control sample of proteins precipitated from wild-type cells. Following SDS-PAGE, the proteins were submitted to mass spectrometry.
B1. List of proteins co-precipitated with mitosomal biotinylated Cia2 protein. B2. Representative SDS-PAGE analysis of proteins coprecipitated with biotinylated Cia2 (Cia2 BirA), and the control sample (wt).
TM, number of transmembrane domains predicted by TMHMM transmembrane prediction software; UP, number of unique peptides identified by mass spectrometry analysis for a given protein. The presence of protein precipitated with GiOR-1 (A) and Cia2 (B) in the interactome of Pam18, Tim44, Hsp70, Tom40, Momp35 (Martincová *et al.*, 2015) and Cia2, and GiOR-1 (this study) is denoted in black; absence is indicated in white. Acc. number, accession number according to GiardiaDB (giardiadb.org).

proteins between *G. intestinalis* and *T. brucei* is surprising. Particularly, the mode of the protein targeting to mitochondria and mitosomes via N-terminal targeting presequences have been shown to be conserved (Doležal *et al.*, 2005). In GiOR-1, there is not obvious N-terminal targeting presequence (Jedelsky *et al.*, 2011), although PSORT II software predicted a putative cleavage site for the mitochondrial processing peptidase between 29th and 30th amino acid residues. Therefore, we tested the cellular localization of the truncated GiOR-1 with deleted 29 amino acid residues at the N-terminus. The truncated GiOR-1 was associated with mitosomes and significant part of the protein was found inside of these organelles (Supporting Information Figure S1). These results suggest that GiOR-1 is targeted to the mitosomes via internal targeting signal, which is not recognized in *T. brucei*.

Phylogeny-based classification of CPR domain-containing proteins in metamonada

To assess the evolution of Tah18-like proteins in Metamonada, we performed a phylogenetic analysis using the CPR domains of various proteins encoded by the representatives of all eukaryotic supergroups. The phylogenetic analysis revealed that the Tah-18-like proteins, including GiOR-1 and GiOR-2, clustered with the CPR-hydrogenase fusion proteins of metamonads and

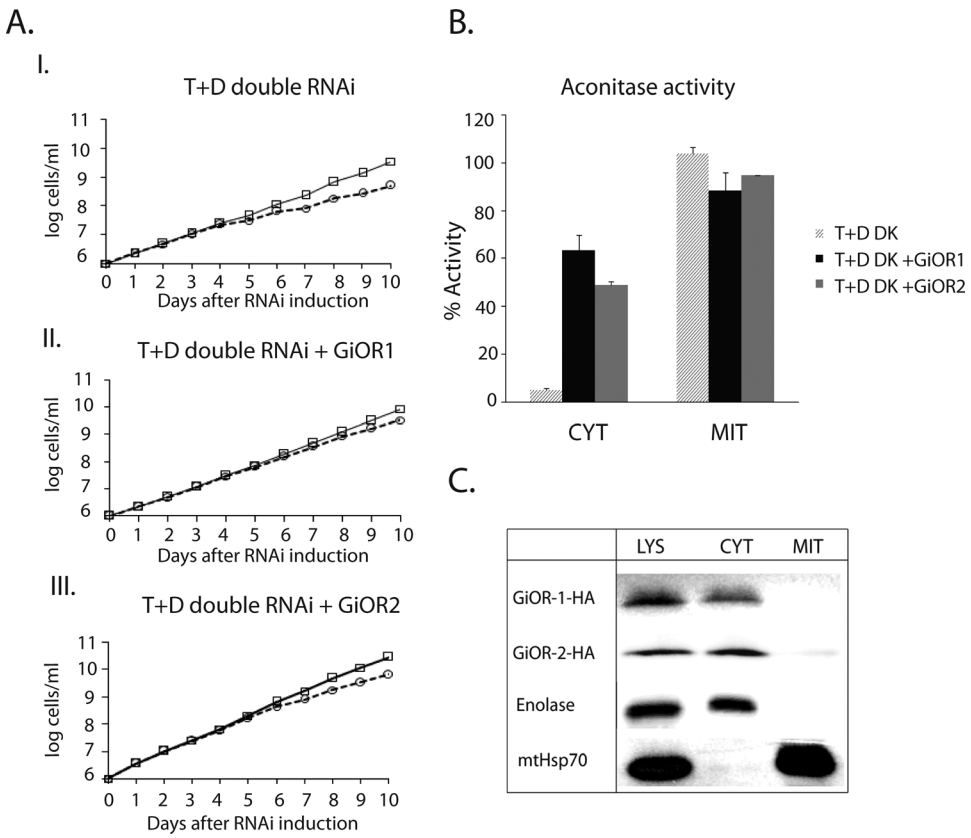

Fig. 4. GiOR rescue experiment in *Trypanosoma brucei*
A. Tah18 and Dre2 knock-down phenotype can be rescued by expressing GiOR-1 and GiOR-2 proteins. A. Growth of *T. brucei* RNAi cell lines is partially rescued by expression of the GiOR proteins. The cumulative density of the cells is indicated by a solid line (non-induced) or broken line (induced). I. The *Tb*Tah18-*Tb*Dre2 double RNAi strain presents a moderate growth effect upon RNAi induction. II & III. The double-RNAi-generated growth effect is partially rescued by the GiOR1 and GiOR2 proteins, respectively. Standard deviations calculated for each time point were below ±0.5 log cell/ml.
B. Aconitase activity is restored in the cytosol of *T. brucei* RNAi cell lines upon expression of GiOR proteins. Measurement was performed after 6 days of RNAi induction. % Activity expresses relative activity determined in RNAi induced cells when the activity in noninduced cells have been set as 100%. Error bars represent standard deviation calculated from three independent experiments. TbTD, *Tb*Tah18-*Tb*Dre2 double RNAi inducible strain; CYT, cytosolic fraction; MIT, mitochondrial fraction.
C. Cellular localization of GiOR proteins in the *Tb*Tah18-*Tb*Dre2 double RNAi strain. HA-tagged GiOR proteins were detected in cellular fractions using western blot analysis. Enolase, and mitochondrial Hsp70 were used as cytosolic, and mitochondrial marker proteins, respectively. LYS, cellular lysate; CYT, cytosolic fraction; MIT, mitochondrial fraction.

Mastigamoeba balamuthi (Nývltová *et al.*, 2015), whereas the Tah18 homologs in all other organisms formed a distinct branch (Fig. 5).

The hydrogenase domain of the CPR-hydrogenase fusion protein in *T. vaginalis* was suggested to correspond to the hydrogenase-like protein Nar1 (Basu *et al.*, 2013). Indeed, similarly to Nar1, the *T. vaginalis* protein possesses a mutated HC1 site for H-cluster binding and therefore likely does not function as a standard hydrogenase (Peters *et al.*, 1998; Basu *et al.*, 2013); however, no corresponding phylogenetic analysis has been performed to date. Therefore, we searched for the evolutionary origin of the N-terminal hydrogenase-like domain of the CPR-hydrogenase fusion proteins in metamonads. The obtained results indicate that these proteins are derived from hydrogenases and not from Nar1 (Supporting Information Figure S2). In contrast to the *T. vaginalis* homologue, the motif for H cluster binding (TSCCP) is present in CPR-hydrogenase fusion proteins of other metamonads (Supporting Information Figure S2).

Discussion

Distribution of CIA pathway components in metamonada

Searches for components of the CIA pathway in the genomes of model excavate protists, such as *T. brucei*, *Naegleria gruberi* and *Bodo saltans*, revealed a complete set of proteins (Basu *et al.*, 2014; Tsaousis *et al.*, 2014; Jackson *et al.*, 2016; Fig. 1). In contrast, the same search for CIA homologs in Metamonada, which

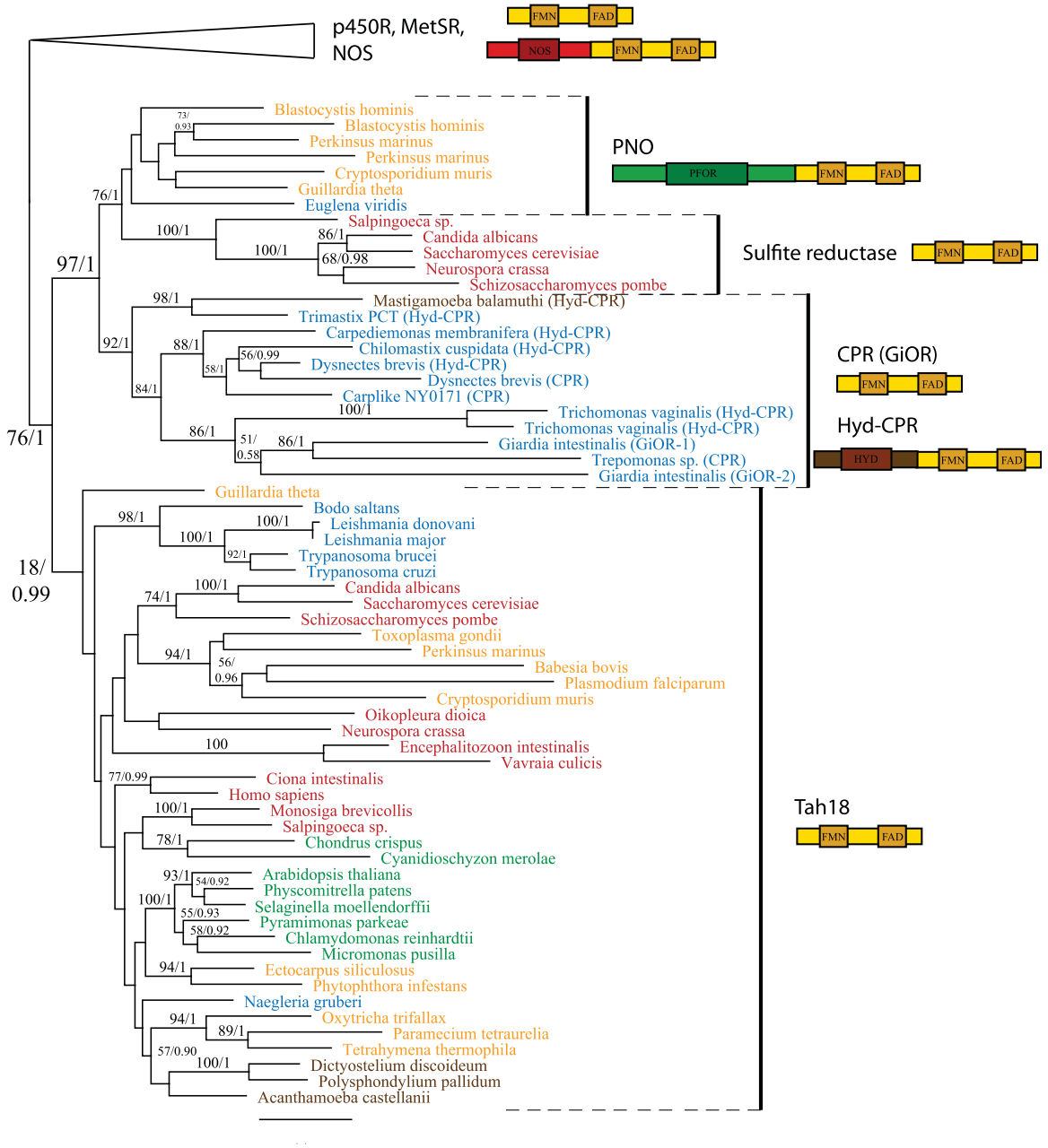

Fig. 5. Phylogeny of CPR domain containing proteins.
Maximum likelihood phylogeny of CPR domain containing proteins in eukaryotes. Numbers indicate statistical support in the form of bootstrap or PP values. The scale bar represents the estimated number of amino acid substitutions per site. Only bootstrap support and PP values greater than 50 and 0.5, respectively, are shown. p450 reductase (p450R), methionine synthase reductase (MetSR) and nitric oxide synthase (NOS) form distant branches of proteins. PNO, pyruvate NADP oxidoreductase; SR, Sulfite reductase alpha; CPR, CPR domain containing protein. Green indicates Viridiplantae, red Opisthokonta, yellow the SAR (Stramenopila, Apicomplexa, Rhizaria) supergroup, brown Amoebozoa, and blue Excavata. The schematic domain architecture for each protein group is displayed. PFOR, pyruvate:ferredoxin oxidoreductase domain; FMN, flavin mononucleotide binding domain; FAD, flavin adenine dinucleotide binding domain; HYD, hydrogenase domain.
Minimal cytosolic iron-sulfur cluster assembly (CIA) pathway of *G. intestinalis* comprises of Nbp35, Nar1, Cia1 and Cia2 proteins whereas essential electron donor Tah18/Dre2 complex, as well as Cfd1 and MMS19 seems to be absent in this parasite.
In addition to the cytosolic localization, Cia2 and Nbp35 are associated with mitosomes and might represent a novel connection between the mitosomal FeS cluster assembly (ISC) and the CIA pathway.

is a subgroup of Excavata, resulted in the identification of only five of them (Nbp35, Cfd1, Nar1, Cia1 and Cia2; Fig. 1). Except for the putative MMS19 of *Trimastix*, Dre2 and MMS19 are likely absent from Metamonada, a surprising finding for such a highly conserved and essential group of proteins. It is noteworthy that Dre2 is

usually absent from anaerobes (Basu *et al*., 2013; Tsaousis *et al*., 2014), and MMS19 has not been found in various members of Stramenophila, Apicomplexa, Viridiplantae and Microsporidia (Tsaousis *et al*., 2014). Moreover, MMS19 is the only non-essential component of the *Arabidopsis thaliana* CIA machinery (Han *et al*., 2015). Because Dre2 was recently implicated in the maturation of diferric-tyrosyl radical cofactor (Zhang *et al*., 2014), we speculated whether the loss of Dre2 in anaerobes was reflected in the absence of the RNR2 proteins. However, because we did not find such correlation (Supporting Information Figure S3), it is unknown how cofactor of RNR2 is assembled in anaerobes.

The patchy distribution of Cfd1 in Metamonada implies multiple losses in *G. intestinalis* and *S. salmonicida* (Fig. 1). Because in plants, which appear to lack Cfd1, Nbp35 acts as a homodimer (Bych *et al*., 2008), its similar function in these two metamonads is an interesting possibility. Furthermore, two key components of the mitochondrial export machinery, Erv1 and Atm1, are also likely absent in Metamonada. The recent finding that decreased enzymatic activities of cytosolic Fe-S proteins in the Erv1 yeast mutant strain are likely caused by glutathione depletion (Ozer *et al*., 2015) questions the generally accepted role of Erv1 as a link between the ISC and CIA pathways (Lill, 2009). Because of its function as a cofactor of Atm1 (Srinivasan *et al*., 2014), the tripeptide glutathione (GSH) is another putative player in cytosolic Fe-S synthesis (Sipos *et al*., 2002). Interestingly, glutathione synthase and glutamate cysteine ligase, two proteins required for the synthesis of GSH, are present in the *G. intestinalis* genome (Morrison *et al*., 2007). Additionally, in this protist, GSH was shown to be important for the stability of glutaredoxin 5 (Rada *et al*., 2009). However, because GSH-synthesizing enzymes and glutaredoxins are absent from *T. vaginalis* and *S. salmonicida* (Carlton *et al*., 2007; Xu *et al*., 2014), it is unlikely that GSH plays any important role in the putative ISC and CIA connection in metamonads. The absence of Atm1 in these flagellates further supports this notion.

The CPR domain-containing proteins in metamonads appear to be non-orthologous to Tah18 protein (Tsaousis *et al*., 2014). We postulate that they actually evolved from the CPR-hydrogenase fusion protein found in the common ancestor of metamonads (Fig. 5). Indeed, a similar scenario was proposed for GiOR-1 and GiOR-2 (Jedelsky *et al*., 2011; Pyrih *et al*., 2014), which cluster with PNO and the α-subunit of sulfite reductase (α-SR), the two of which are related proteins (Rotte *et al*., 2001). Although a connection between GiORs and PNO had previously been suggested (Tsaousis *et al*., 2014), it lacked statistical support. The architecture of these CPR-hydrogenase fusion proteins is unique for metamonads. Despite its different origin, we cannot exclude the possibility that GiOR proteins might be functional Tah18 analogs in *G. intestinalis*. However, this is rather unlikely as Tah18 related activity is dependent on Dre2 (Netz *et al*., 2010), which seems to be absent in metamonads. Interestingly, in a heterologous rescue, the GiOR proteins were able to restore the Fe-S cluster assembly in the Tah18-depleted procyclic stage of *T. brucei*. We propose that this phenomenon reflects a functional versatility of the CPR domain that enables several proteins to reduce various electron acceptors, such as Dre2, cytochrome p450 or methionine synthase (Netz *et al*., 2010). Similarly, the previously reported reduction of cytosolic cytochrome b_5 by GiOR-1 (Pyrih *et al*., 2014) appears to be nonphysiological because GiOR-1 is localized inside the mitosomes. Furthermore, artificial interaction with cytochromes was previously described for the human Tah18 homolog (Olteanu and Banerjee, 2003). Fe-S cluster assembly in mitosomes that is mediated by ISC machinery requires supply of electrons. Ferredoxin has been shown to be the main electron donor for ISC components. However, the metabolic source of electrons in mitosomes is unknown. We can speculate that GiOR-1 is somehow involved in electron transport associated with the function of ISC machinery. Previously, we tested an ability of GiOR-1 to transfer electrons to ferredoxin; however, we did not observe such an activity (Jedelsky *et al*., 2011). Thus, the function of GiOR-1 remains unclear.

Intracellular localization of CIA components in G. Intestinalis

All known components of the CIA pathway in *G. intestinalis* are localized in the cytosol; however, Nbp35-1, Nbp35-2 and Cia2 are also associated with the mitosomes. Indeed, immunofluorescence microscopy shows that both Nbp35 proteins exhibit dual cytosolic and mitosomal localization. However, only a small portion of each of them was found to be associated with the organellar fraction, as revealed by cell fractionation. The faint signal detected in the organellar fraction likely resulted from a transient interaction between Nbp35 and the mitosomes, which were disrupted during the fractionation procedure and washing steps. A similar phenomenon was observed in the case of Dre2, which is found throughout the cytosol as well as on the surface of yeast mitochondria (Peleh *et al*., 2014).

To investigate the localization of Cia2 within the mitosome in greater detail, putative interacting proteins were subjected to precipitation, and the obtained lists of proteins were compared with those co-precipitated with other mitosomal proteins (Martincová *et al*., 2015). It is

worth noting that the majority of proteins pulled down by Cia2 were previously identified as partners of integral outer mitochondrial proteins Tom40 and GiMomp35, whereas only a slight overlap with lists of proteins obtained via mitosomal matrix components GiOR-1, Pam18 and Tim44 was observed (Martincová *et al.*, 2015). Combined, the data obtained from subcellular fractionation and protease protection assay are compatible with Cia2 being localized both in the cytosol and in the intermembrane space of the mitosome.

Dual mitochondrial and cytosolic localization are not unprecedented for the CIA components; they were previously reported for Tah18 and Dre2 in yeast (Banci *et al.*, 2011). Tah18 is relocated from the cytosol to mitochondria upon the induction of oxidative stress conditions (Vernis *et al.*, 2009). A fraction of Dre2 is present in the mitochondrial intermembrane space and in the cytosol (Zhang *et al.*, 2008; Banci *et al.*, 2011), although this distribution was recently questioned by Peleh and colleagues, who suggested that the protein is present on the surface of the outer mitochondrial membrane (Peleh *et al.*, 2014). Whether mitochondrion-localized Tah18 and Dre2 play a role in the CIA pathway remains to be established. However, the dual localization reported herein for Nbp35 and Cia2 is novel. The recently described connection between Cia2 and plant mitochondria, reflected by unexpectedly reduced activity of mitochondrial aconitase along with an expected decrease in the activities of several Fe-S proteins in the cytosol (Luo *et al.*, 2012), may be particularly relevant in this context. In fact, any mechanism linking Cia2 and the ISC machinery remains unknown. The two human Cia2 proteins have different functions. Whereas CIA2B is responsible for the maturation of a wide range of nuclear and cytosolic Fe-S proteins, CIA2A is dedicated to the maturation of iron regulatory protein 1 (Stehling *et al.*, 2013). Homologs of both Cia2 variants are also present in the *T. brucei* genome, but no information is available regarding their function. It is tempting to speculate that *G. intestinalis* has solved the functional diversification of Cia2 by dual localization.

Possible connection between ISC and CIA pathways in G. intestinalis

In yeasts, plants and humans, the CIA pathway depends on the mitochondrial ISC pathway (Leighton and Schatz, 1995; Kispal *et al.*, 1999; Lange *et al.*, 2001; Mühlenhoff *et al.*, 2004). Although no data are available about such connection in metamonads, the best studied excavate protist *T. brucei* also appear to retain this arrangement (Horáková *et al.*, 2015). The ISC and protein import pathways are the only known ones identified within the *G. intestinalis* mitosome (Jedelsky *et al.*, 2011; Martincová *et al.*, 2015). Counterintuitively, there is no known putative Fe-S protein in the mitosome apart from components of the ISC pathway itself, although several novel proteins have been recently identified in this highly reduced organelle (Martincová *et al.*, 2015). Therefore, one has to contemplate the possibility that the ISC pathway mediates the formation of Fe-S clusters for the extramitosomal targets. Cysteine desulfurases catalyze the removal of sulfur from L-cysteine and are essential for all Fe-S cluster assembly pathways (Netz *et al.*, 2014), yet they were not found in the cytosol of any member of the Metamonada. Still, the activities of several Fe-S containing enzymes were measured in the cytosol of *G. intestinalis* (Townson *et al.*, 1996; Emelyanov and Goldberg, 2011). Therefore, it is plausible that in this group of diverged and reduced protists, the CIA machinery depends on the mitosomal cysteine desulfurase (Tachezy *et al.*, 2001; Tovar *et al.*, 2003). The existence of paralogs of scaffold proteins Nbp35 on the surface of the mitosomes supports this assumption. Whether in *G. intestinalis* Cia2 partially substitutes for the function of the missing intermembrane space protein Erv1 and the inner membrane internal protein Atm1 will be the subject of future investigations.

In conclusion, our data suggest that *G. intestinalis* belongs to a handful of eukaryotes with CIA machinery lacking the electron donor complex Tah18/Dre2. Moreover, it is possible that this essential machinery is dependent on the mitosomal ISC pathway, even in the absence of the well-characterized Atm1 and Erv1 linker proteins. We speculate that the scaffold proteins Nbp35-1 and Nbp35-2 located on the surface of the mitosome and the cluster delivery protein Cia2 in its intermembrane space might be components of this noncanonical connection. Additional research will be needed to support or disprove this interesting possibility.

Experimental procedures

Cultivation and transformation of G. Intestinalis

Trophozoites of *G. intestinalis* strain WB (ATCC 30957) were grown in TY-S-33 medium (Keister, 1983) supplemented with 10% heat-inactivated bovine serum (PAA Laboratories), 0.1% bovine bile and antibiotics. For episomal expression, the CIA genes (GiardiaDB gene ID: GL50803_15324, GL50803_10969, GL50803_14604, GL50803_33030, GL50803_17550, GL50803_8819) were PCR-amplified and the amplicons were inserted into the plasmid pTG3039 (Lauwaet *et al.*, 2007), which was modified for the expression of proteins that contain the C-terminal hemagglutinin (HA) tag (Martincová *et al.*, 2015). The cells were transformed and selected as previously described (Singer *et al.*, 1998). Genes for co-

precipitation experiments (GL50803_8819 and GL50803_91252) were subcloned into pONDRA plasmid with a C-terminal BAP and coexpressed with the cytosolic BirA gene on pTG plasmid as previously described (Martincová *et al*., 2015).

Immunofluorescence microscopy

G. intestinalis cells were fixed with 1% formaldehyde as described elsewhere (Dawson *et al*., 2007). Proteins of interest were stained for immunofluorescence microscopy using α-HA tag rat monoclonal antibody (Roche). Additionally, we raised α-GiOR-1 rabbit polyclonal antibody and α-Nbp35-1 rat polyclonal antibody for the detection of GiOR-1 and Nbp35-1 proteins. α-TOM40 rabbit polyclonal antibody (Dagley *et al*., 2009) and α-Grx5 polyclonal rat antibody (Rada *et al*., 2009) were used as mitosomal markers. Alexa Fluor 488 (green) donkey α-rat and α-rabbit antibodies and Alexa Fluor 594 (red) donkey α-rabbit and α-rat antibodies (Invitrogen) were used as secondary antibodies. Nuclei were stained with 4',6-diamidin-2-phenylindol (DAPI). The slides were examined using an Olympus IX81 microscope equipped with an MT20 illumination system, and the images were processed using ImageJ 1.41e software (NIH).

Preparation of subcellular fractions and immunoblot analysis

Giardia trophozoites were harvested, washed twice in phosphate-buffered saline (PBS), pH 7.4, and resuspended in SM buffer (250 mM sucrose and 20 mM morpholinepropanesulfonic acid, pH 7.2) supplemented with protease inhibitors (Complete EDTA-free Protease Inhibitor Cocktail; Roche). The cells were disrupted by sonication (∼15 × 1-s pulses) at an amplitude of 40 (Bioblock Scientific Vibra-Cell 72405) and centrifuged twice at 2,750*g* for 10 min to remove undisrupted cells. The supernatant was then centrifuged at 180,000*g* for 30 min to obtain the organellar fraction. Proteins were detected using the same sets of antibodies applied for immunofluorescence, and a signal was developed using corresponding secondary antibodies fused to alkaline phosphatase (Invitrogen). For protease protection assay, the organellar fraction (2 mg/ml) in SM buffer supplemented with protease inhibitors (Roche) was incubated with trypsin (200 μg/ml) for 10 min at 37°C.

Coprecipitation of in vivo *biotinylated proteins and their interacting partners*

We used a strategy recently developed for the study of mitosomal protein import machinery (Martincová *et al*., 2015). Briefly, the organellar fraction (∼10 mg) was resuspended in PBS (pH 7.4) at a final protein concentration of 1.5 mg/ml. The crosslinker DSP (Thermo Scientific) was then added (final concentration 25 μM) and incubated for 1 h on ice. Following centrifugation at 30,000 × g for 10 min at 4°C, the resulting pellet was resuspended in boiling buffer (50 mM Tris, 1 mM EDTA, 1% SDS, pH 7.4) and incubated for 10 min at 80°C. The obtained supernatant was diluted 1:10 in incubation buffer (50 mM Tris, 150 mM NaCl, 5 mM EDTA, 1% Triton X 100; pH 7.4) supplemented with protease inhibitors. Then, 100 μl of streptavidin coupled magnetic beads (Dynabeads® MyOne™ Streptavidin C1, Invitrogen) was mixed with the sample and incubated overnight at 4°C with gentle rotation. The beads were then washed in the following order (each step lasting 5 min): 3 times in incubation buffer, once in boiling buffer, once in washing buffer (60 mM Tris, 2% SDS, 10% glycerol) and twice in incubation buffer supplemented with 0.1% SDS. Finally, proteins were eluted from the beads in SDS PAGE sample buffer supplemented with 20 mM biotin for 5 min at 95°C. The eluate was resolved by SDS PAGE and stained with Coomassie brilliant blue. Separated proteins were destained, trypsin digested and analyzed by mass spectrometry. The same procedure was performed with wild-type *Giardia* and cells overexpressing BirA protein only, both used as negative controls.

Mass spectrometry

The trypsine digested proteins were loaded onto UltiMate 3000 RSLCnano system (Thermo Scientific - Dionex) coupled to a TripleTOF 5600 mass spectrometer with a NanoSpray III source (AB Sciex) for LC-MS/MS analysis. The instrument was operated with Analyst TF 1.6 (AB Sciex). TOF MS mass range was set to 350–1500 m/z, in MS/MS mode the instrument acquired fragmentation spectra within 100–2000 m/z. Spectra were searched against *G. intestinalis* database (GiardiaDB 28, http://giardiadb.org/giardiadb/), and the common contaminants database cRAP (http://www.thegpm.org/crap/) with Mascot 2.2. The results from Mascot were postprocessed with Percolator software (http://percolator.ms/) and resulting datasets were evaluated with the Scaffold software version 4.4.6 (Proteome Software, Portland) using False Discovery Rate (FDR) set to 1% for peptide and protein. All proteins identified in the negative controls (at least 95% protein identification probability) were subtracted from the dataset of immunoprecipitated proteins. Only proteins with 100% protein identification probability that were identified based on at least two peptides were considered as putative interactive proteins. The mass spectrometry proteomics data have been deposited to the ProteomeXchange Consortium via the PRIDE (Vizcaíno *et al*., 2016) partner repository with the dataset identifier PXD004722.

Bioinformatic analyses

To classify the copurified proteins, their amino acid sequences were analyzed by BLASTP against the NCBI nr database and using the HHpred algorithm available at http://toolkit.tuebingen.mpg.de/hhpred# (Soding *et al*., 2005). For phylogenetic analysis of Nar1 and CPR domain-containing proteins in eukaryotes, amino acid sequences were retrieved from a non-redundant GenBank protein database. EST sequences of various metamonads are available in SRA ncbi database under accession ID PRJNA315708. The sequences were aligned using the Mafft program

(Katoh *et al*., 2002), and non-informative sites were removed using BMGE software (Criscuolo and Gribaldo, 2010). The best substitutional model (LG + G4 + I for both analyses) was calculated using the IQ tree program (Nguyen *et al*., 2015), and phylogenetic analysis was performed using PhyML 3.0 (Guindon and Gascuel, 2003) and MrBayes (Huelsenbeck and Ronquist, 2001). Support values are shown next to the branches as the maximum-likelihood bootstrap support (PhyML) or posterior probabilities (MrBayes).

Rescue experiment in T. brucei

Procyclic *T. brucei* 29-13 were cultivated in SDM-79 medium (Carruthers and Cross, 1992) containing 10% fetal bovine serum, 15 μg/ml of geneticin and 50 μg/ml of hygromycin. The genes for GiOR-1 and GiOR-2 were cloned into pABPURO vector possessing an HA_3 tag. The resulting GiOR-1-pABPURO and GiOR-2-pABPURO constructs were linearized using NotI and electroporated individually into the TbTah18-TbDre2 RNAi double knock-down PS cells (Basu *et al*., 2014) using a BTX electroporator, as described elsewhere (Vondrušková *et al*., 2005). Positive transfectants were selected by clonal dilution using puromycin as a marker. In the presence of puromycin (1 μg/ml), RNAi was induced by the addition of tetracycline (1 μg/ml). Cell densities were measured using a Beckman Coulter Z2 counter every 24 h over a period of 10 days after induction. The cytosolic and mitochondrial fractions were obtained by digitonin fractionation (Šmíd *et al*., 2006). Aconitase activity was in both subcellular compartments measured spectrophotometrically at 240 nm via the production of cis-aconitate from isocitrate (Long *et al*., 2011).

Acknowledgements

The authors thank Frances Gillin (University of San Diego) for kindly providing plasmid pTG3039, and Jitka Štáfková for a critical reading of the manuscript. They thank Paul Michels (Universidad de los Andes/University of Edinburgh) and Alena Zíková (Institute of Parasitology, Biology Centre ASCR) for anti enolase and anti mtHsp70 antibodies, respectively. This work was supported by LQ1604 NPU II provided by MEYS, CZ.1.05/1.1.00/02.0109 BIOCEV provided by ERDF and MEYS to J.T., and the Czech Science Foundation 15-21974S provided to J.L. The work by M.K. and A.J.R. was supported by grant MOP-142349 from the Canadian Institutes of Health Research awarded to A.J.R

References

Balk, J., Pierik, A.J., Netz, D.J.A., Mühlenhoff, U., and Lill, R. (2004) The hydrogenase-like Nar1p is essential for maturation of cytosolic and nuclear iron-sulphur Proteins. *embo J* **23**: 2105–2115.

Balk, J., Netz, D.J.A., Tepper, K., Pierik, A.J., and Lill, R. (2005) The essential WD40 protein Cia1 is involved in a late step of cytosolic and nuclear iron-sulfur protein assembly. *Mol Cell Biol* **25**: 10833–10841.

Banci, L., Bertini, I., Ciofi-Baffoni, S., Boscaro, F., Chatzi, A., Mikolajczyk, M., *et al*. (2011) Anamorsin is a [2Fe-2S] cluster-containing substrate of the Mia40-dependent mitochondrial protein trapping machinery. *Chem Biol* **18**: 794–804.

Basu, S., Leonard, J.C., Desai, N., Mavridou, D.A.I., Tang, K.H., Goddard, A.D., *et al*. (2013) Divergence of Erv1-associated mitochondrial import and export pathways in Trypanosomes and anaerobic protists. *Eukaryot Cell* **12**: 343–355.

Basu, S., Netz, D.J., Haindrich, A.C., Herlerth, N., Lagny, T.J., Pierik, A.J., *et al*. (2014) Cytosolic iron-sulphur protein assembly is functionally conserved and essential in procyclic and bloodstream *Trypanosoma brucei*. *Mol Microbiol* **93**: 897–910.

Bych, K., Netz, D.J.A., Vigani, G., Bill, E., Lill, R., Pierik, A.J., and Balk, J. (2008) The essential cytosolic iron-sulfur protein Nbp35 acts without Cfd1 partner in the green lineage. *J Biol Chem* **283**: 35797–35804.

Carlton, J.M., Hirt, R.P., Silva, J.C., Delcher, A.L., Schatz, M., Zhao, Q., *et al*. (2007) Draft genome sequence of the sexually transmitted pathogen *Trichomonas vaginalis*. *Science* **315**: 207–212.

Carruthers, V.B. and Cross, G.A.M. (1992) High efficiency clonal growth of blood stream form and insect form *Trypanosoma brucei* on agarose plates. *Proc Natl Acad Sci U S A* **89**: 8818–8821.

Criscuolo, A. and Gribaldo, S. (2010) BMGE (Block Mapping and Gathering with Entropy): A new software for selection of phylogenetic informative regions from multiple sequence alignments. *BMC Evol Biol* **10**: 210.

Dagley, M.J., Doležal, P., Likic, V.A., Šmíd, O., Purcell, A.W., Buchanan, S.K., *et al*. (2009) The protein import channel in the outer mitosomal membrane of *Giardia intestinalis*. *Mol Biol Evol* **26**: 1941–1947.

Dawson, S.C., Sagolla, M.S., Mancuso, J.J., Woessner, D.J., House, S.A., Fritz-Laylin, L., and Cande, W.Z. (2007) Kinesin-13 regulates flagellar, interphase, and mitotic microtubule dynamics in *Giardia intestinalis*. *Eukaryot Cell* **6**: 2354–2364.

Doležal, P., Šmíd, O., Rada, P., Zubáčová, Z., Bursac, D., Sutak, R., *et al*. (2005) Giardia mitosomes and trichomonad hydrogenosomes share a common mode of protein targeting. *Proc Natl Acad Sci U S A* **102**: 10924–10929.

Emelyanov, V.V. and Goldberg, A.V. (2011) Fermentation enzymes of *Giardia intestinalis*, pyruvate:ferredoxin oxidoreductase and hydrogenase, do not localize to its mitosomes. *Microbiol SGM* **157**: 1602–1611.

Gari, K., Ortiz, A.M.L., Borel, V., Flynn, H., Skehel, J.M., and Boulton, S.J. (2012) MMS19 links cytoplasmic Iron-Sulfur cluster assembly to DNA metabolism. *Science* **337**: 243–245.

Guindon, S. and Gascuel, O. (2003) A simple, fast, and accurate algorithm to estimate large phylogenies by maximum likelihood. *Syst Biol* **52**: 696–704.

Han, Y.F., Huang, H.W., Li, L., Cai, T., Chen, S., and He, X.J. (2015) The cytosolic iron-sulfur cluster assembly protein MMS19 regulates transcriptional gene silencing, DNA repair, and flowering time in Arabidopsis. *PLoS One* **10**:

Hausmann, A., Netz, D.J.A., Balk, J., Pierik, A.J., Mühlenhoff, U., and Lill, R. (2005) The eukaryotic P loop NTPase Nbp35: An essential component of the cytosolic and nuclear iron-sulfur protein assembly machinery. *Proc Natl Acad Sci U S A* **102**: 3266–3271.

Horáková, E., Changmai, P., Paris, Z., Salmon, D., and Lukeš, J. (2015) Simultaneous depletion of Atm and Mdl rebalances cytosolic Fe-S cluster assembly but not heme import into the mitochondrion of *Trypanosoma Brucei*. *febs J* **282**: 4157–4175.

Huelsenbeck, J.P. and Ronquist, F. (2001) MRBAYES: Bayesian inference of phylogenetic trees. *Bioinformatics* **17**: 754–755.

Iyanagi, T., Xia, C., and Kim, J.J. (2012) NADPH-cytochrome P450 oxidoreductase: Prototypic member of the diflavin reductase family. *Arch Biochem Biophys* **528**: 72–89.

Jackson, A.P., Otto, T.D., Aslett, M., Armstrong, S.D., Bringaud, F., Schlacht, A., *et al*. (2016) Kinetoplastid phylogenomics reveals the evolutionary innovations associated with the origins of parasitism. *Curr Biol* **26**: 161–172.

Jedelsky, P.L., Doležal, P., Rada, P., Pyrih, J., Šmíd, O., Hrdý, I., *et al*. (2011) The minimal proteome in the reduced mitochondrion of the parasitic protist *Giardia intestinalis*. *PLoS One* **6**: e17285.

Katoh, K., Misawa, K., Kuma, K., and Miyata, T. (2002) MAFFT: A novel method for rapid multiple sequence alignment based on fast Fourier transform. *Nucl Acids Res* **30**: 3059–3066.

Keister, D.B. (1983) Axenic culture of *Giardia lamblia* in Tyi-S-33 medium supplemented with bile. *Trans Roy Soc Trop Med Hyg* **77**: 487–488.

Kispal, G., Csere, P., Prohl, C., and Lill, R. (1999) The mitochondrial proteins Atm1p and Nfs1p are essential for biogenesis of cytosolic Fe/S Proteins. *embo J* **18**: 3981–3989.

Kolísko, M., Silberman, J.D., Cepicka, I., Yubuki, N., Takishita, K., Yabuki, A., *et al*. (2010) A wide diversity of previously undetected free-living relatives of diplomonads isolated from marine/saline habitats. *Environ Microbiol* **12**: 2700–2710.

Kuhnke, G., Neumann, K., Müehlenhoff, U., and Lill, R. (2006) Stimulation of the ATPase activity of the yeast mitochondrial ABC transporter Atm1p by thiol compounds. *Mol Membr Biol* **23**: 173–184.

Lange, H., Lisowsky, T., Gerber, J., Mühlenhoff, U., Kispal, G., and Lill, R. (2001) An essential function of the mitochondrial sulfhydryl oxidase Erv1p/ALR in the maturation of cytosolic Fe/S proteins. *EMBO Rep* **2**: 715–720.

Lauwaet, T., Davids, B.J., Torres-Escobar, A., Birkeland, S.R., Cipriano, M.J., Preheim, S.P., *et al*. (2007) Protein phosphatase 2A plays a crucial role in *Giardia lamblia* differentiation. *Mol Biochem Parasitol* **152**: 80–89.

Leighton, J. and Schatz, G. (1995) An ABC transporter in the mitochondrial inner membrane is required for normal growth of Yeast. *embo J* **14**: 188–195.

Lill, R. (2009) Function and biogenesis of iron-sulphur proteins. *Nature* **460**: 831–838.

Lill, R., Dutkiewicz, R., Freibert, S.A., Heidenreich, T., Mascarenhas, J., Netz, D.J., *et al*. (2015) The role of mitochondria and the CIA machinery in the maturation of cytosolic and nuclear iron-sulfur proteins. *Eur J Cell Biol* **94**: 280–291.

Long, S.J., Changmai, P., Tsaousis, A.D., Skalicky, T., Verner, Z., Wen, Y.Z., *et al*. (2011) Stage-specific requirement for Isa1 and Isa2 proteins in the mitochondrion of *Trypanosoma brucei* and heterologous rescue by human and *Blastocystis* orthologues. *Mol Microbiol* **81**: 1403–1418.

Luo, D.X., Bernard, D.G., Balk, J., Hai, H., and Cui, X.F. (2012) The DUF59 family gene AE7 acts in the cytosolic Iron-Sulfur cluster assembly pathway to maintain nuclear genome integrity in Arabidopsis. *Plant Cell* **24**: 4135–4148.

Martincová, E., Voleman, L., Pyrih, J., Žárský, V., Vondráčková, P., Kolísko, M., *et al*. (2015) Probing the biology of *Giardia intestinalis* mitosomes using in vivo enzymatic tagging. *Mol Cell Biol* **35**: 2864–2874.

Morrison, H.G., McArthur, A.G., Gillin, F.D., Aley, S.B., Adam, R.D., Olsen, G.J., *et al*. (2007) Genomic minimalism in the early diverging intestinal parasite *Giardia lamblia*. *Science* **317**: 1921–1926.

Mühlenhoff, U., Balk, J., Richhardt, N., Kaiser, J.T., Sipos, K., Kispal, G., and Lill, R. (2004) Functional characterization of the eukaryotic cysteine desulfurase Nfs1p from *Saccharomyces cerevisiae*. *J Biol Chem* **279**: 36906–36915.

Netz, D.J.A., Pierik, A.J., Stuempfig, M., Mühlenhoff, U., and Lill, R. (2007) The Cfd1-Nbp35 complex acts as a scaffold for iron-sulfur protein assembly in the yeast cytosol. *Nat Chem Biol* **3**: 278–286.

Netz, D.J.A., Stumpfig, M., Dore, C., Mühlenhoff, U., Pierik, A.J., and Lill, R. (2010) Tah18 transfers electrons to Dre2 in cytosolic iron-sulfur protein biogenesis. *Nat Chem Biol* **6**: 758–765.

Netz, D.J.A., Pierik, A.J., Stumpfig, M., Bill, E., Sharma, A.K., Pallesen, L.J, *et al*. (2012) A bridging [4Fe-4S] cluster and nucleotide binding are essential for function of the Cfd1-Nbp35 complex as a scaffold in Iron-Sulfur protein maturation. *J Biol Chem* **287**: 12365–12378.

Netz, D.J.A., Mascarenhas, J., Stehling, O., Pierik, A.J., and Lill, R. (2014) Maturation of cytosolic and nuclear iron-sulfur proteins. *Trends Cell Biol* **24**: 303–312.

Nguyen, L.T., Schmidt, H.A., von Haeseler, A., and Minh, B.Q. (2015) IQ-TREE: A fast and effective stochastic algorithm for estimating maximum-likelihood phylogenies. *Mol Biol Evol* **32**: 268–274.

Nishimura, A., Kawahara, N., and Takagi, H. (2013) The flavoprotein Tah18-dependent NO synthesis confers high-temperature stress tolerance on yeast cells. *Biochem Biophys Res Commun* **430**: 137–143.

Nývltová, E., Stairs, C.W., Hrdý, I., Rídl, J., Mach, J., Pačes, J, *et al*. (2015) Lateral gene transfer and gene duplication played a key role in the evolution of *Mastigamoeba balamuthi* hydrogenosomes. *Mol Biol Evol* **32**: 1039–1055.

Olteanu, H. and Banerjee, R. (2003) Redundancy in the pathway for redox regulation of mammalian methionine synthase - Reductive activation by the dual flavoprotein, novel reductase 1. *J Biol Chem* **278**: 38310–38314.

Ozer, H.K., Dlouhy, A.C., Thornton, J.D., Hu, J., Liu, Y., Barycki, J.J, *et al*. (2015) Cytosolic Fe-S cluster protein

maturation and iron regulation are independent of the mitochondrial Erv1/Mia40 import system. *J Biol Chem* **290**: 27829–27840.
Peleh, V., Riemer, J., Dancis, A., and Herrmann, J.M. (2014) Protein oxidation in the intermembrane space of mitochondria is substrate-specific rather than general. *Microbial Cell* **1**: 81–93.
Peters, J.W., Lanzilotta, W.N., Lemon, B.J., and Seefeldt, L.C. (1998) X-ray crystal structure of the Fe-only hydrogenase (Cpl) from *Clostridium pasteurianum* to 1.8 angstrom resolution. *Science* **282**: 1853–1858.
Pyrih, J., Harant, K., Martincová, E., Sutak, R., Lesuisse, E., Hrdý, I., and Tachezy, J. (2014) *Giardia intestinalis* incorporates heme into cytosolic cytochrome b(5). *Eukaryot Cell* **13**: 231–239.
Rada, P., Šmíd, O., Sutak, R., Doležal, P., Pyrih, J., Žárský, V., *et al*. (2009) The monothiol single-domain glutaredoxin is conserved in the highly reduced mitochondria of *Giardia intestinalis*. *Eukaryot Cell* **8**: 1584–1591.
Rotte, C., Stejskal, F., Zhu, G., Keithly, J.S., and Martin, W. (2001) Pyruvate: NADP(+) oxidoreductase from the mitochondrion of *Euglena gracilis* and from the apicomplexan *Cryptosporidium parvum*: A biochemical relic linking pyruvate metabolism in mitochondriate and amitochondriate protists. *Mol Biol Evol* **18**: 710–720.
Singer, S.M., Yee, J., and Nash, T.E. (1998) Episomal and integrated maintenance of foreign DNA in *Giardia lamblia*. *Mol Biochem Parasitol* **92**: 59–69.
Sipos, K., Lange, H., Fekete, Z., Ullmann, P., Lill, R., and Kispal, G. (2002) Maturation of cytosolic iron-sulfur proteins requires glutathione. *J Biol Chem* **277**: 26944–26949.
Šmíd, O., Horáková, E., Vilímová, V., Hrdý, I., Cammack, R., Horvath, A., *et al*. (2006) Knock-downs of iron-sulfur cluster assembly proteins IscS and IscU down-regulate the active mitochondrion of procyclic *Trypanosoma brucei*. *J Biol Chem* **281**: 28679–28686.
Soding, J., Biegert, A., and Lupas, A.N. (2005) The HHpred interactive server for protein homology detection and structure prediction. *Nucl Acids Res* **33**: W244–W248.
Srinivasan, V., Pierik, A.J., and Lill, R. (2014) Crystal structures of nucleotide-free and glutathione-bound mitochondrial ABC transporter Atm1. *Science* **343**: 1137–1140.
Stehling, O., Vashisht, A.A., Mascarenhas, J., Jonsson, Z.O., Sharma, T., Netz, D.J.A., *et al*. (2012) MMS19 assembles iron-sulfur proteins required for DNA metabolism and genomic integrity. *Science* **337**: 195–199.
Stehling, O., Mascarenhas, J., Vashisht, A.A., Sheftel, A.D., Niggemeyer, B., Rosser, R., *et al*. (2013) Human Cia2A-Fam96A and Cia2B-Fam96B integrate iron homeostasis and maturation of different subsets of cytosolic-nuclear Iron-Sulfur proteins. *Cell Metabol* **18**: 187–198.
Tachezy, J., Sanchez, L.B., and Müller, M. (2001) Mitochondrial type iron-sulfur cluster assembly in the amitochondriate eukaryotes *Trichomonas vaginalis* and *Giardia intestinalis*, as indicated by the phylogeny of IscS. *Mol Biol Evol* **18**: 1919–1928.
Takishita, K., Kolisko, M., Komatsuzaki, H., Yabuki, A., Inagaki, Y., Čepička, I., *et al*. (2012) Multigene phylogenies of diverse Carpediemonas-like organisms identify the closest relatives of 'Amitochondriate' Diplomonads and Retortamonads. *Protist* **163**: 344–355.
Tanaka, N., Kanazawa, M., Tonosaki, K., Yokoyama, N., Kuzuyama, T., and Takahashi, Y. (2015) Novel features of the ISC machinery revealed by characterization of *Escherichia coli* mutants that survive without iron-sulfur clusters. *Mol Microbiol* **99**: 835–848.
Tovar, J., Leon-Avila, G., Sanchez, L.B., Sutak, R., Tachezy, J., van der Giezen, M., *et al*. (2003) Mitochondrial remnant organelles of Giardia function in iron-sulphur protein maturation. *Nature* **426**: 172–176.
Townson, S.M., Upcroft, J.A., and Upcroft, P. (1996) Characterisation and purification of pyruvate:ferredoxin oxidoreductase from *Giardia duodenalis*. *Mol Biochem Parasitol* **79**: 183–193.
Tsaousis, A.D., Gentekaki, E., Eme, L., Gaston, D., and Roger, A.J. (2014) Evolution of the cytosolic iron-sulfur cluster assembly machinery in Blastocystis species and other microbial eukaryotes. *Eukaryot Cell* **13**: 143–153.
Vernis, L., Facca, C., Delagoutte, E., Soler, N., Chanet, R., Guiard, B., *et al*. (2009) A newly identified essential complex, Dre2-Tah18, controls mitochondria integrity and cell death after oxidative stress in yeast. *PLoS One* **4**:
Vizcaíno, J.A., Csordas, A., del-Toro, N., Dianes, J.A., Griss, J., Lavidas, I., *et al*. (2016) 2016 update of the PRIDE database and related tools. *Nucleic Acids Res* **44**: D447–D456.
Vondrušková, E., van den Burg, J., Zíková, A., Ernst, N.L., Stuart, K., Benne, R., and Lukeš, J. (2005) RNA interference analyses suggest a transcript-specific regulatory role for mitochondrial RNA-binding proteins MRP1 and MRP2 in RNA editing and other RNA processing in *Trypanosoma brucei*. *J Biol Chem* **280**: 2429–2438.
Weerapana, E., Wang, C., Simon, G.M., Richter, F., Khare, S., Dillon, M.B.D., *et al*. (2010) Quantitative reactivity profiling predicts functional cysteines in proteomes. *Nature* **468**: 790–U79.
Xu, F.F., Jerlstrom-Hultqvist, J., Einarsson, E., Astvaldsson, A., Svard, S.G., and Andersson, J.O. (2014) The genome of *Spironucleus salmonicida* highlights a fish pathogen adapted to fluctuating environments. *PLoS Genetics* **10**:
Zhang, Y., Lyver, E.R., Nakamaru-Ogiso, E., Yoon, H., Amutha, B., Lee, D.W., *et al*. (2008) Dre2, a conserved eukaryotic Fe/S cluster protein, functions in cytosolic Fe/S protein biogenesis. *Mol Cell Biol* **28**: 5569–5582.
Zhang, Y., Li, H.R., Zhang, C.G., An, X.X., Liu, L.L., Stubbe, J., and Huang, M.X. (2014) Conserved electron donor complex Dre2-Tah18 is required for ribonucleotide reductase metallocofactor assembly and DNA synthesis. *Proc Natl Acad Sci U S A* **111**: E1695–E1704.

Supporting information

Additional supporting information may be found in the online version of this article at the publisher's web-site.

SINGLE TIM TRANSLOCASE IN THE MITOSOMES OF *GIARDIA INTESTINALIS* ILLUSTRATES THE CONVERGENCE OF THE PROTEIN IMPORT MACHINES IN ANAEROBIC EUKARYOTES.

Eva Pyrihová[1], Alžběta Krupičková[1], Luboš Voleman[1], Natalia Wandyszewska[1], Andrew Roger[2], Martin Kolísko[2,3#], Pavel Doležal[1#]

[1]Department of Parasitology, Faculty of Science, Charles University, BIOCEV, Průmyslová 595, Vestec, 252 42, Czech Republic

[2]Centre for Comparative Genomics and Evolutionary Bioinformatics, Department of Biochemistry and Molecular Biology, Dalhousie University, Halifax, Nova Scotia, Canada

[3]Biology Centre CAS, Branišovská 1160/31, 370 05,ČeskéBudějovice, Czech Republic

[#]corresponding authors: Martin Kolísko: kolisko@paru.cas.cz, Pavel Doležal: pavel.dolezal@natur.cuni.cz

ABSTRACT

The evolution of eukaryotes has stemmed into a range of mitochondrial forms, of which mitosomes are the simplest but also the least known. Transport of proteins via TIM complexes build around three proteins from Tim17 protein family (Tim17/22/23), is one of the key unifying aspects of mitochondrial organelles. However, so far multiple experimental and bioinformatic attempts failed to identify nature of the TIM complex in the mitosomes of *Giardia intestinalis*, one of few experimental models for mitosome biology. Here, we present the identification of single Tim17 (GiTim17) from this anaerobic metamonad, which was possible only by the use of metamonad-specific hidden Markov model. While very divergent in primary sequence and in predicted membrane topology, the experimental data suggest that GiTim17 is an inner membrane mitosomal protein, forming a disulphide linked dimer. We suggest that peculiar GiTim17 sequence reflects the unusual detergent resistance of the inner mitosomal membrane. Nevertheless, specific pull-down experiments indicate contact of GiTim17 with mitosomal Tim44, the import motor complex tethering component. The analysis of TIM complexes in eukaryotes indicates that “single Tim” translocase is a convergent adaptation of mitosomes in the anaerobic protists, with Tim22 and Tim17 but not Tim23 providing the protein backbone.

BACKGROUND

The endosymbiotic acquisition of mitochondria was a key event in the evolution of eukaryotes [1]. The subsequent formation of an effective system for import of proteins from the cytosol into the mitochondria involved the redesign of the endosymbiont membranes and the creation of novel protein transport machines [2]. In canonical mitochondria, the protein import machinery is a complex network of specialized protein translocases, comprising of more than 35 different protein components [3].

The unicellular anaerobic parasite, *Giardia intestinalis*, possesses highly reduced mitochondria, tiny organelles called mitosomes. Currently, its only known function is the iron-sulfur cluster synthesis through the ISC pathway [4]. The mitosome has lost most of other canonical

mitochondrial functions [5]. It does not carry its own genome and is devoid of cristae, yet it is still surrounded by two membranes [4].

Canonical mitochondria employ several independent protein transport machines, including the TOM and the SAM complexes in the outer membrane, the MIA pathway in the intermembrane space and the TIM23 and TIM22 complexes transporting protein across or into the inner membrane, respectively [3]. Proteins from Tim17/22/23 protein family form the core of both TIM complexes. The protein-conducting channel of TIM23 complex is formed by two Tim17/22/23 family proteins, Tim23 and Tim17 [6]. The transport through TIM23 complex is initially energized by the membrane potential, while the translocation is driven by mtHsp70 chaperone [7]. mtHsp70 is part of the PAM motor complex, which is tethered to the TIM23 complex via protein Tim44 [8]. The channel of the TIM22 complex is formed by single Tim17 family protein, Tim22, and the TIM22 translocase requires only the membrane potential to insert proteins into the inner mitochondrial membrane [9].

The presence of similar protein targeting signals and homologous SAM, TOM and TIM machineries have been considered as the crucial support for the common origin of mitochondria, mitosomes and hydrogen-producing hydrogenosomes [10,11]. However, of the three molecular machines only bare bone TOM complex is known from *Giardia*[12], even though its genome has been fully sequenced [13] and proteomic data from mitosomes are available [5,14,15]. Only three components of the import motor complex, PAM, are known. The hidden Markov model (HMM) search identified mitosomal Pam18 [11], while proteomics of density gradient-derived cell fractions resulted in the identification of Pam16 [5]. Recently, another mitosomal component Tim44 has been identified using high-affinity co-precipitation of *in vivo* biotin-tagged mitosomal bait proteins [14].

Despite all these combined efforts, the crucial channel forming protein of Tim17 protein family remained elusive. Two alternate hypotheses explaining the absence of Tim17 family protein in *Giardia* have been drawn: 1) the import into mitosomes is facilitated through lineage-specific protein channel or other molecular mechanism; this would be in line with the presence of many unique *Giardia*-specific proteins with no clear orthologues in other eukaryotes [14,15], 2) Tim17 primary structure has diverged beyond the sensitivity of bioinformatic approaches. Given that the protein sequences of *Giardia* proteins are frequently highly divergent, it is not surprising that bioinformatics tend to fail to identify clear homology to known mitochondrial components, even when they are present as it was the case for mitosomal Tom40 [12] and Tim44 [14]. It can be said that the mechanism of protein translocation across the inner mitosomal membrane remains one of the “last great mysteries” of these organelles.

Moreover, until today there is virtually no information on the transport of any biomolecules across the inner mitosomal membrane in *Giardia*. It appears that biochemical properties of the membrane, including the nature of the protein translocase remain one of the “last mysteries” of *Giardia* mitosomes.

RESULTS AND DISCUSSION

We performed three rounds of hmm search against our Metamonada protein database [17] including predicted proteome of *Giardia* [18]. The HMM model was enriched each round by newly identified sequences. After the third round there were no new sequences recovered. The search returned single *Giardia* sequence GL50803_10452 encoding a protein of 180 amino acids and molecular mass of 19,4 kDa. Hereafter the protein has been referred to as GiTim17. Interestingly, currently one of the most sensitive protein homology detection tools, HHpred [19], failed to recognize GiTim17 as a member of Tim17/22/23 protein family, while putative Tim17 homologues in all other metamonad sequences were clearly identified as Tim17/22/23 proteins (Fig. 1A). Enriching the HMM profile for phylogenetically related orthologues has thus proved crucial for the identification of GiTim17 [20].

Attempts to recover well resolved phylogenetic tree of Tim17/22/23 are mostly hindered by the extreme divergence of the proteins across species as well as their relatively short length. However, our phylogenetic analyses have clearly demonstrated, with high statistical support, that GiTim17 is closely related to Tim17 proteins from *Giardia's* closest relatives the so called *Carpediemonas*-like organisms (BP support 91, Figure 1B). Moreover, GiTim17 also shares a short deletion between TMD1 and 2 with its closest free-living relative *Dysnectes brevis* [17](Fig 1A). These results strongly suggest that GiTim17 is, at least from the evolutionary standpoint, the so far absent Tim17 homolog in *Giardia*. To test whether GiTim17 is a mitosomal protein, it was expressed with the C-terminal HA-tag in *Giardia*. Western blot analysis showed that GiTim17 is enriched in the high speed pellet fraction (HSP) containing mitosomes and other membrane-bounded organelles (Fig. 2A). Moreover, fluorescence microscopy showed that GiTim17 co-localized with the mitosomal marker protein GL50803_9296 [14] (Fig. 2B).

GiTim17 possesses four hydrophobic regions corresponding to the four putative transmembrane domains (TMDs) of canonical Tim17 family proteins (Fig. 1C), however they are not recognized as TMDs by widely used HMM-based predictors such as TMHMM [21]. This can be likely attributed to the stringent nature of the diagnostic model in TMHMM predictor. Only one of the four putative TMDs bears typical glycine zipper (GxxxG) motif for the intramembrane interaction of TMDs (Fig. 1A). The extreme divergence of the putative TMDs in GiTim17 could be explained as loss of functional membrane insertion or adaptation to unusual biological properties of mitosomal inner membrane.

The resolution of stimulated emission depletion (STED) microscopy enables to discriminate soluble and membrane proteins in the mitochondria [22]. Detection of GiTim17 by STED showed specific presence of the protein in the periphery of the mitosomes (Fig. 2C), thus supporting its insertion into the mitosomal membrane. In order to distinguish whether GiTim17 occupies the outer or the inner mitosomal membrane, the organelles were treated with detergent for membrane differentiation based on their lipid composition. The HSP (high speed pellet) was incubated in different detergents (digitionin, DDM, deoxycholate, Triton X-114, Zwittergent)

and the resulted soluble and insoluble fractions were probed for the mitosomal proteins. Repeatedly, the outer mitosomal membrane protein Tom40 was efficiently solubilised, whereas GiTim17 was always retained in the pellet fraction along with the inner membrane anchored GiPam18 and peripheral membrane protein GiTim44 as shown for the experiment with 2% digitonin (Fig. 2D). These results strongly implied that that GiTim17, indeed, is localized into the inner mitosomal membrane. The overall resistance of the mitosomal inner membrane to detergent treatment suggest its highly unusual lipid composition, when compared to the properties of canonical mitochondria [23]. In light of these results it is possible that the non-conformity of putative TMDs in GiTim17 are results of adaptation to the unusual composition of mitosomal inner membrane.

The TIM23 complex includes more than one subunit from Tim17/22/23 protein family - Tim17 and Tim23. Moreover, both TIM22 and TIM23 complexes homodimerize into superior assemblies of twin pore architecture [24,25]. Given that we were able to identify only one member of the family in *Giardia*, we hypothesized that the GiTim17 forms dimers in order to form functional pore. Indeed, three lines of evidence suggest the capability of GiTim17 to dimerize; 1) *In-vivo*, GiTim17 is part of a protein complex bound by disulfide bond and of approximately doubled size of single GiTim17 (Fig. 4A); 2) Upon in-vitro translation it forms a complex of doubled size in experimental membrane (Fig. 4B) It specifically interacts with itself in yeast two-hybrid assay (Fig. 4C).

Tim17 family proteins constitute the core protein-conducting channels, activity and specificity of which are controlled by other components of the TIM and PAM complexes. Therefore, the interaction of GiTim17 with the other mitosomal components was investigated. Unfortunately, without the convenient solubilisation conditions the association of GiTim17 within putative translocation complex could not be tested by blue native PAGE or by co-precipitations under native conditions. Instead, the *in-vivo* biotinylation approach coupled to chemical cross-linking of adjacent sulfhydryl groups by DTME was used to isolate interacting partners of GiTim17. This technique previously allowed to obtain highly specific protein profiles of mitosomal interactome [14]. Briefly, the HSP isolated from *Giardia* cell line expressing GiTim17 *in vivo* biotinylated by biotin ligase (BirA) (Fig. 3A) was chemically crosslinked and GiTim17-containing complexes were purified on streptavidin magnetic beads (Fig. 3B). The sample was analyzed by mass spectrometry and quantified against the negative control isolated from a strain expressing only BirA. Of the identified proteins, GiTim44 was found among the most enriched proteins. Some of them were entirely absent in the control samples (the enrichment ratio could not be determined) (Fig. 3C). The function of Tim44 is to tether the Hsp70 motor to the translocase [26]. Therefore the presence of conserved arginine residue in GiTim17 shown to be responsible for Tim44 binding (Fig. 1A) [27], suggests that possibly analogous link exists between the translocase and the motor in the mitosomes.

In addition, single subunit matrix processing peptidase (βMPP) [28], responsible for the cleavage of mitosomal targeting presequences, as well as multiple components of ISC pathway were co-

purified with GiTim17. However, none of other known Tim proteins could be identified in the dataset, which was further supported by their absence in our Metamonada protein database [17].

Of three paralogues Tim17, Tim22 and Tim23, which mediate the protein transport across the inner mitochondrial membrane several eukaryotes have simplified the set to just a single Tim17/22/23 family protein like *Giardia* [29]. Commonly, these eukaryotes highly reduced their mitochondria to minimalist mitosomes such as *Giardia*-related *Carpediemonas*-like eukaryotes (CLO, Metamonada) [17], Microsporidia [30] and *Cryptosporidumparvum* (Apicomplexa) [31]. The only exception is the mitochondrion of kineplastids such as *Trypanosoma brucei* [32]. Their mitochondria are complex organelles with fully developed cristae and capable of oxidative phosphorylation, and yet they contain single Tim17/22/23 family protein, which was verified to function as an inner membrane transporter [33]. This protein was also shown to function in complex with several trypanosome-specific proteins [34]. Similarly, several *Giardia*-specific proteins of unknown function were co-purified with GiTim17 and may represent lineage specific protein import apparatus components.

Taken together, it appears, that the evolutionarily independent reduction of mitochondria resulted in the convergence evolution towards the “single Tim17 family protein translocase”. Based on the recent classification of Tim17/22/23 family and suggested presence of all there paralogues in the last eukaryotic common ancestor (LECA) [29], it appears that „single Tim” design is not derived from one and only paralogue (Fig. 5). That a “single Tim” of trimastix, microsporidia, and kinetoplastidsis likely derived from Tim22, while the counterpart of *C. parvum*, *Giardia* and CLO from Tim17 proteins indicates, that both proteins have capacity to build functional protein conduction channel.

MATERIALS AND METHODS

Bioinformatics

Cell culture and fractionation

Trophozoites of *G. intestinalis* strain WB (ATCC 30957) were grown in TY-S-33 medium [35] supplemented with 10% heat-inactivated bovine serum (PAA Laboratories), 0.1% bovine bile and antibiotics. Cells containing BirA were grown in medium supplemented with 50 μM biotin.

Cloning and transfection

Table S1 in the supplemental material presents the primers used in this study. For the determination of cellular localization, GL50803_10452 gene was amplified from genomic DNA and subcloned into pTG vector containg HA-tag [36] using NdeI and PstI restriction sites. For the biotinylation assay, we used pTG plasmid containing *E. coli* BirA and GL50803_10452 gene was subcloned to pONDRA with the C-terminal BAP-tag using NdeI and XhoI restriction sites [14]. Transfection was performed asi previously described [37]. Genes for Y2H system were

PCR aplified and subcloned into pGADT7 and pGBKT7 vectors using NdeI (AseI) and BamHI (BglII) restriction sites.

Fluorescence microscopy

G. intestinalis trophozoites were fixed with 1% formaldehyde as previously described [38]. Protein GL50803_9296 was recognized by specific antibody produced in rabbit, and the hemagglutinin epitope (HA tag) was recognized by a rat monoclonal antibody (Roche). The primary antibodies were detected by a donkey Alexa 594 (red)-conjugated anti-rabbit antibody and or Alexa 488 (green)-conjugated anti-rat antibodies (Life Technologies). Alexa 488 (green)-conjugated streptavidin (Life Technologies) was used to detect biotinylation. Slides were mounted with Vectashield containing DAPI (Vector Laboratories). The slides were imaged with an OLYMPUS Cell-R, IX81 microscope system, and the images were processed using ImageJ 1.41e software (NIH).

STED experiment was performed on commercial Abberior STED 775 QUAD Scanning microscope (Abberior Instruments GmbH, Germany) equipped with Ti-E Nikon body, QUAD beam scanner, Easy3D STED Optics Module, and Nikon CFI Plan Apo Lambda objective (60x Oil, NA 1.40). Sample was illuminated by pulsed 561 nm and 640 nm lasers and depleted by pulsed 775 nm STED laser of 2D donut shape (all lasers: 40 MHz repetition rate). Fluorescence signal was detected with single photon counting modules (Excelitas Technologies). Line-interleaved acquisition enabled separated detection of individual channels in spectral range from 605 nm to 625 nm and from 650 nm to 720 nm. The confocal pinhole was set to 1 AU.

Co-precipitation and mass spectrometry

G. intestinalis Tim17-BirA cells were grown in standard medium supplemented with 50 M biotin for 24 h prior to harvesting. The cells were harvested and fractionated as previsously described [14]. The HSP (40 mg) was used for the crosslinking and protein isolation. Crosslinking was performed as previously described [14] using 10uM DTME and 1h incubationon ice. Proteins were eluted from the beads in SDS-sample buffer supplemented with 20 mM bitotin, 5 min, 95 °C. The samples were analyzed by Western blotting using streptavidin conjugated Alexa Fluor 488 and were visualized using a Molecular Imager FX imager (Bio-Rad). The rest of the eluate was analysed with Mass spectrometry.

Samples were dissolved in 100mM TEAB (Triethylammoniumbicarbonate, Thermofisher) buffer with 2% sodiumdeoxycholate (SDC, Sigma) and sonicated. Samples were reduced with 5mM TCEP (Tris(2-carboxyethyl)phosphinehydrochloride, Sigma) for 30 min at 60 °C and alkylated with 10mM MMTS (S-Methylmethanethiosulfonate , Sigma) for 10 min, RT. Total amount of protein was measured with BCA kit (Sigma). 100ug of proteins were digested with trypsin (trypsin:protein ratio 1:50) overnight at 37 ºC. After digestion 1% TFA (Trifluoroacetic acid,

Sigma) was added. SDC was removed by extraction to ethylacetate as previously described [39]. Briefly, 200 µl of ethylacetate was added, vortexed for 1 min and centrifuged at 4000 x g fo 30 s and supernatants were discarded. This step was repeated five times. Remaining ethylacetate was removed using vacuum centrifugation at 45°C for 10 min. After ethylacetate removal 1% TFA was added.

Sample desalting was performed in home made tips columns. Each tip was filled with three layers of C18 sorbent (Sulpeco) as previously described [40]. 15ug of protein was loaded on each pre-equilibrated tip. Eluents were dryed on vacuum dryer, resuspended in 20ul of 1%TFA. 2ug of samples were used for LC/MS measurement.

NanoReversed phase column (EASY-Spray column, 50 cm x 75 µm ID, PepMap C18, 2µm particles, 100 Å poresize) was used for LC/MS analysis. Mobile phase buffer A was composed of water, 2% acetonitrile and 0.1% formic acid. Mobile phase B was composed of 80 % acetonitrile, 0.1% formic acid. Samples were loaded on to the trap column (Acclaim PepMap300, C18, 5 µm, 300 Å WidePore, 300 µm x 5 mm) at a flow rate of 15 µl/min. Loading buffer was composed of water, 2% acetonitrile and 0.1% trifluoroacetic acid. Peptides were eluted with gradient of B from 2% to 40% over 60 min at a flow rate of 300nl/min. Eluting peptide cations were converted to gas-phase ions by electrospray ionization and analyzed on a Thermo Orbitrap Fusion (Q-OT- qIT, Thermo).

Spectra were acquired on Orbitrap Fusion massspectrometer (ThermoScientific) with 2 seconds duty cycle. Full MS spectra were acquired in orbitrap within massrange 350 - 1400 m/z with resolution 120 000 at 200 m/z and maximum injection time 50 ms. Most intense precursors were isolated by quadrupole with 1,6 m/z isolation window and fragmented using HCD with collision energy set to 30 %. Fragment ions were detected in ion trap with scan range mode set to normal and scan rate set to rapid with maximum injection time 35 ms. Fragmented precursors were excluded from fragmentation for 60 seconds.

Raw data were processed in MaxQuant LFQ [41]. LFQ quantification was used for estimation of relative amount of each protein. Just proteins with valid values at least in two replicates (in control or treated group) were used for further processing. Search were done for latest vision of *G. intestinalis* database from EuPathDb (http://eupathdb.org/eupathdb/) and common contaminant database. Modifications were set: Cystein (unimod nr:39) as static, and methionine oxidation (unimod : 1384) and protein N terminus acetylation (unimod : 1) as variable. Further Max Quant results data processing were done in Perseus [42].

Yeast two hybrid assay.

Yeast strain AH109 was inoculated into 5ml 2xYPAD media and incubated over night, 30°C, 200 RPM. Grown culture was diluted with 2xYPAD medium to OD_{600} = 0,2 and incubated (30°C, 200 RPM) until OD_{600} = 0,8. Cells were harvested (3000 x g, 5min), washed in H_2O and resuspended in 1ml H_2O. The carrier DNA (Salmonsperm) was denatured (95°C, 5min) and

placed on ice. Cells were pelleted (3000G, 1min) and the supernatant was discarded. 100 µl of the cells were resuspended in 400ml H_2O and dividend into separate tubes – 50µl for each transformation. Cells were pelleted (3000 x g, 1min) and the supernatant discarded. Solutions were added to tubes in following order: 240µl PEG3500 50% w/v, 36 µl 1M LiAc, 50 µl Salmonsperm DNA, 5 + 5 µl of each plasmid DNA, 24 µl H_2O. Each transformation was vortexed thoroughly for 1 min. Transformed cells were incubated in 42°C, 40 min, then pelleted (3000G, 1min) and the supernatant discarded. Yeast cells were resuspended in 500 µl H_2O, divided into two and spreaded on SD -Trp/-Leu plates with kanamycin (50 µg/ml) (for verification of succesful transformation) and on SD -Trp/-Leu/-His with kanamycin (for interaction test). Plates were incubated in 30°C until colonies appeared (3-4 days).

Serial dilution test

One colony was inoculated into 5ml SD -Trp/-Leu with kanamycin (50 µg/ml) and incubated overnight, 30°C, 200RPM. Cells were pelleted (3000x g, 1min) and the supernatant discarded. Yeast were resuspended in H_2O to OD_{600} = 0,2 and serial dilution was made (40 µl of cell suspension in 160 µl H_2O, 20x – 200 000x). 2µl of each dilution was dropped on SD -Trp/-Leu plate, which were incubated in 30°C until colonies appeared.

***In vitro* protein expression.**

GiTim17 was *in vitro* synthetized using the PURExpress In Vitro Protein Synthesis Kit (NEB). The gene was cloned to DHFR control plasmid (provided in the Kit). The 25 µl translation reaction contained 10 µl of solution A, 7,5 µl of solution B, 250 ng of the template DNA, 1 µl of RNase inhibitor (RNAsin, Promega), radioactively labeled ^{35}S-methionin and 50 µg of lecithin liposomes. The liposomes were prepared from the stock solution of soybean 1-α- lecithin in chloroform by evaporating the chloroform under a nitrogen flow, resuspending the lipid film in dH_20 and subsequent sonication in the water bath sonicator. The translation reaction was incubated for 2 hours in 37°C and then centrifuged for 45 minutes at 13000 g. The pellet was resuspended in 50mM sodium phosphate buffer (pH = 8) with 2M urea, centrifuged and then washed in clear 50mM sodium phosphate buffer. The output was analyzed on Blue Native PAGE, using 2% digitonin and NativePAGE Novex 4-16% Bis-Tris Protein Gel (Thermo Fisher Scientific).

ACKNOWLEDGEMENT

This work was supported by Czech Science Foundation grant 13-29423S to PD and by Charles University Grant Agency grant 98214 to EP/LV. This work was also supported by the Ministry of Education, Youth and Sports of CR within the National Sustainability Program II (Project BIOCEV-FAR) LQ1604 and by the project BIOCEV (CZ.1.05/1.1.00/02.0109).

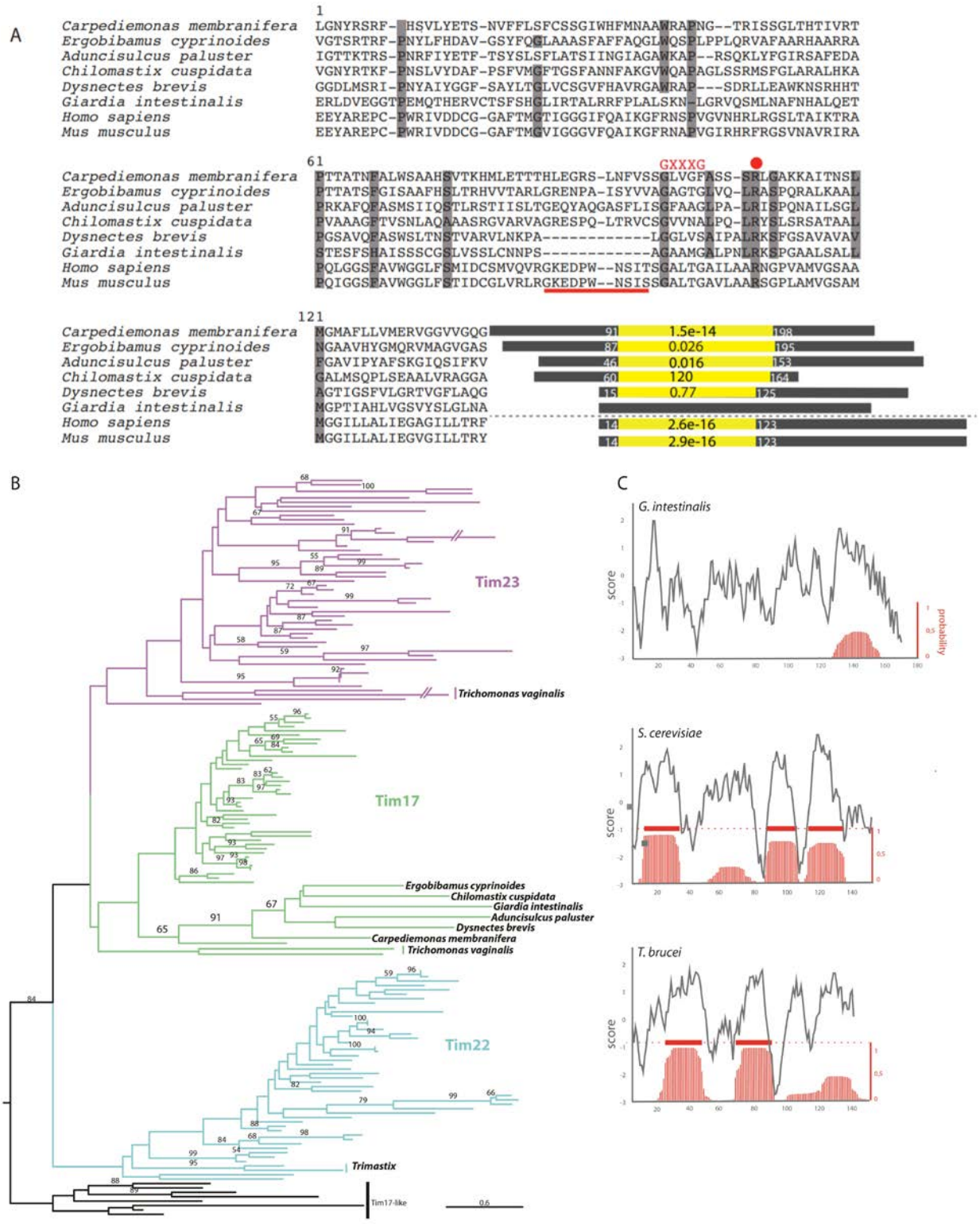

Figure 1. *Giardia* has a single Tim17 family protein. A, Protein sequence alignment of GiTim17 with the orthologues from other metamonads, *Homo sapiens* and *Mus musculus.* Red dot depicts the conserved arginine residue essential for the interaction with Tim44, red line represents the deletion conserved in

G. intestinalis and *D. brevis*. The diagrams next to the alignment correspond to the particular Tim17 proteins (gray rectangle) with highlighted Tim17/22/23 domain identified by HHpred against Pfam (yellow rectangle). The e-value and start and end positions of the domain are shown. **B**, Phylogenetic reconstruction of Tim17, Tim22 and Tim23 proteins including the metamonad sequences. **C**, Hydrophobicity profiles (gray line) by Protscale - (Kyte and Doolittle scale) and transmembrane domain prediction (red lines) by TMHMM of Tim17 proteins from *G. intestinalis*, *S. cerevisiae* and *T. brucei*.

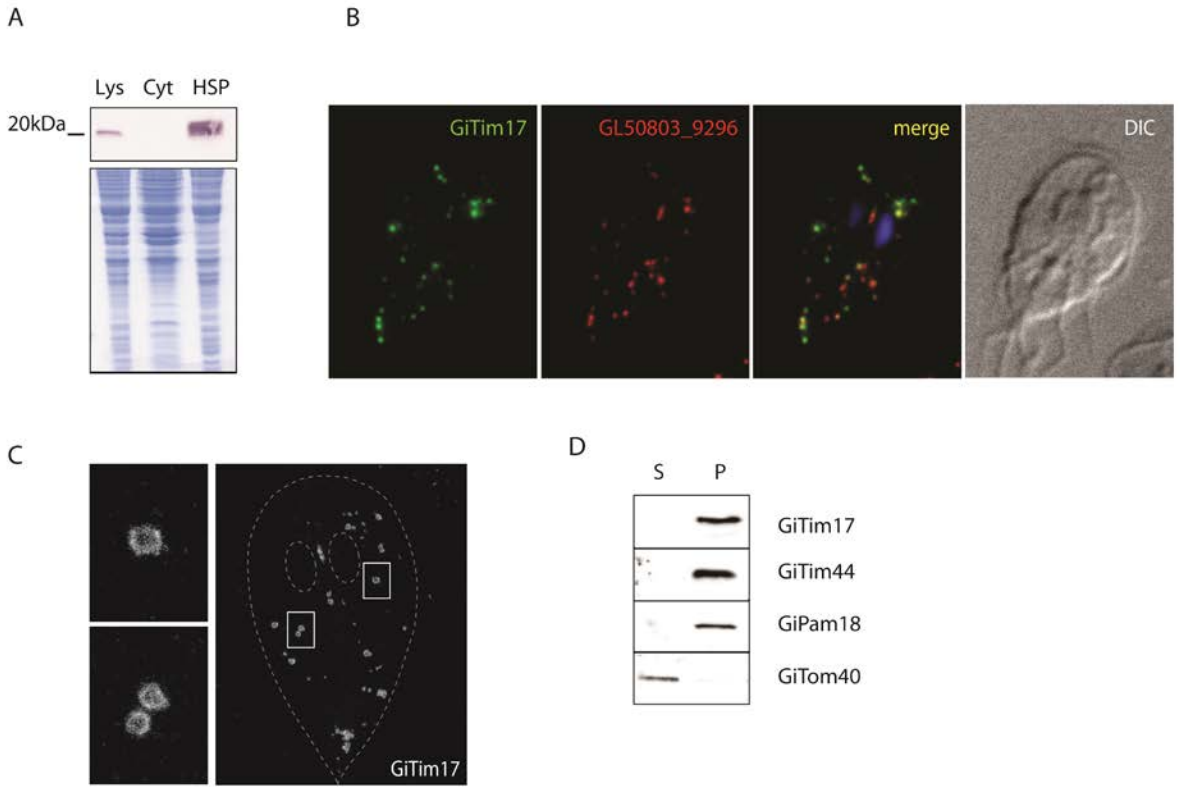

Figure 2. GiTim17 is the inner mitosomal membrane protein. A, GiTim17 was expressed with the C-terminal HA-tag and the protein was detected on the western blot of *G. intestinalis* cellular fractions. The protein was present in the lysate and the high speed pellet fraction, which is enriched for the mitosomes. Lys-lysate, Cyt-cytosol, HSP-high speed pellet. **B**, mitosomal localization of GiTim17 was confirmed by the immunofluorescence microscopy using GL50803_9296 as the mitosomal marker. **C**, STED microscopy of the HA-tagged GiTim17 showed its discrete localization on the periphery of the mitosomes, corresponding to the mitosomal membrane. Two images on the left depict the details of the displayed cell. **D**, western blot analysis of digitonin-solubilized HSP fraction shows differential distribution of the outer mitosomal membrane marker GiTom40 and GiTim17 along with GiPam18 and GiTim44, which are associated with the inner mitosomal membrane. S – supernatant, P – pellet.

A

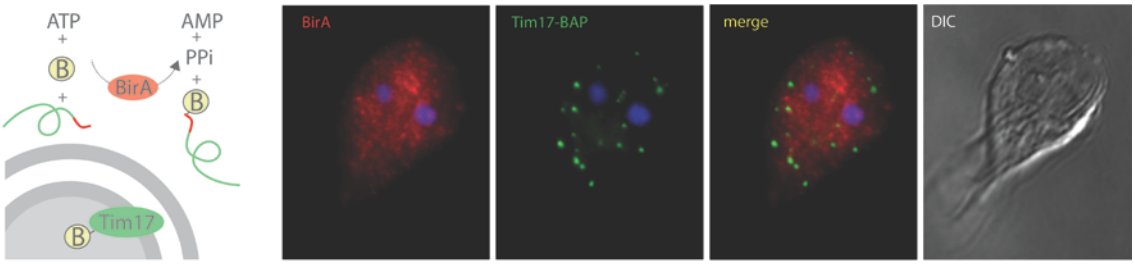

B

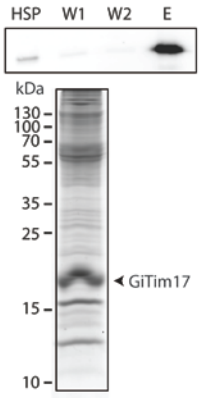

C

Gene ID	annotation (GiardiaDB)	enrichment sample/control
GL50803_10452	Tim17	ND in control
GL50803_14845	Tim44	ND in control
GL50803_17276	hypothetical	ND in control
GL50803_9827	thioredoxin reductase	ND in control
GL50803_10971	hypothetical	ND in control
GL50803_9478	α-MPP	35,1
GL50803_91252	GiOR-1	31,5
GL50803_27266	Ferredoxin	18,3
GL50803_103891	Cpn60	12,1
GL50803_14519	IscS	8,8
GL50803_2013	Glutaredoxin	6,8
GL50803_15196	NifU	6,4
GL50803_17520	ClpB protein	6,2
GL50803_14457	DDTFR19	6,0
GL50803_15049	NEK kinase	4,4
GL50803_3491	hypothetical	4,2
GL50803_16424	hypothetical	4,1
GL50803_14581	Hsp70	3,8
GL50803_32838	Nfu	3,5
GL50803_14821	IscA	3,4
GL50803_3098	hypothetical	3,3

Figure 3. GiTim17 is localized in the proximity to GiTim44. A, BAP-tagged GiTim17 (green) is biotinylated *in vivo* by the HA-tagged cytosolic BirA (red). **B**, The proteins chemically cross-linked to GiTim17 by DTME were co-purified and analyzed by the mass spectrometry.The illustrative SDS-PAGE gel of the purified protein profile. **C**, The identified proteins were ordered according to the enrichment score**.** Only the proteins enriched more than three times are shown (the complete list of the proteins is shown at Supplementary Table 2). Proteins previously verified as mitosomal are highlited in red. ND – not detected in control sample.

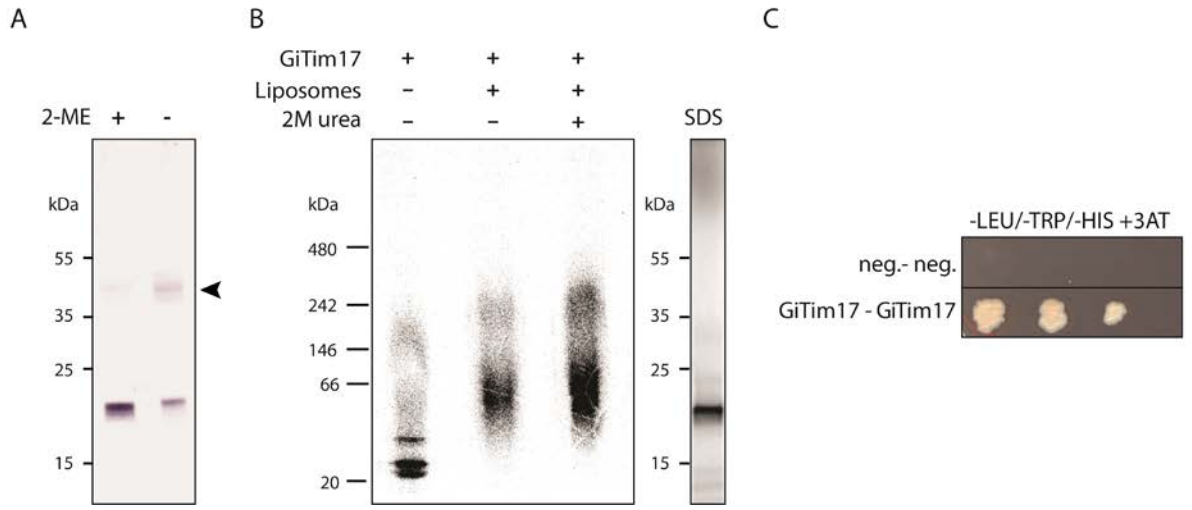

Figure 4. GiTim17 forms dimers in the mitosomal membrane. A. GiTim17 forms about 40kDa complex on non-reducing SDS-PAGE. The complex depicted by the arrowhead brakes apart in the presence of reducing agent such as 2-mercapthoethanol (2-ME). **B**, The complex of higher molecular weight corresponding approximately to the dimer of GiTim17 assembled in the liposomes upon the *in vitro* translation. The complex was resistant to 2M urea, which indicated its membrane insertion. The control SDS-PAGE of the translated GiTim17 is shown on the right. **C**, The mutual interaction of two GiTim17 was positively tested in yeast two hybrid assay under stringent conditions of 3-amino-1,2,4-triazole (3-AT).

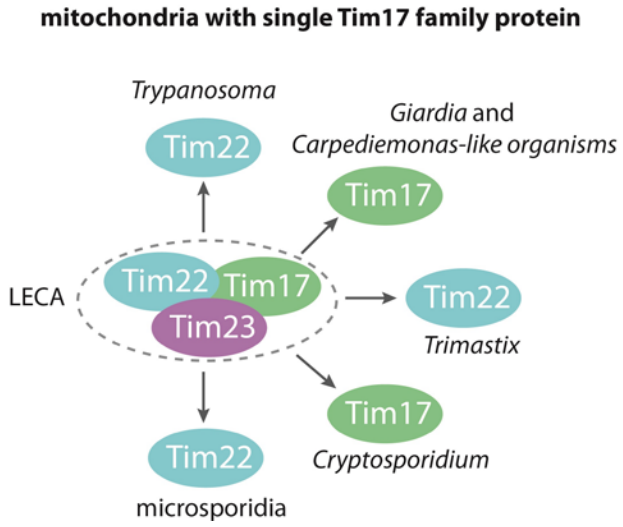

Figure 5. Schematic representation of the mitochondria converging on the single Tim17 family protein translocase. Distinct lineages of eukaryotes have indepently reduced their mitochondrial protein import pathways to just a „single Tim“ translocase in the inner membrane. According to the phylogenetic reconstruction and classification of the protein family members [29], such translocase was derived either from Tim22 or Tim17 subunit.

REFERENCES

1. Embley TM, Martin W. Eukaryotic evolution, changes and challenges. Nature. 2006;440: 623–30. doi:10.1038/nature04546

2. Dolezal P, Likic V, Tachezy J, Lithgow T. Evolution of the molecular machines for protein import into mitochondria. Science. 2006;313: 314–8. doi:10.1126/science.1127895

3. Dudek J, Rehling P, van der Laan M. Mitochondrial protein import: Common principles and physiological networks. Biochim Biophys Acta - Mol Cell Res. 2013;1833: 274–285. doi:10.1016/j.bbamcr.2012.05.028

4. Tovar J, León-Avila G, Sánchez LB, Sutak R, Tachezy J, van der Giezen M, et al. Mitochondrial remnant organelles of Giardia function in iron-sulphur protein maturation. Nature. 2003;426: 172–6. doi:10.1038/nature01945

5. Jedelský PL, Doležal P, Rada P, Pyrih J, Smíd O, Hrdý I, et al. The minimal proteome in the reduced mitochondrion of the parasitic protist Giardia intestinalis. PLoS One. 2011;6: e17285. doi:10.1371/journal.pone.0017285

6. Mokranjac D, Neupert W. The many faces of the mitochondrial TIM23 complex. Biochim Biophys Acta. 1797: 1045–54. doi:10.1016/j.bbabio.2010.01.026

7. Chacinska A, Koehler CM, Milenkovic D, Lithgow T, Pfanner N. Importing mitochondrial proteins: machineries and mechanisms. Cell. 2009;138: 628–44. doi:10.1016/j.cell.2009.08.005

8. Schneider H-C, Berthold J, Bauer MF, Dietmeier K, Guiard B, Brunner M, et al. Mitochondrial Hsp70/MIM44 complex facilitates protein import. Nature. 1994;371: 768–774. doi:10.1038/371768a0

9. Kovermann P, Truscott KN, Guiard B, Rehling P, Sepuri NB, Jensen RE, et al. Tim22 , the Essential Core of the Mitochondrial Protein Insertion Complex , Forms a Voltage-Activated and Signal-Gated Channel. Mol Cell. 2002;9: 363–373.

10. Lithgow T, Schneider A. Evolution of macromolecular import pathways in mitochondria, hydrogenosomes and mitosomes. Philos Trans R Soc Lond B Biol Sci. The Royal Society; 2010;365: 799–817. doi:10.1098/rstb.2009.0167

11. Dolezal P, Smíd O, Rada P, Zubácová Z, Bursać D, Suták R, et al. Giardia mitosomes and trichomonad hydrogenosomes share a common mode of protein targeting. Proc Natl Acad Sci U S A. 2005;102: 10924–9. doi:10.1073/pnas.0500349102

12. Dagley MJ, Dolezal P, Likic VA, Smid O, Purcell AW, Buchanan SK, et al. The protein import channel in the outer mitosomal membrane of Giardia intestinalis. Mol Biol Evol. 2009;26: 1941–7. doi:10.1093/molbev/msp117

13. Morrison HG, McArthur AG, Gillin FD, Aley SB, Adam RD, Olsen GJ, et al. Genomic minimalism in the early diverging intestinal parasite Giardia lamblia. Science. 2007;317: 1921–6. doi:10.1126/science.1143837

14. Martincová E, Voleman L, Pyrih J, Žárský V, Vondráčková P, Kolísko M, et al. Probing the Biology of *Giardia intestinalis* Mitosomes Using In Vivo Enzymatic Tagging. Mol Cell Biol. 2015;35: 2864–74. doi:10.1128/MCB.00448-15

15. Rout S, Zumthor JP, Schraner EM, Faso C, Hehl AB. An Interactome-Centered Protein Discovery Approach Reveals Novel Components Involved in Mitosome Function and Homeostasis in Giardia lamblia. Kumar K, editor. PLOS Pathog. 2016;12: e1006036. doi:10.1371/journal.ppat.1006036

16. Dolezal P, Dagley MJ, Kono M, Wolynec P, Likić VA, Foo JH, et al. The essentials of protein import in the degenerate mitochondrion of *Entamoba histolytica*. PLoS Pathog. 2010;6: e1000812. doi:10.1371/journal.ppat.1000812

17. Leger MM, Kolisko M, Kamikawa R, Stairs CW, Kume K, Čepička I, et al. Organelles that illuminate the origins of Trichomonas hydrogenosomes and Giardia mitosomes. Nat Ecol Evol. 2017;1: 92. doi:10.1038/s41559-017-0092

18. Aurrecoechea C, Barreto A, Basenko EY, Brestelli J, Brunk BP, Cade S, et al. EuPathDB: the eukaryotic pathogen genomics database resource. Nucleic Acids Res. 2017;45: D581–D591. doi:10.1093/nar/gkw1105

19. Alva V, Nam S-Z, Söding J, Lupas AN. The MPI bioinformatics Toolkit as an integrative platform for advanced protein sequence and structure analysis. Nucleic Acids Res. Oxford University Press; 2016;44: W410–W415.

doi:10.1093/nar/gkw348

20. Likic VA, Dolezal P, Celik N, Dagley M, Lithgow T. Using hidden markov models to discover new protein transport machines. Methods Mol Biol. 2010;619: 271–84. doi:10.1007/978-1-60327-412-8_16

21. Krogh A, Larsson B, von Heijne G, Sonnhammer EL. Predicting transmembrane protein topology with a hidden Markov model: application to complete genomes. J Mol Biol. 2001;305: 567–80. doi:10.1006/jmbi.2000.4315

22. Jakobs S, Wurm CA. Super-resolution microscopy of mitochondria. Curr Opin Chem Biol. 2014;20: 9–15. doi:10.1016/j.cbpa.2014.03.019

23. Schagger H, Pfeiffer K. Supercomplexes in the respiratory chains of yeast and mammalian mitochondria. EMBO J. 2000;19: 1777–1783. doi:10.1093/emboj/19.8.1777

24. Rehling P, Model K, Brandner K, Kovermann P, Sickmann A, Meyer HE, et al. Protein insertion into the mitochondrial inner membrane by a twin-pore translocase. Science. 2003;299: 1747–51. doi:10.1126/science.1080945

25. Martinez-Caballero S, Grigoriev SM, Herrmann JM, Campo ML, Kinnally KW. Tim17p Regulates the Twin Pore Structure and Voltage Gating of the Mitochondrial Protein Import Complex TIM23. J Biol Chem. 2006;282: 3584–3593. doi:10.1074/jbc.M607551200

26. Blom J, Kübrich M, Rassow J, Voos W, Dekker PJ, Maarse AC, et al. The essential yeast protein MIM44 (encoded by MPI1) is involved in an early step of preprotein translocation across the mitochondrial inner membrane. Mol Cell Biol. 1993;13: 7364–71. Available: http://www.ncbi.nlm.nih.gov/pubmed/8246957

27. Demishtein-Zohary K, Günsel U, Marom M, Banerjee R, Neupert W, Azem A, et al. Role of Tim17 in coupling the import motor to the translocation channel of the mitochondrial presequence translocase. Elife. 2017;6. doi:10.7554/eLife.22696

28. Šmíd O, Matušková A, Harris SR, Kučera T, Novotný M, Horváthová L, et al. Reductive Evolution of the Mitochondrial Processing Peptidases of the Unicellular Parasites Trichomonas vaginalis and Giardia intestinalis. Goldberg DE, editor. PLoS Pathog. 2008;4: e1000243. doi:10.1371/journal.ppat.1000243

29. Žárský V, Doležal P. Evolution of the Tim17 protein family. Biol Direct. 2016;11: 54. doi:10.1186/s13062-016-0157-y

30. Burri L, Williams BAP, Bursac D, Lithgow T, Keeling PJ. Microsporidian mitosomes retain elements of the general mitochondrial targeting system. Proc Natl Acad Sci. 2006;103: 15916–15920. doi:10.1073/pnas.0604109103

31. Henriquez FL, Richards TA, Roberts F, McLeod R, Roberts CW. The unusual mitochondrial compartment of Cryptosporidium parvum. Trends Parasitol. 2005;21: 68–74. doi:10.1016/j.pt.2004.11.010

32. Schneider A, Bursać D, Lithgow T. The direct route: a simplified pathway for protein import into the mitochondrion of trypanosomes. Trends Cell Biol. 2008;18: 12–8. doi:10.1016/j.tcb.2007.09.009

33. Singha UK, Peprah E, Williams S, Walker R, Saha L, Chaudhuri M. Characterization of the mitochondrial inner membrane protein translocator Tim17 from *Trypanosoma brucei*. Mol Biochem Parasitol. 2008;159: 30–43. doi:10.1016/j.molbiopara.2008.01.003

34. Singha UK, Hamilton V, Duncan MR, Weems E, Tripathi MK, Chaudhuri M. Protein Translocase of Mitochondrial Inner Membrane in *Trypanosoma brucei*. J Biol Chem. 2012;287: 14480–14493. doi:10.1074/jbc.M111.322925

35. Keister DB. Axenic culture of Giardia lamblia in TYI-S-33 medium supplemented with bile. Trans R Soc Trop Med Hyg. 1983;77: 487–8. Available: http://www.ncbi.nlm.nih.gov/pubmed/6636276

36. Martincová E, Voleman L, Najdrová V, De Napoli M, Eshar S, Gualdron M, et al. Live imaging of mitosomes and hydrogenosomes by HaloTag technology. PLoS One. 2012;7: e36314. doi:10.1371/journal.pone.0036314

37. Voleman L, Najdrová V, Ástvaldsson Á, Tůmová P, Einarsson E, Švindrych Z, et al. Giardia intestinalis mitosomes undergo synchronized fission but not fusion and are constitutively associated with the endoplasmic reticulum. BMC Biol. 2017;15: 27. doi:10.1186/s12915-017-0361-y

38. Dawson SC, Sagolla MS, Mancuso JJ, Woessner DJ, House SA, Fritz-Laylin L, et al. Kinesin-13 regulates flagellar, interphase, and mitotic microtubule dynamics in Giardia intestinalis. Eukaryot Cell. American Society for Microbiology;

2007;6: 2354–64. doi:10.1128/EC.00128-07

39. Masuda T, Tomita M, Ishihama Y. Phase Transfer Surfactant-Aided Trypsin Digestion for Membrane Proteome Analysis. J Proteome Res. 2008;7: 731–740. doi:10.1021/pr700658q

40. Ishihama Y, Rappsilber J, Mann M. Modular Stop and Go Extraction Tips with Stacked Disks for Parallel and Multidimensional Peptide Fractionation in Proteomics. J Proteome Res. 2006;5: 988–994. doi:10.1021/pr050385q

41. Cox J, Hein MY, Luber CA, Paron I, Nagaraj N, Mann M. Accurate Proteome-wide Label-free Quantification by Delayed Normalization and Maximal Peptide Ratio Extraction, Termed MaxLFQ. Mol Cell Proteomics. 2014;13: 2513–2526. doi:10.1074/mcp.M113.031591

42. Tyanova S, Temu T, Sinitcyn P, Carlson A, Hein MY, Geiger T, et al. The Perseus computational platform for comprehensive analysis of (prote)omics data. Nat Methods. 2016;13: 731–740. doi:10.1038/nmeth.3901